International Journal of

Cancer Therapy and Oncology

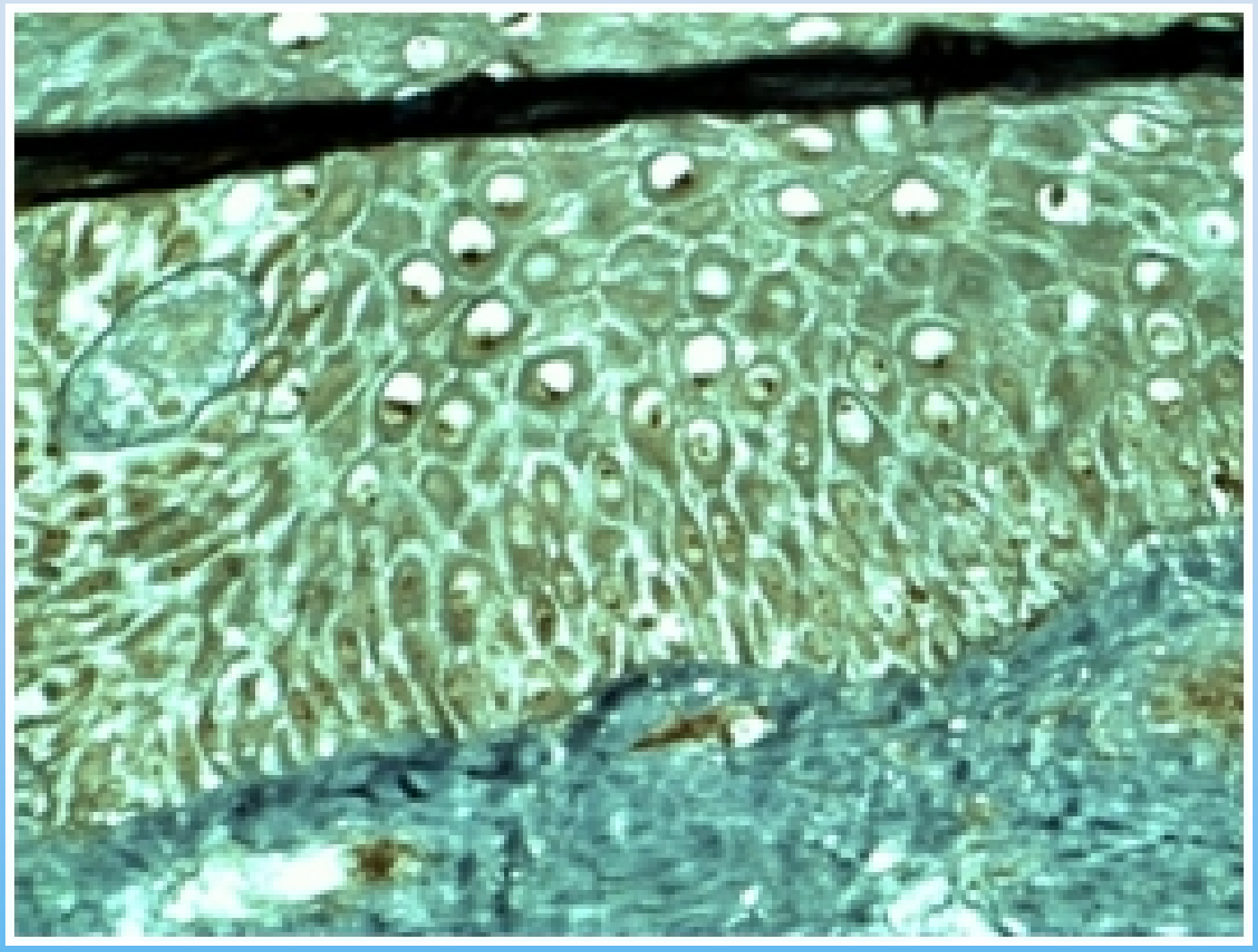

Volume 1, Number 2

(*December 2013*)

www.ijcto.org **ISSN 2330-4049**

Editorial Board

TABLE OF CONTENTS

(The image used in this issue cover is from **Wong *et al.*** **DOI:10.14319/ijcto.0102.7**)

International Journal of Cancer Therapy and Oncology
www.ijcto.org

Dose calculation algorithms in external beam photon radiation therapy

Lanchun Lu

Department of Radiation Oncology, The James Cancer Hospital, Ohio State University, Columbus, Ohio, USA.

Received October 30, 2013; Revised November 12, 2013; Accepted November 13, 2013; Published Online November 22, 2013

Editorial

The ultimate goal of radiation therapy is to deliver a prescribed dose to a tumor precisely while minimizing dose to the critical structures. Radiation dose is the core of the regime, which also includes dose calculation and delivery of radiation beam. The former is the key component of a treatment planning system. Its accuracy directly impacts the quality of a treatment while its speed heavily affects the clinical flow. This review is focused on photon beam dose calculation algorithms, although some basic concepts can also be applied to other beam modalities.

Why is dose calculation required in radiation therapy? One of the reasons is that we need to plan and simulate the treatment prior to the actual delivery of radiation beam to the tumor. To kill a tumor with radiation, a specific dose needs to be absorbed by the tumor. To make sure this tumor gets the prescribed dose, we need to perform dose calculation by managing radiation beams which are characterized by various parameters in the treatment machine used to deliver the radiation. This process is called treatment planning. In modern radiation therapy, treatment planning is generally performed with computing software by using the patient's images to identify and locate the anatomical structures and the machine parameters to simulate the actual treatment. The result of simulation gives the calculated doses for the target as well as for other regions of interest. The accuracy of dose calculation and the strict quality assurance program is essential in order to make sure that dose delivery to the tumor is 100% or close to 100% of the calculated dose.

Radiation dose is defined as the total amount of ionizing radiation energy absorbed by the material or tissues per unit of mass. Hence, dose calculation is computing the energy absorbed by the media at any points that radiation beam particles pass or may not pass through, where various physical processes are underway due to the interaction between beam particles and the media. At any point of interest, the dose is contributed by primary beam particles interacting at the point, then scattering from other interacting points in the patient, and the non-primary beam particles leaking from the gantry head. A good dose calculation algorithm is the one that not only can take into account accurately all the physical processes involved in the beam particle-media interaction so that the calculated dose is accurate, but also is fast enough to be used in clinic. Hence, accuracy and speed are the two key factors for a dose calculation algorithm.

The dose calculation algorithm for radiation therapy has been evolving rapidly since the 1950s, mainly attributed to the rapid development in the fields of particle/nuclear physics and computer science which enable us to better understand the physical processes involved in the beam particle-media interaction and to simulate and calculate doses for a complex system within a short time period. **Figure 1** illustrates this evolution. From the developing history of dose calculation and the mechanisms used for the dose calculation, we can categorize the dose calculation algorithms into three major groups: (1) correction-based; (2) model-based; and (3) principle-based.

Correction-based algorithm is a type of empirical dose calculation which interpolates or extrapolates dose from some basic measurements in water such as percentage depth dose (PDD) for different field sizes at a certain source surface distance (SSD). The introduction of concepts of tissue-air ratio (TAR) [1], tissue-phantom ratio (TPR) [2], and tissue-maximum ratio (TMR) [3] made this algorithm rather successful in the regime of homogenous media. A typical example of this algorithm is Clarkson's technique [4] and IRREG[5-6] that are still commonly used in clinic for manual dose calculation and in some commercial software used for second-hand dose check (RadCalc, Lifeline Software Inc., Austin, Texas, USA). For homogenous media, such as water, this calculation algorithm gives rather accurate results. For a heterogeneous system

Corresponding author: Lanchun Lu, PhD; The James Cancer Hospital, Department of Radiation Oncology, Ohio State University, 300 W 10th Avenue, Columbus, OH 43210, USA. Email: lu.281@osu.edu

Cite this article as:
Lu L. Dose calculation algorithms in external beam photon radiation therapy. Int J Cancer Ther Oncol 2013; **1**(2):01025.
DOI: 10.14319/ijcto.0102.5

ISSN 2330-4049

such as a human body with bones and lungs, applying equivalent beam path length can correct part of the heterogeneous effect, but the accuracy is not enough because it cannot take into account the lateral scattering when beam transports in media.

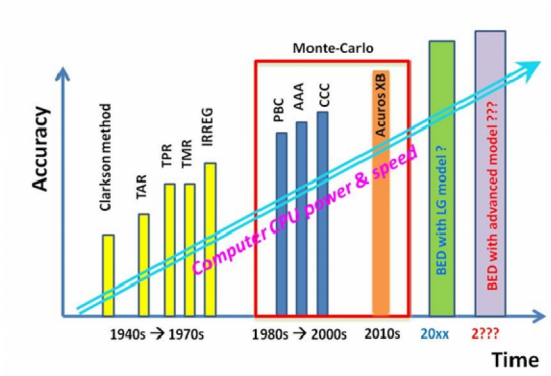

FIG. 1: Evolution of photon dose calculation algorithms.

Model-based algorithm starts first from physics principles and then simplifying the procedure describing the actual physical transport to expedite the calculation. These physical processes have been well studied and are unambiguous: A beam particle interacts with media at a point, releases energy, and then is deposited or scattered away from the primary interaction site. During this process it may create secondary photons and electrons, releasing energy in the scattering path. These physical processes are simplified by using a convolution equation that convolutes the primary photon energy fluence (*terma* – total energy released in unit of mass) with a kernel that describes the contribution from scattering photons and electrons, and the method is called the convolution algorithm.[7-20] If the path length is replaced by radiological path length to describe the inhomogeneity of media, the method is called convolution-superposition. The details of how to handle this convolution kernel give rise to sub-difference algorithms that are applied in different commercial treatment plan systems: Pencil Beam Convolution (PBC)[12-14], the Analytical Anisotropic Algorithm (AAA) [15,18] (Varian Medical System, Inc. Palo Alto, CA, USA), and Collapse Cone Convolution (CCC) algorithms[16, 19, 20] (Pinnacle, CMS XiO, etc). For homogeneous media such as water, there is not much difference in accuracy for these calculation algorithms. For heterogeneous media, radiological path length is used in place of the actual length to account for the difference in electron density from water, and convolution evolutes to convolution-superposition. The difference in the accuracy of dose calculation on heterogeneous media is determined by how well the kernels of these algorithms can simulate the actual scattering. In PBC, the lateral scattering is considered to be homogeneous, and the inhomogeneity correction only happens in the longitudinal direction which is accounted for by using the equivalent path length converted from mass attenuation (hence the electron density of media).

For AAA and CCC, both consider the heterogeneous effect not only in the longitudinal direction, but also in the lateral one. AAA uses Gaussian functions to describe the mean heterogeneous effect in four lateral directions (± x and ± y).[15, 18] In CCC, the kernel is replaced by a certain number of discrete elements and the mean for all elements is used to simplify and reduce the calculation time.[16, 19, 20] Many research results imply that CCC is more accurate than AAA when an inhomogeneity correction needs to be applied[21-23], which indicates that CCC handles the lateral scattering better than does AAA in a heterogeneous environment. Monte-Carlo algorithm is not a new technique but has been used as a benchmark to check the accuracy of other dose calculation algorithms.[22, 24-28] Starting from the first principles of physics, Monte-Carlo simulates the actual physical processes in two major steps which are initiated by a random number seed generation in the target: (1) the radiation beams travel through the accelerator gantry head including the collimator system; (2) collimated beam particles from the gantry head travel through and distribute dose in the patient's body. As Monte-Carlo simulates all the real physical processes in which the beam particles are involved during transportation, the result of its dose calculation should be very accurate.

However, the accuracy is mainly determined by the number of events generated, and this statistical uncertainty is proportional to the inverse square root of the event numbers scored.[29] For this reason, the speed of Monte-Carlo dose calculation is slow and the process is very time-consuming. The rapid development of computer CPU power greatly enhances the speed of Monte-Carlo dose calculation and makes it possible to be applied in clinic – even though only until very recently the electron Monte-Carlo dose calculation was just implemented into the Varian Eclipse treatment plan system.[30] The photon Monte-Carlo dose calculation is still very slow and not feasible for use in the clinic. To take advantage of the accuracy of the Monte-Carlo algorithm and avoid its slow speed, simplification of beam particle transport in patient body was made, leading to the AAA and CCC algorithms.[15-21]

Similar to Monte-Carlo algorithm, Acuros XB tries to simulate all the physical processes that beam particles involve – instead of generating beam particles one by one in the simulation process, Acuros XB uses a group of Boltzmann transport equations (BTE) to describe all the physical processes involved[31], and these equations are solved using numerical methods in the computer world, which is much faster than Monte-Carlo (and even the AAA algorithm) but still provides a comparable accuracy to the Monte-Carlo algorithm. The Acuros XB algorithm was recently implemented in the Varian Eclipse Version 10.1, and is available in clinic.[32-34]

ISSN 2330-4049

To test and evaluate the accuracy of a dose calculation algorithm, the best approach is to perform measurements and then compare the measured results with the calculated dose in both homogeneous and heterogeneous media. Many works have been done to evaluate the above-mentioned dose calculation algorithms[21-23, 30, 32-42], and the hierarchy of accuracy is as follows: Monte-Carlo algorithm > Acuros XB > CCC > AAA > PBC > Correction-based methods.[21-23, 30, 32-42]

With Monte-Carlo and Acuro XB algorithms, you can expect a close to 100% accuracy of dose calculation if time permits. After more than 60 years of dedicated efforts on the dose calculation algorithm and the development of powerful computer CPUs, the accuracy of dose calculation seems to meet our requirements, and the time needed for calculation in the clinic no longer matters. Are Monte-Carlo and Acuros XB algorithms the end of the dose calculation game? We should not forget that the ultimate goal of radiation therapy is to kill cancer cells while sparing normal tissues as much as possible. A pure physical dose in non-life media, which does not directly associate with any biological factor in tissues, has no more significance than does a dose calculation algorithm with less accuracy. The next generation of dose calculation algorithms should and is expected to include biological equivalent dose or biological effectiveness dose, which can take into account the actual biological effect for different types of ionization radiation beams and different types of irradiated tissues, and can allow physicians to relate the biological dose more closely to the treatment outcome than what we have today. This is heavily reliant on the progress of radiation biology. Is that going to be a simply biological equivalent dose (BED) with Linear-Quadratic model or BED with a more advanced model?

Conflict of interest

The authors declare that they have no conflicts of interest. The authors alone are responsible for the content and writing of the paper.

References

1. Johns HE, Whitmore G, Watson T, et al: A system of dosimetry for rotation therapy with typical rotation distributions. *J Can Assn Radiol* 1953; **4**:1.
2. Karzmark CJ, Deubert A, Loevinger R. Tissue-phantom ratios — an aid to treatment planning. *Br J Radiol* 1965; 38:158.
3. Holt JG, Laughlin JS, Moroney JP. The extension of the concept of tissue-air ratios (TAR) to high-energy x-ray beams. *Radiology* 1970; 96:437-46.
4. Clarkson JR. A note on depth doses in fields of irregular shape. *Br J Radiol* 1941; 14:265. 24.
5. Cunningham JR. Scatter-air ratios. *Phys Med Biol* 1972; 17:42-51.
6. Khan FM, Levitt SH, Moore VC, Jones TK Jr. Computer and approximation methods of calculating depth dose in irregularly shaped fields. *Radiology* 1973; 106:433-6.
7. Woo MK, Scora DJ, Wong E. The regional Monte Carlo method: a dose calculation method based on accuracy requirement. *Med Phys* 1998; 25:1866-71.
8. Mackie TR, Bielajew AF, Rogers DW, Battista JJ. Generation of photon energy deposition kernels using the EGS Monte Carlo code. *Phys Med Biol* 1988; 33:1-20.
9. Ahnesjö A, Aspradakis MM. Dose calculations for external photon beams in radiotherapy. (Topical Review), *Phys Med Biol* 1999; 44:R99-155.
10. Nilsson M and Knoos T. Application of the Fano theorem in inhomogeneous media using a convolution algorithm. *Phys Med Biol* 1992; 37: 69-83.
11. Ahnesjo A. Collapsed cone convolution of radiant energy for photon dose calculation in heterogeneous media. *Med Phys* 1989; 16: 577-92.
12. Mohan R, Chui C, Lidofsky L. Differential pencil beam dose computation model for photons. *Med Phys* 1986; 13:64-73.
13. Ahnesjö A, Saxner M, Trepp A. A pencil beam model for photon dose calculation. *Med Phys* 1992; 19:263-73.
14. Bourland JD, Chaney EL. A finite-size pencil beam model for photon dose calculations in three dimensions. *Med Phys* 1992; 19:1401-12.
15. Sievinen J, Ulmer W, Kaissl W. AAA photon dose calculation model in Eclipse. Varian Medical Systems 2005; RAD #7170B.
16. McNutt T. The ADAC Pinnacle Collapsed Cone Convolution Superposition Dose Model. ADAC Radiation Therapy Products. www.adaclabs.com
17. Sharpe MB, Battista JJ. Dose calculations using convolution and superposition principles: the orientation of dose spread kernels in divergent x-ray beams. *Med Phys* 1993; 20:1685-94.
18. Ulmer W, Harder D. A Triple Gaussian Pencil Beam Model for Photon Beam Treatment Planning, *Z. Med Phys* 1995; 5:25-30.
19. Mackie TR, Bielajew AF, Rogers DW, Battista JJ. Generation of photon energy deposition kernels using the EGS Monte Carlo code. *Phys Med Biol* 1988; 33:1-20.
20. MackieTR, Reckwerdt PJ, Holmes TW, Kubsad SS, Review of convolution/superposition methods for photon beam dose computation. *Proceedings of the Xth ICCR* 1990; 20-23.
21. Hasenbalg F, Neuenschwander H, Mini R, Born EJ. Collapsed cone convolution and analytical anisotropic algorithm dose calculations compared to

 ISSN 2330-4049

VMC++ Monte Carlo simulations in clinical cases. *Phys Med Biol* 2007; 52:3679-91.
22. Aarup LR, Nahum AE, Zacharatou C, Juhler-Nøttrup T, Knöös T, Nyström H, Specht L, Wieslander E, Korreman SS. The effect of different lung densities on the accuracy of various radiotherapy dose calculation methods: implications for tumour coverage. *Radiother Oncol* 2009; 91:405-14.
23. Gray A, Oliver LD, Johnston PN. The accuracy of the pencil beam convolution and anisotropic analytical algorithms in predicting the dose effects due to attenuation from immobilization devices and large air gaps. *Med Phys* 2009; 36:3181-91.
24. Ma CM, Li JS, Pawlicki T, Jiang SB, Deng J, Lee MC, Koumrian T, Luxton M, Brain S. A Monte Carlo dose calculation tool for radiotherapy treatment planning. *Phys Med Biol* 2002; 47:1671-89.
25. Webb S, Parker RP. A Monte Carlo study of the interaction of external beam X-radiation with inhomogeneous media. *Phys Med Biol* 1978; 23:1043-59.
26. Kawrakow I. VMC++, Electron and Photon Monte Carlo Calculations Optimized for Radiation Treatment Planning in Advanced Monte Carlo for Radiation Physics, Particle Transport Simulation and Applications: *Proc. Monte Carlo 2000 Meeting Lisbon*, A. Kling, F. Barao, M. Nakagawa, L. Tavora, and P. Vaz (eds.), Berlin: Springer 2001; 229-236.
27. Reynaert N, Van der Marck SC, Schaart DR, et al. Monte Carlo treatment planning for photo and electron beams. *Radiation Physics and Chemistry* 2007; 76:643-686.
28. Tertel J, Wulff J, Karle H, Zink K. Verification of a commercial implementation of the Macro-Monte-Carlo electron dose calculation algorithm using the virtual accelerator approach. *Z Med Phys* 2010; 20:51-60.
29. Jeraj R, Keall P. The effect of statistical uncertainty on inverse treatment planning based on Monte Carlo dose calculation. Phys Med Biol 2000; 45:3601-13.
30. Hu YA, Song H, Chen Z, Zhou S, Yin FF. Evaluation of an electron Monte Carlo dose calculation algorithm for electron beam. *J Appl Clin Med Phys* 2008; 9:2720.
31. Vassiliev ON, Wareing TA, McGhee J, Failla G, Salehpour MR, Mourtada F. Validation of a new grid-based Boltzmann equation solver for dose calculation in radiotherapy with photon beams. *Phys Med Biol* 2010; 55:581-98.
32. Kroon PS, Hol S, Essers M. Dosimetric accuracy and clinical quality of Acuros XB and AAA dose calculation algorithm for ste-reotactic and conventional lung volumetric modulated arc therapy plans. *Radiat Oncol* 2013; 8:149.
33. Fogliata A, Nicolini G, Clivio A, Vanetti E, Cozzi L. Critical appraisal of Acuros XB and Anisotropic Analytic Algorithm dose calculation in advanced non-small-cell lung cancer treatments. *Int J Radiat Oncol Biol Phys* 2012; 83:1587-95.
34. Han T, Mikell JK, Salehpour M, Mourtada F. Dosimetric comparison of Acuros XB deterministic radiation transport method with Monte Carlo and model-based convolution methods in heterogeneous media. *Med Phys* 2011; 38:2651-2664.
35. Mesbahi A, Thwaites DI, Reilly AJ. Experimental and Monte Carlo evaluation of Eclipse treatment planning system for lung dose calculations. *Rep Pract Onc Radiother* 2006; 11:123-133.
36. Van Esch A, Tillikainen L, Pyykkonen J, Tenhunen M, Helminen H, Siljamäki S, et al. Testing of the analytical anisotropic algorithm for photon dose calculation. *Med Phys* 2006; 33:4130-48.
37. Nishio T, Kunieda E, Shirato H, Ishikura S, Onishi H, Tateoka K, et al. Dosimetric verification in participating institutions in a stereotactic body radiotherapy trial for stage I non-small cell lung cancer: Japan clinical oncology group trial (JCOG0403). *Phys Med Biol* 2006; 51:5409-17.
38. Knöös T, Wieslander E, Cozzi L, Brink C, Fogliata A, Albers D, Nyström H, Lassen S. Comparison of dose calculation algorithms for treatment planning in external photon beam therapy for clinical situations. *Phys Med Biol* 2006; 51:5785-807.
39. Lu LC, Yembi-Goma G, Wang JZ, et al. A practical method to evaluate and verify dose calculation algorithms in the treatment planning system of radiation therapy. *Int J Med Phys Clin Eng Radiat Oncl* 2013; 2:76-87.
40. Rana S, Rogers K. Dosimetric evaluation of Acuros XB dose calculation algorithm with measurements in predicting doses beyond different air gap thickness for smaller and larger field sizes. *J Med Phys* 2013; 38: 9-14.
41. Kathirvel M, Subramanian S, Clivio A, et al. Critical appraisal of the accuracy of Acuros-XB and Anisotropic Analytical Algorithm compared to measurement and calculations with the compass system in the delivery of RapidArc clinical plans. *Radiat Oncol* 2013; 8:140.
42. Rana S, Rogers K, Lee T, Reed D, Biggs C. Verification and Dosimetric Impact of Acuros XB Algorithm for Stereotactic Body Radiation Therapy (SBRT) and RapidArc Planning for Non-Small-Cell Lung Cancer (NSCLC) Patients. *Int J Med Phys Clin Eng Radiat Oncl* 2013; 2:6-14.

(Dr. Lanchun Lu is an editorial board member of International Journal of Cancer Therapy and Oncology)

 ISSN 2330-4049

International Journal of Cancer Therapy and Oncology
www.ijcto.org

Recent advances in treatment of childhood cancer : role of targeted therapy

Youssef Al-Tonbary

Department of Pediatric Oncology, Mansoura University Children Hospital, Mansoura University, Egypt.

Received November 17, 2013; Revised November 25, 2013; Accepted November 27, 2013; Published Online December 02, 2013

Editorial

Advances in the basic science of cancer, genetic studies, molecular biology and different modalities of therapy including chemotherapy, radiotherapy, surgery and supportive care have occurred in the last few decades. Improvement in histological, immunological and cytogenetic techniques has made the diagnosis and classification more accurate. The development of multiple-agent chemotherapy, targeted and pharmacogenetic therapies as well as hematopoietic stem cell transplantation hold great promise for the future. Molecular HLA-typing techniques and the international donor registries have solved the problem of finding appropriate donors for transplantation. In addition, progress in palliative care has provided a degree of comfort for patients undergoing chemotherapy, radiotherapy and surgery.

Recently targeted cancer therapy has made a good impact in treatment of childhood chronic myeloid leukemia (CML) and Philadelphia positive acute lymphoblastic leukemia (Ph+ ALL). The Ph+ is due to reciprocal translocation of the long arms of chromosomes 9 and 22, t (9:22) (q34; q11), which results in a fusion gene BCR-ABL, encoding a constitutively active tyrosine kinase. The BCR-ABL tyrosine kinase inhibitor (TKI), imatinib, is now used in treatment of Pediatric CML as well as Ph+ALL. It selectively inhibits the tyrosine kinase domain in the Abelson proto-oncogene (ABL) and targets the tyrosine kinase C-kit and platelet – derived growth factor receptor (PDGF-R) which causes the mutations found in both myeloid and lymphoid malignancies.[1, 2] As a result, phosphorylation of ABL-tyrosine kinase substrates fails to occur and prevent activation of leukemogenic signal transduction. It was approved in 2001 for treatment of CML and in 2013 for treatment of Pediatric Ph+ALL.

Corresponding author: Youssef Al-Tonbary; Department of Pediatric Oncology, Mansoura University Children Hospital, Mansoura University, Egypt.
Email: ytonbary@gmail.com

Cite this article as:
Al-Tonbary Y. Recent advances in treatment of childhood cancer: role of targeted therapy. Int J Cancer Ther Oncol 2013; 1(2):01028. **DOI**: 10.14319/ijcto.0102.8

A report from the children's Oncology group has recorded success in treatment of de-novo chronic phase CML in children in 80% of cases.[3] CML comprises 2-3% of all childhood leukemia. Response to treatment with imatinib appears to be better in children than in adults.[4, 5, 6] Recently, the use of imatinib alone in treating CML in children is considered when no HLA-identical donor for stem cell transplantation is available.

The high-risk Ph+ALL represents 3-5% of childhood ALL.[7] The use of chemotherapy alone in its treatment results in less than 30% event-free survival rates.[8] Children Oncology Group (COG) reported improved outcomes of children with Ph+ALL treated with imatinib and chemotherapy.[9] Its role in pre-and post-hematopoietic stem cell transplantation is still under study and evaluation.[10] In conclusion, the targeted imatinib therapy dramatically improved the outcomes of children with CML and Ph+ALL.

Currently, several novel targeted therapeutic strategies are being investigated. They include Troxacitabine (a nucleoside analogue), Decitabine (a hypomethylating agent), R15777 SCH66336 (farnesyl transferase inhibitor), Homoharringtone (a plant alkaloid), PS-341 (a proteosome inhibitor), PR1 vaccine, polyethylene glycol IFN-α preparations, and inhibitor of heat shock protein 90 (a molecular chaperone required for stability of signal proteins). Success of these novel drugs will add a major advance in combating malignancy.

Conflict of interest

The authors declare that they have no conflicts of interest. The authors alone are responsible for the content and writing of the paper.

References

1. Hatzimichael E, Georgiou G, Benetatos L, Briasoulis E. Gene mutations and molecularly targeted therapies in acute myeloid leukemia. *Am J Blood Res* 2013; **3**: 29-51.

ISSN 2330-4049

2. Roberts KG, Morin RD, Zhang J et al. Genetic alterations activating kinase and cytokine receptor signaling in high-risk acute lymphoblastic leukemia. *Cancer cell* 2012; **22**: 153-166.
3. Champagne MA, Fu CH, Chang M et al. Higher dose imatinib for children with de novo chronic phase chronic myelogenous leukemia: a report from the Children's Oncology Group. *Pediatr Blood Cancer* 2011; **57**: 56-62.
4. Suttorp M, Thiede C, Tauer JT, Roettgers S, Sedlacek P, Harbott J. Chronic Myeloid Leukemia in Pediatrics -- First Results From Study CML-PAED II. *ASH Annual Meeting Abstracts* 2009; **114**: 342.
5. Roy L, Guilhot J, Krahnke T et al. Survival advantage from imatinib compared with the combination interferon-alpha plus cytarabine in chronic-phase chronic myelogenous leukemia: historical comparison between two phase 3 trials. *Blood* 2006; **108:** 1478-1484.
6. O'Brien SG, Guilhot F, Larson RA et al. Imatinib compared with interferon and low-dose cytarabine for newly diagnosed chronic-phase chronic myeloid leukemia. *N Engl J Med* 2003**; 348**: 994-1004.
7. Jones LK, Saha V. Philadelphia positive acute lymphoblastic leukaemia of childhood. *Br J Haematol* 2005; **130**: 489-500.
8. Arico M, Valsecchi MG, Camitta B et al. Outcome of treatment in children with Philadelphia chromosome-positive acute lymphoblastic leukemia. *N Engl J Med* 2000; **342**: 998-1006.
9. Schultz KR, Bowman WP, Aledo A et al. Improved early event-free survival with imatinib in Philadelphia chromosome-positive acute lymphoblastic leukemia: a children's oncology group study. *J Clin Oncol* 2009; **27**: 5175-5181.
10. Burke MJ, Cao Q, Trotz B et al. Allogeneic hematopoietic cell transplantation (allogeneic HCT) for treatment of pediatric Philadelphia chromosome-positive acute lymphoblastic leukemia (ALL). *Pediatr Blood Cancer* 2009; **53**: 1289-1294.

(Dr. Youssef Al-Tonbary is an editorial board member of International Journal of Cancer Therapy and Oncology)

 ISSN 2330-4049

International Journal of Cancer Therapy and Oncology
www.ijcto.org

Radiation exposure for coronary artery calcium score at prospective 320 row multi-detector computed tomography

Faisal Khosa[1], Atif Khan[2], Waqas Shuaib[1], Melvin Clouse[2], Matthew Budoff[5], Ron Blankstein[4], Khurram Nasir[3]

[1]*Department of Radiology, Emory University Hospital-Midtown, Atlanta, GA, USA.*
[2]*Department of Radiology, Beth Israel Deaconess Medical Center, Harvard University, Boston, MA, USA.*
[3]*Yale University School of Medicine, New Haven, CT, USA.*
[4]*Brigham and Women's Hospital Harvard Medical School, Boston, MA, USA.*
[5]*Los Angeles Biomedical Research Institute, Torrance, CA, USA.*

Received October 16, 2013; Revised November 03, 2013; Accepted November 10, 2013; Published Online November 15, 2013

Original Article

Abstract

Purpose: To date there is extensive data on the radiation dose for assessing coronary artery calcium scores (CACS) with 4-64 row multidetector MDCT. However with the advent of 320 row MDCT, the entire heart can be imaged in one beat and thus potentially reduce the radiation dose. The aim of this study was to evaluate radiation dose for CACS on low-dose prospective EKG-triggered 320 row MDCT. **Materials and Methods**: Informed consent for this retrospective HIPAA-compliant study was waived and approved by our institution's institutional review board IRB. One hundred and sixty eight consecutive patients (Male 133 (79%): female 35 (21%), mean body mass index BMI 29±5 and mean heart rate 58± bpm) underwent coronary calcium scoring with prospective gating. The scan parameters were 300 mA, 120 kVp, volume scan length (VSL) 160 mm, gantry rotation 0.350 msec and 320 x 0.5 mm detectors at 320 MDCT. Beta blockers were given to patients in a case heart rate HR > 65 bpm. The effective dose (ED) estimates were calculated for all patients from the dose length product and the conversion factor k (0.014 mSv/mGy/cm) as recommended by current guidelines. **Results:** The mean SD radiation was 1.89±0.79 mSv. Overall the range varied from 0.28-2.48 mSv. The radiation was significantly less in females as compared to males (2.02±0.73 vs. 1.41±0.87, p<0.0001). No differences were noted whether HR was <60 vs. >=60 bpm (1.87±0.79 vs. 1.77±0.84 mSv, p=0.45). On the other hand a higher radiation was noted among obese individuals as compared to those with BMI<30 (1.84±0.82 vs. 1.91±0.80 mSv, p=0.62). **Conclusion**: Radiation dose obtained from 320-MDCT is similar to those obtained with 4-64 row MDCT. Further studies are needed to assess the feasibility of further lowering the tube current and tube voltage.

Keywords: Calcium Score; Coronary Artery; MDCT; Radiation

Introduction

Vascular calcification is a constituent of atherosclerosis and in case of coronary arteries this is a strong indicator of presence of coronary artery disease (CAD).[1,2] Several studies have shown that the amount of coronary artery calcium (CAC) correlates with the risk for severe cardiac events, detection and quantification of CAC therefore can be a valuable diagnostic tool in the workup of patients with suspected coronary artery disease.[3-5] Overall, the presence of CAC is highly sensitive and moderately specific for detection of CAD. The negative predictive value of a CAC score of zero (0) can be as high as 99% and is associated with a 0.1% annual risk of cardiovascular events[6,7] and over 99% survival for 10 years.[8] CAC as detected and quantified using noninvasive cardiac computed tomography (CCT) represents a reliable linear anatomic estimate of total plaque burden[9] and is represented clinically as a "calcium score."

Corresponding author: Waqas Shuaib, MD; Department of Radiology and Imaging Sciences, Emory University Hospital 550 Peachtree Street NE. Atlanta, GA 30308, USA.
E-mail: Waqas1184@hotmail.com

Cite this article as:
Khosa F, Khan A, Shuaib W, Clouse M, Budoff M, Blankstein R, Nasir K. Radiation exposure for coronary artery calcium score at prospective 320 row multi-detector computed tomography. Int J Cancer Ther Oncol 2013; 1(2):01023. **DOI:** 10.14319/ijcto.0102.3

(Dr. Faisal Khosa is an American Roentgen Ray Scholar (2013-2015))

ISSN 2330-4049

In 1990, Agatston et al. described a method to determine the amount of coronary calcium from tomographic images.[10] This method depends on the area and the maximum CT density of the calcification detected by electron beam computed tomography (EBCT). EBCT has been regarded the standard of reference method for detection and quantification of coronary calcium, and studies indicating the risk for coronary artery disease are based on EBCT investigations.[8, 11, 12] Calcium score investigations are increasingly performed by using multi-detector CT (MDCT) techniques. It has been shown that MDCT calcium scores correlate well with that of EBCT.[13-17]

MDCT technology has evolved with the current 320 row MDCT, offering improved coverage in the z axis and better temporal & spatial resolution. These technical improvements in scanners lead to better radiation dose efficiency and improved image acquisitions of non-invasive CCTA at high quality with less radiation. The aim of this study was to evaluate radiation dose for CAC scoring on low-dose prospective EKG-triggered CCTA using 320 row MDCT.

Methods and Materials

Patient Characteristics

Informed consent for this retrospective HIPAA-compliant study was waived and approved by our institution's IRB. Retrospective review of CCTA data-base yielded 168 consecutive patients who had undergone CCTA between March 2008 and December 2009 using prospective ECG gating on 320 MDCT (Toshiba Aquilion One Dynamic volume CT, Tochigi-ken, Japan). At our institution as part of the protocol CCS is also performed on all patients. The indication for CCTA comprised the assessment of the coronary arteries or bypass grafts, chest pain, and visualization of cardiac anatomy before or after electrophysiological procedures. Typical sized patients were defined by a body mass index (BMI calculated as weight in pounds divided by height in inches) of 20-35. One hundred and sixty eight consecutive patients (Male 133 (79%): female 35 (21%), mean BMI 29±5 and mean heart rate 58± bpm) underwent coronary calcium scoring with prospective gating. Beta blockers were given to patients in case HR > 65 bpm (Table 1).

MDCT Technique

Aquilion ONE is a cone beam MDCT with 320 rows of 0.5 mm detector array capable of covering 160 mm of anatomy in the z-direction in one rotation without table movement. However, Aquilion ONE has two operating modes, the 64-row, and the 320-row modes. Under the 64-row mode, Aquilion ONE functions just like another 64 MDCT scanner in which both axial scans and helical scans are available with a maximum beam width (BW) of (64 × 0.5 mm = 32 mm).

The 320-row mode, at present, functions primarily as a cardiac scanner (volume scan mode). Under the volume scan mode, the unit acts as an axial scanner and can cover up to 160 mm per rotation. For cardiac scanning the BW coverage is usually 120, 140 or 160mm depending on the length of the heart. The tabletop translation movement is disabled via software control during image acquisition under the volume scan mode and the data set is acquired in one 360-degree rotation and image is reconstructed from 180 degrees using the remaining 180 degrees for cone beam correction.

The scan parameters during CACS measurement were 300 mA, 120 kVp, volume scan length (VSL) 160mm, gantry rotation 0.350 msec and 320 x 0.5mm detectors at 320 MDCT (Table 2).

TABLE 1: Summary of patient's characteristics

Patient's Characteristics	Values
Total subjects (n)	168
Mean Age (SD) years	61±10
Male: Female	133:35
Mean BMI (SD)	29±4
Current Smoker No/total (%)	13/168 (7.7%)
Past smoker No/total (%)	74/168 (44%)
Hypertension No/total (%)	112/168 (66.6%)
Hyperlipedemia No/total (%)	121/168 (72%)
Diabetes No/total (%)	23/168 (13.7%)
Family H/O of CAD (%)	113/168 (67.2%)
H/O CAD (%)	91/168 (54.1%)
H/O of MI (%)	55/168 (32.7%)

Abbreviations: SD = Standard Deviation; No = Number; H/O = History of; CAD = Coronary Artery Disease; MI = Myocardial Infarction

TABLE 2: Scanning parameters and radiation dose for Coronary artery calcium score at 320 MDCTA

Scanning parameters & Radiation	Values
Typical collimation	(64 x 5) x 0.5 mm (160mm)
Rotation time	350 sec
Tube voltage	120 kVp
Tube current-time product	300 mA
Scan length (mm)	160 mm
Mean radiation dose (SD)	1.89 (0.79)

Abbreviations: SD = Standard Deviation

Radiation Dose measurement

Radiation dose is calculated from the parameters included the volume CT dose index (CTDI vol) and dose length product (DLP). The CTDI value can be calculated as a mathematical integral under the radiation dose profile of a single rotation scan that would produce one tomographic image at a fixed table position. CTDI vol is the average radiation dose over a specific investigated volume. The dose length product (DLP) can be calculated by multiplying CTDI vol with re-

 ISSN 2330-4049

spective scan length. DLP shows the radiation a patient is exposed to by the entire CT. This was the primary parameter in our study (Table 2).

CT dose index volume (CTDI vol) and dose length product (DLP) were recorded as direct data output from prospective ECG gated examinations. Scanner provided a protocol summary containing dose-length product for each image series. The effective radiation dose was derived from the summed dose-length product multiplied by the European working group for guidelines on Quality criteria in computed tomography conversion coefficient (k = 0.014 mSv/mGy x cm).

Statistical Analysis

The statistical software packages used for data analysis were Stata\MP 10.0 (Stata, college station, Tex).

Results

The mean ± SD radiation was 1.89 ± 0.79 mSv. Overall the range varied from 0.28-2.48 mSv. The radiation was significantly less in females as compared to males (2.02 ± 0.73 vs. 1.41 ± 0.87, p < 0.0001). No differences were noted whether HR was <60 vs. >=60 bpm (1.87 ± 0.79 vs. 1.77 ± 0.84 mSv, p = 0.45). On the other hand a higher radiation was noted among obese individuals as compared to those with BMI<30 (1.84 ± 0.82 vs. 1.91 ± 0.80 mSv, p = 0.62) (Figure 1).

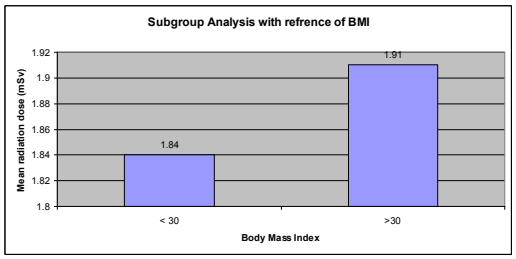

FIG. 1: Subgroup analysis of radiation dose with reference of BMI for patients that underwent Coronary calcium score with 320 MDCTA.

Discussion

CAC scoring being a screening tool requires the use of low radiation techniques in order to outweigh the potential risks associated with the examination. A major disadvantage is the radiation exposure with the use of Computed Tomography (CT) and radiation dose has been the single most significant concern in the context of widespread clinical applications of CCTA. Medical radiation exposure has risen more than 700% between 1980 and 2006, largely contributing to increased public awareness of medical radiation burden.[18] As a reference for radiation exposure it should be noted that annually background accounts for 82 %, and man made for 18 % of the total radiation exposure to the general population. Amongst medical x-rays such as diagnostic studies, computed tomography of the chest, abdomen and pelvis accounts for 58 %, nuclear medicine studies for 21 %, and consumer products for 18 % of all man made exposure. CCTA contributes about 1.5 % to the overall CT dose.[18] Emergence of the 320 row detector CT scanner allows for even faster image acquisition for CCTA which will likely further increase the use of CCTA and be associated with a corresponding rise in radiation exposure to the public in the future.[18] Calcium scoring is usually routinely performed in addition to contrast enhanced MDCTA with single rotations and prospective gating. Our measurements for the calcium score protocol at 120 kVp compare favorably to those of prior investigations using prospective gating.[16, 19] Our data along with those of others also indicate that occurrence of deterministic skin effects secondary to MDCTA with the dual source and 320-detector row scanner is fundamentally inconceivable, even in the setting of performance of multiple studies in a short time span in the same individual as deterministic effects have a threshold between 2,000 and 20,000 mGy, depending on the severity.[17]

It is believed that transient erythema, the earliest radiation effect, is unlikely to occur with radiation doses of less than 4000–5000 mGy.[17, 20] Rutten *et al.* reported 2.6 mSv ED for CAC scoring with retrospectively gated 64 MDCTA but after application of maximum dose in a single phase of R-R interval and at heart rate < 60 bpm , ED was reduced from 2.6 to 1.6 mSv.[21] While at prospectively gated 64 MDCT using step and shoot method, Malago R et al. and Husmann L. et al documented the ED of 1.547 and 1.1 mSv respectively for CAC scoring.[22, 23] Mahnken *et al.* obtained a mean ED of 4.44 mSv (3.28-588) and 3.01 mSv (2.52-4.18) for women and men with BMI > 26 respectively using a four channel MDCT scanner but in comparison radiation was reduced by 11.6% for men and 24.8% for women using body weight–adapted tube current settings in case of patients with BMI below 25.[24] While Hunold *et al.* compared the ED for electron beam and four-detector MDCT using anthropomorphic phantom. ED using electron beam CT were 1.0 and 1.3 mSv for male and female respectively while ED were 1.5-5.2 mSv and 1.8-6.2 mSv for male and female respectively at 4 rows MDCT.[25]

We must acknowledge several limitations of our study. First, it was a retrospective review of medical records and study design was not prospective. For the retrospective study design, we reduced the bias by selecting consecutive patients. We did not assess the factors affecting the diagnostic quality of these examinations, however, the goal of this study was to assess radiation dose associated with CAC if this were to be incorporated as a screening tool to reclassify risk in patients at intermediate risk based on traditional scores such as the Framingham and Procam Algorithms.[9]

 ISSN 2330-4049

Conclusion

The 320-slice MDCT is a robust potential diagnostic tool for non-invasive coronary artery assessment with novel single rotation acquisition capabilities with single cardiac cycle. Dose optimization remains an exceedingly significant concern. Radiation dose obtained from 320-MDCT for measuring CAC is similar to those obtained with 4-64 row MDCT. Prospective studies are needed to assess the feasibility of further lowering the tube current, tube voltage, and optimizing the volume scan length to minimize radiation doses.

Conflict of interest

The authors declare that they have no conflicts of interest. The authors alone are responsible for the content and writing of the paper.

References

1. Schmermund A, Mohlenkamp S, Erbel R. Coronary artery calcium and its relationship to coronary artery disease. *Cardiol Clin* 2003; **21**:521-534.
2. Frink RJ, Achor RW, Brown AL, Jr., Kincaid OW, Brandenburg RO. Significance of calcification of the coronary arteries. *Am J Cardiol* 1970; **26**:241-247.
3. Guerci AD, Spadaro LA, Goodman KJ, Lledo-Perez A, Newstein D, Lerner G, et al. Comparison of electron beam computed tomography scanning and conventional risk factor assessment for the prediction of angiographic coronary artery disease. *J Am Coll Cardiol* 1998; **32**:673-679.
4. Janssen CH, Kuijpers D, Vliegenthart R, Overbosch J, van Dijkman PR, Zijlstra F, et al. Coronary artery calcification score by multislice computed tomography predicts the outcome of dobutamine cardiovascular magnetic resonance imaging. *Eur Radiol* 2005; **15**:1128-1134.
5. Becker CR, Majeed A, Crispin A, Knez A, Schoepf UJ, Boekstegers P, et al. CT measurement of coronary calcium mass: impact on global cardiac risk assessment. *Eur Radiol* 2005; **15:96**-101.
6. Haberl R, Becker A, Leber A, Knez A, Becker C, Lang C, et al. Correlation of coronary calcification and angiographically documented stenoses in patients with suspected coronary artery disease: results of 1,764 patients. *J Am Coll Cardiol* 2001; **37**:451-457.
7. Sarwar A, Shaw LJ, Shapiro MD, Blankstein R, Hoffman U, Cury RC, et al. Diagnostic and prognostic value of absence of coronary artery calcification. *JACC Cardiovasc Imaging* 2009; **2**:675-688.
8. Budoff MJ, Shaw LJ, Liu ST, Weinstein SR, Mosler TP, Tseng PH, et al. Long-term prognosis associated with coronary calcification: observations from a registry of 25,253 patients. *J Am Coll Cardiol* 2007; **49**:1860-1870.
9. Budoff MJ, Achenbach S, Blumenthal RS, Carr JJ, Goldin JG, Greenland P, et al. Assessment of coronary artery disease by cardiac computed tomography: a scientific statement from the American Heart Association Committee on Cardiovascular Imaging and Intervention, Council on Cardiovascular Radiology and Intervention, and Committee on Cardiac Imaging, Council on Clinical Cardiology. *Circulation* 2006; **114**:1761-1791.
10. Agatston AS, Janowitz WR, Hildner FJ, Zusmer NR, Viamonte M, Jr., Detrano R. Quantification of coronary artery calcium using ultrafast computed tomography. J Am Coll Cardiol 1990;**15**:827-832.
11. Arad Y, Spadaro LA, Goodman K, Newstein D, Guerci AD. Prediction of coronary events with electron beam computed tomography. *J Am Coll Cardiol* 2000; **36**:1253-1260.
12. Shaw LJ, Raggi P, Schisterman E, Berman DS, Callister TQ. Prognostic value of cardiac risk factors and coronary artery calcium screening for all-cause mortality. *Radiology* 2003; **228**:826-833.
13. Becker CR, Kleffel T, Crispin A, Knez A, Young J, Schoepf UJ, et al. Coronary artery calcium measurement: agreement of multirow detector and electron beam CT. *AJR Am J Roentgenol* 2001; **176**:1295-1298.
14. Becker CR, Jakobs TF, Aydemir S, Becker A, Knez A, Schoepf UJ, et al. Helical and single-slice conventional CT versus electron beam CT for the quantification of coronary artery calcification. *AJR Am J Roentgenol* 2000; **174**:543-547.
15. Kopp AF, Ohnesorge B, Becker C, Schroder S, Heuschmid M, Kuttner A, et al. Reproducibility and accuracy of coronary calcium measurements with multi-detector row versus electron-beam CT. *Radiology* 2002; **225**:113-119.
16. Ulzheimer S, Kalender WA. Assessment of calcium scoring performance in cardiac computed tomography. *Eur Radiol* 2003; **13**:484-497.
17. Stanford W, Thompson BH, Burns TL, Heery SD, Burr MC. Coronary artery calcium quantification at multi-detector row helical CT versus electron-beam CT. *Radiology* 2004; **230**:397-402.
18. Gerber TC, Carr JJ, Arai AE, Dixon RL, Ferrari VA, Gomes AS, et al. Ionizing radiation in cardiac imaging: a science advisory from the American Heart Association Committee on Cardiac Imaging of the Council on Clinical Cardiology and Committee on Cardiovascular Imaging and Intervention of the Council on Cardiovascular Radiology and Intervention. *Circulation* 2009; **119**:1056-1065.

 ISSN 2330-4049

19. Kim SM, Chung MJ, Lee KS, Choe YH, Yi CA, Choe BK. Coronary calcium screening using low-dose lung cancer screening: effectiveness of MDCT with retrospective reconstruction. *AJR Am J Roentgenol* 2008; **190**:917-922.
20. Wagner LK, Eifel PJ, Geise RA. Potential biological effects following high X-ray dose interventional procedures. *J Vasc Interv Radiol* 1994; **5**:71-84.
21. Rutten A, Krul SP, Meijs MF, de Vos AM, Cramer MJ, Prokop M. Variability of coronary calcium scores throughout the cardiac cycle: implications for the appropriate use of electrocardiogram-dose modulation with retrospectively gated computed tomography. *Invest Radiol* 2008; **43**:187-194.
22. Malago R, D'Onofrio M, Baglio I, Brunelli S, Tavella D, Beltrame F, et al. Choice strategy of different dose-saving protocols in 64-slice MDCT coronary angiography. *Radiol Med* 2009; **114**:1196-1213.
23. Husmann L, Herzog BA, Burger IA, Buechel RR, Pazhenkottil AP, von Schulthess P, et al. Usefulness of additional coronary calcium scoring in low-dose CT coronary angiography with prospective ECG-triggering impact on total effective radiation dose and diagnostic accuracy. *Acad Radiol* 2010; **17**:201-206.
24. Mahnken AH, Wildberger JE, Simon J, Koos R, Flohr TG, Schaller S, et al. Detection of coronary calcifications: feasibility of dose reduction with a body weight-adapted examination protocol. *AJR Am J Roentgenol* 2003; **181**:533-538.
25. Hunold P, Vogt FM, Schmermund A, Debatin JF, Kerkhoff G, Budde T, et al. Radiation exposure during cardiac CT: effective doses at multi-detector row CT and electron-beam CT. *Radiology* 2003; **226**:145-152.

 ISSN 2330-4049

International Journal of Cancer Therapy and Oncology
www.ijcto.org

Assessment of pulmonary toxicities in breast cancer patients undergoing treatment with anthracycline and taxane based chemotherapy and radiotherapy- a prospective study

Aramita Saha[1], Subrata Chattopadhyay[2]

[1]*Department of Medical Oncology, Apollo Gleangles Cancer Hospital, Kolkata, India.*
[2]*Department of Radiation Oncology, Medical College, Kolkata, India.*

Received October 02, 2013; Revised October 27, 2013; Accepted October 27, 2013; Published Online November 22, 2013

Original Article

Abstract

Background: Anthracycline based regiments and/or taxanes and adjuvant radiotherapy; the main modalities of treatment for breast cancers are associated with deterioration of pulmonary functions and progressive pulmonary toxicities. **Aim**: Assessment of pulmonary toxicities and impact on pulmonary functions mainly in terms of decline of forced vital capacity (FVC) and the ratio of forced expiratory volume (FEV) in 1 Second and FEV1/FVC ratio with different treatment times and follow ups in carcinoma breast patients receiving anthracycline and/or taxane based chemotherapy and radiotherapy. **Materials and methods**: A prospective single institutional cohort study was performed with 58 breast cancer patients between January 2011 to July 2012 who received either anthracycline based (37 patients received 6 cycles FAC= 5 FU, Adriamycin, Cyclophosphamide regime) and radiotherapy or anthracycline and taxane based chemotherapy (21 patients received 4cycles AC= Adriamycin, Cyclophosphamide; followed by 4 cycles of T=Taxane) and radiotherapy. Assessment of pulmonary symptoms and signs, chest x-ray and pulmonary function tests were performed at baseline, midcycle, at end of chemotherapy, at end radiotherapy, at 1 and 6 months follow ups and compared. By means of a two-way analysis of variance (ANOVA) model, the course of lung parameters across the time points was compared. **Results and Conclusion**: Analysis of mean forced vital capacities at different points of study times showed definitive declining pattern, which is at statistically significant level at the end of 6th month of follow up (p=0.032) .The FEV1/FVC ratio (in percentage) also revealed a definite decreasing pattern over different treatment times and at statistically significant level at 6th month follow up with p value 0.003. Separate analysis of mean FEV1/FVC ratios over time in anthracycline based chemotherapy and radiotherapy group as well as anthracycline and taxane based chemotherapy and radiotherapy group showed a similar declining pattern.

Keywords: Anthracycline, Taxane, Radiotherapy, Pulmonary, FEV1/FVC

Introduction

Breast cancer is the leading cause of cancer death among women around the world.[1] It accounts for 26% of all malignancies in women and second most common cause of cancer death in women.[2] In India it shows mixed incidence pattern with breast cancer being second to cancer of the cervix in rural areas[1, 2]; however, in metropolitan cities the incidence of breast cancer has crossed that of cervix.[2] Mathematical models suggest that both the adoption of screening mammography and the availability of adjuvant chemotherapy, radiotherapy and tamoxifen have contributed approximately equally to the improvement of breast cancer outcomes.[3]

Adjuvant chemotherapy reduces local recurrence after radiation therapy in breast cancer. Anthracycline (doxorubicin)-based regimens (± taxanes for high-risk disease) have been associated with superior outcomes as compared to nonanthracycline containing regimens. Recent evidence suggests that disease free survival (DFS) and overall survival (OS) of breast cancers has been increased with taxane-based therapy as compared to anthracycline-based therapy. Neoadjuvant chemotherapy is considered standard of care in

Corresponding author: Aramita Saha; Department of Medical Oncology, Gleangles Cancer Hospital, Kolkata, India.
Email: docaramita@gmail.com

Cite this article as:
Saha A, Chattopadhyay S. Assessment of pulmonary toxicities in breast cancer patients undergoing treatment with anthracycline and taxane based chemotherapy and radiotherapy- a prospective study. Int J Cancer Ther Oncol 2013; **1**(2):01021.
DOI: 10.14319/ijcto.0102.1

ISSN 2330-4049

high-risk populations such as young patients and/or advanced stage disease, and has been evaluated in Stage II–IIIa breast cancer in randomized trials.[3, 4]

Paclitaxel (Taxol) is one of the most potent chemotherapeutic agents in the treatment of breast cancers has experienced widespread use over the past 5 years. . A limited number of case reports are available concluding that Taxol is associated with respiratory symptoms, including dyspnea, cough, wheezing and chest tightness.[5] Interstitial and reticulonodular infiltrates have been described on chest radiographic examination in few studies with paclitaxel in breast cancers.[6] Cases of transient pulmonary infiltrates and suspected interstitial pneumonitis have been reported, although the true incidence of lung toxicity that is directly related to paclitaxel is not well understood. A prospective study of lung function in 33 patients who received paclitaxel with carboplatin (an agent with little evidence for direct lung toxicity) for nonthoracic malignancy revealed an isolated decrease in diffusing capacity without other clinical or radiographic evidence of pulmonary toxicity .[7] Clinicians should be aware of the potential for paclitaxel to impair pulmonary function.

Randomized trials have found that addition of adjuvant therapy with taxane to an anthracycline-based chemotherapy regimen, compared with anthracycline-based chemotherapy alone, led to improved survival for high grade breast cancer patients.[8, 9] Irradiation is also an important adjuvant therapy for breast cancer. Specifically, adjuvant radiation therapy for selected patients with breast cancer reduces locoregional recurrence and improves overall survival.[10, 11]
One serious potential risk of radiation therapy for breast cancer is symptomatic radiation pneumonitis. Fortunately, with modern irradiation techniques, the risk of radiation pneumonitis is low (5%), and its course is usually self-limited .[12] However, the risk of radiation pneumonitis has recently become a greater clinical concern because of reports suggesting that this risk may increase in patients who receive taxanes.

It is well known that post-operative adjuvant loco-regional radiotherapy in breast cancer is associated with pulmonary complications. The frequency and grade of pulmonary complications following radiotherapy for breast cancer are, however, still debated. Few investigators have quantified this problem by using objective methods such as pulmonary function tests (PFTs).[13, 14] The PFTs have the advantage of being widely available and reproducible methods for detecting parenchymal lung damage, if they are performed under strict standardized conditions.[15] We performed a prospective study from January 2011 to August 2012 for pulmonary status and pulmonary toxicities assessment on 58 Breast cancer patients attended and registered Radiotherapy department of Medical College, Kolkata, who received either anthracycline based and/or taxane based chemotherapy followed by radiotherapy .The effects of anthracycline and taxane based chemotherapy and radiotherapy on pulmonary functions were assessed and variation of pulmonary toxicities with different treatment times and follow up were analysed.

Methods and Materials

The lung is one of the major dose-limiting organs for radiotherapy within the thorax. Therefore, the total dose that can safely be delivered to patients with malignant tumors like carcinoma breast has to be limited because of the risk of radiation pneumonitis (developing 1 to 6 months after treatment) and radiation fibrosis (developing from 6 months onward). Chemotherapy (regardless of the type of drug) primarily affected the diffusion capacity. So the aim of our study was to analyze whether and how much the course in pulmonary function changes over time, forced vital capacity [FVC], ratio of forced expiratory volume in 1second [FEV1/FVC ratio] varied between the different treatment regimens and whether recovery of early pulmonary damage occurred or not. In general, when chemotherapy and radiotherapy are combined, two different effects may occur as an interaction between both modalities, resulting in an enhancement of radiation-induced damage or an additional effect.

Study Area: Department of Radiotherapy, Medical College and Hospitals, Kolkata.

Study Population: All biopsy proven cases of left sided female carcinoma breast attending the Radiotherapy Out Patients' Department and conforming to inclusion /exclusion criteria mentioned herein.

Study Period: Case accrual started from January 2011 and it was divided into preparatory phase, data collection phase data compilation phase, data analysis phase and preparation phase.

Sample Size: 60 patients

Sample Design: All the population with carcinoma breast (female) who conform to the inclusion / exclusion criteria mentioned herein and gave consent to be included in the study.

Inclusion Criteria:

- Female carcinoma breast patients.
- Age above 20 years and below 70 years.
- Those who are eligible to receive anthracycline and/or taxane based chemotherapy and external beam radiotherapy.
- Stage II and onwards (American Joint Committee on Cancer Stage Grouping).
- Karnofsky performance status >70.

 ISSN 2330-4049

- Baseline normal hematological, renal and hepatic profile.
- Baseline normal cardiac and pulmonary function status.
- Informed Consent to participate in this study.

Exclusion Criteria:

- Male carcinoma breast patients.
- Patients undergoing breast conservation surgery.
- Pregnant and lactating patients.
- Any evidence of Metastasis at presentation.
- Previous history of any malignancy.
- Previously received / currently receiving chemotherapy / radiotherapy.
- Not enrolled in any other study on Breast cancer.

Study Design: Prospective observational single-Institutional trial.

Parameters studied

- History.
- Detailed physical examination.
- Pulmonary function test (FEV1, FVC, FEV1/FVC ratio and VC)
- Chest X Ray (PA and lateral view).

Study Techniques: All biopsy proven cases of left sided carcinoma breast attending the OPD of Radiotherapy, Medical College Hospitals, Kolkata, satisfying the specified Inclusion and Exclusion Criteria who are willing to participate in the study were included.

Patients were treated with Anthracycline and / or Taxane based chemotherapy in the Neo-Adjuvant or Adjuvant setting in combination with Modified Radical Mastectomy (Timing of surgery depending on operability). In addition all patients will receive adjuvant External Beam Radiotherapy (Dose, Portals etc depending on stage and tumour features). Hormone receptor positive patients will receive adjuvant Endocrine therapy for a minimum duration of five years.

All patients were subjected to chest X-ray and Pulmonary function tests (Clinical assessment, Chest X ray, FEV1, FVC, FEV1/FVC) at baseline, during and at the end of chemotherapy, at the end of radiation and during first month and sixth month follow up.Mid cycle chemotherapy means after completion of 3rd cycle of chemotherapy in FAC group and after completion of 4th cycle of chemotherapy in Anthracycline, Cyclophosphamide (AC) followed by Taxane (T group).

Statistical analysis:

Quantitative variables were compared between two groups using an unpaired t test for normally distributed variables or Wilcoxon two sample tests for skewed distributed variables. Normally distributed variables are reported as mean, standard deviation, and variance. Skewed distributed variables are reported as median and range (minimum to maximum).

By means of a two-way ANOVA model, the course of lung parameters (decline of pulmonary function tests) across the time points was compared between patients. Correlations between variables were calculated using Pearson's or Spearman correlation coefficient test as appropriate. All P values were two-sided and $P < 0.05$ was considered statistically significant. Medcalc and Vassarstats were used to perform the statistical analysis.

Results

Case Accrual

Initially, 60 patients were selected for accrual. Of these, after careful scrutiny towards meeting of inclusion and exclusion criteria, 58 breast cancer patients were actually found suitable. All patients under study had left sided breast cancer. However, 4 patients were expired during and at the end of chemotherapy and were consequently excluded from the study. Ultimately 54 patients underwent the study till end.

Baseline Patient Characteristics

TABLE 1: Baseline age distribution of the study population

Age Groups	No of Patients	Percentage (%)
20-32 years	9	15.52
33-45 years	18	31.03
46-58 years	23	39.65
>58 years	8	13.79

The baseline age distributions of patients under are depicted in Table 1. The Mean age is 51.5 yrs. Inclusion criteria of our study was lump size more than 5cm and / or node positive disease. All N0 patients must have T3 (tumour>5cm) according to our study inclusion criteria otherwise node positive.

All the patients in the study population received anthracycline and/or taxane based chemotherapy and post chemotherapy radiation of chest flap alone or in combination with supraclavicular field radiotherapy or chest flap+supraclavicular field +axillary field radiation. All patients have undergone mastectomy as the very first treatment or initially received 2-3 cycles of neoadjuvant chemotherapy, downstaged and then undergone mastectomy; after that completed chemotherapy. After completion of chemotherapy they received radiation .At the end of chemotherapy the study population came down to 54.Two patients died after 4 cycles,1 patient after 5th cycle of chemotherapy and 1 patient after 2nd cycle of chemotherapy. So, 54 patients have undergone radiotherapy.
Among the 58 patients, 37 patients (63.79%) received only

 ISSN 2330-4049

anthracycline based (doxorubicin) chemotherapy and 21 patients (36.2%) received both anthracycline and taxane both based chemotherapy. Moreover, majority of the patients belonged to poor socio-economic status; received doxorubicin, which is supplied free of cost from government fund in our ward. So we have chosen doxorubicin not epirubicin as anthracycline regime. For those 37 patients who received only anthracycline based chemotherapy, the regime chosen was 6cycles of FAC every 21days(Inj 5FU 500mg/m2 iv D1;Inj Doxorubicin 50mg/m2 iv D1; Inj Cyclophosphamide 500mg/m2 iv D1).Rest 21 patients received both anthracycline and taxane based chemotherapy with 4 cycles of AC followed by 4 cycles of T(Inj Doxorubicin 60mg/m2 iv D1,Inj Cyclophosphamide 600mg/m2 iv D1 every 21 days 4 cycles followed by Paclitaxel 175 mg/m2 iv D1 every 21days 4 cycles. Among 58 patients, 42 patients received neoadjuvant chemotherapy 2-3 cycles, thereafter achieved complete or partial response, undergone MRM and axillary clearance, thereafter completed remaining cycles of chemotherapy. Remaining 16 patients have undergone MRM with axillary clearance first, thereafter received adjuvant chemotherapy.54 patients have undergone radiotherapy after completion of chemotherapy.

Evaluation of pulmonary toxicities following chemotherapy and radiotherapy in breast cancer patients

The baseline pulmonary function tests and chest x-ray including clinical features were within normal limits in all patients of the study population.

Assessment of respiratory symptoms: Cough and respiratory distress were considered as respiratory symptoms.

a) Respiratory distress: Total seven patients, three in the anthracycline based CT+RTgroup (one during third cycle of chemotherapy, two during first cycle of chemotherapy) complained of respiratory distress. Two patients in the anthracycline and taxane based CT+RT group developed respiratory distress during first cycle of chemotherapy; two patients during radiotherapy.1 patient during 1month follow up and 3 patients in 6th month of follow up complained of moderate respiratory distress. From symptoms only we couldn't distinguish that whether the distress was due to cardiological or pulmonary damage .Patients were urgently sent for immediate cardiological evaluation -and chest x-ray. None revealed any significant cardiological abnormality. The patient who developed respiratory distress during 1 month follow up revealed bilateral lung metastasis in chest x-ray and among those 3 who developed distress at 6th month follow up; 1 revealed lung metastasis and 2 showed overt features of radiation pneumonitis in chest x-ray. So, only 2 patients (3.44%) of the entire study group revealed radiation pneumonitis at 6th month of follow up.

b) Cough: Total 9 patients in the entire study group developed cough. Two during 3rd cycle chemotherapy, three during 1 month follow up and four during 6th month of follow ups. Investigations revealed lung metastasis in total 2 patients and 2 patients developed radiation pneumonitis.

Evaluation of respiratory signs: None of the patients revealed any overt respiratory signs.

Evaluation of pulmonary toxicities by study tools: All the patients have undergone chest x ray and pulmonary function tests(FVC and FEV1/FVC ratio) at baseline ,at mid cycle chemotherapy, at the end of chemotherapy,at completion of radiotherapy, at 1moth and 6th month of follow ups.

Interpretation of chest x-ray: Two patients in the entire study group revealed features of lung metastases in chest x-ray, one at 1st month of follow up and one at 6th month of follow up. Only 2 patients (3.44%) in the entire study group developed features of radiation pneumonitis on chest x-ray at 6th month of follow up. Both the patients received anthracycline and taxane based chemotherapy and radiotherapy.

Interpretation of pulmonary function tests:

TABLE 2: Variation of mean FEV1/FVC ratios (%) at different points of time and follow ups.

	Mean	Median	SD	Variance (SD)	Population (SD)
Baseline FEV1/FVC (N=58)	79.17 (0.791)	78.9 (0.789)	9.24	10.05	1.14
Mid cycle CT FEV1/FVC (N=58)	78.19 (0.781)	77.9 (0.779)	6.87	5.82	1.38
End CT FEV1/FVC N=54)	76.15 (0.761)	75.2 (0.752)	1.94	3.78	1.96
End RT FEV1/FVC (N=54)	74.24 (0.742)	74.56 (0.745)	2.32	5.4	2.3
1 month FU FEV1/FVC (N=52)	72.59 (0.725)	72.2 (0.722)	2.45	6.7	2.42
6 months FU FEV1/FVC (N=50)	69.52 (0.695)	69.075 (0.69)	2.74	74	7.20

Analysis of mean forced vital capacities at different points of study time (baseline, mid cycle chemotherapy, end of chemotherapy, end of radiotherapy, 1 month and 6 months follow ups showed definitive declining pattern, which is at statistically significant level at the end of 6 th month of follow up ($p=0.032$) in the entire study population (Table 2, Table 3, and **Figure 1**).

 ISSN 2330-4049

TABLE 3: Variation of means of FVCs (forced vitals capacities in liters) over different treatment times:

	Mean FVCs	P-value
Baseline	2.84	--
MID CT	2.69	0.99
END CT	2.54	0.867
END RT	2.19	0.740
1month follow up	2.06	0.632
6 month follow up	1.81	0.032

P values were compared to baseline; P < 0.05 "means statistically significant"

TABLE 4: Comparison of mean FEV1/FVC ratios with baseline at different times of study time

Different points of study time	P-value
Baseline and mid cycle chemotherapy	0.98
Baseline and end of chemotherapy	0.76
Baseline and end of radiotherapy	0.71
Baseline and 1 month follow up	0.068
Baseline and 6 months follow up	0.003

P values of mean FEV1/FVC ratio as compared to baseline; P < 0.05 "means statistically significant"

TABLE 5: Variation of mean FEV1/FVC ratios (%) s at different points of time and follow up period in anthracycline based chemotherapy and radiotherapy group

	Mean	Median	SD	Variance (SD)	Population (SD)
Baseline FEV1/FVC (N=37)	79.82(0.798)	79.2(0.792)	1.32	1.75	1.3
Mid cycle CT FEV1/FVC (N=37)	78.36(0.736)	77.8(0.778)	1.97	2.1	1.48
End CT FEV1/FVC (N=34)	76.59(0.765)	76.5(0.765)	2.06	4.02	1.97
End RT FEV1/FVC (N=34)	75.05(0.75)	75.45(0.754)	2.23	5.01	2.02
1 month FU FEV1/FVC (N=33)	73.45(0.734)	73.5(0.735)	2.4	5.77	2.36
6 months FU FEV1/FVC (N=31)	69.9(0.699)	69.5(0.695)	3.2	10.24	3.14

Abbreviations: CT = Chemotherapy; FU = Follow up

TABLE 6: Variation of mean FEV1/FVC ratios with baseline at different times of study time of the study group received anthracycline+ taxane based CT+RT group

	Mean	Median	SD	Variance (SD)	Population (SD)
Baseline FEV1/FVC (N=21)	78.92 (0.789)	78.7 (0.787)	3.46	8.48	6.45
Mid cycle CT FEV1/FVC (N=21)	77.86 (0.778)	77.6 (O.776)	1.93	6.7	5.98
End CT FEV1/FVC (N=20)	75.4 (0.754)	75.2 (0.752)	1.61	2.61	1.57
End RT FEV1/FVC (N=20)	72.85 (O.728)	72.5 (0.725)	1.78	3.17	1.73
1 month FU FEV1/FVC (N=19)	71.09 (0.719)	72.01 (0.721)	1.74	3.03	1.69
6 months FU FEV1/FVC(N=19)	68.79 (0.687)	68.45 (0.684)	1.6	2.56	1.55

Abbreviations: CT = Chemotherapy; FU = Follow up; RT = Radiation therapy

ISSN 2330-4049

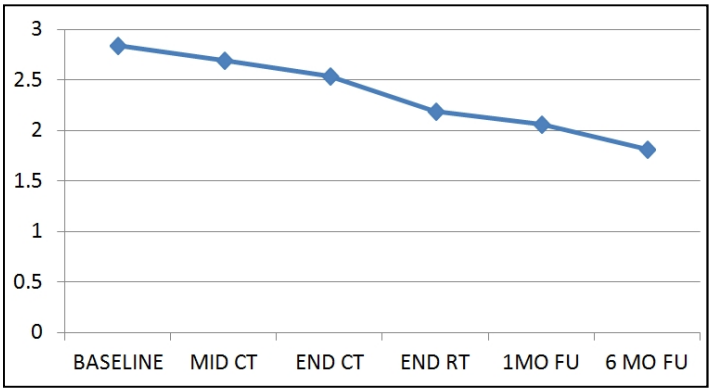

FIG. 1: Graphical representation of variations of mean forced vital capacities (FVC) over different treatment times and follow ups
Y –axis represents Mean FVC s over time
Abbreviations: CT = Chemotherapy, RT= Radiotherapy, FU= Follow up, FAC=5 Fluorouracil, Adriamycin, Cyclophosthamide, AC= Adriamycin, Cyclophosphamide, T = Taxane

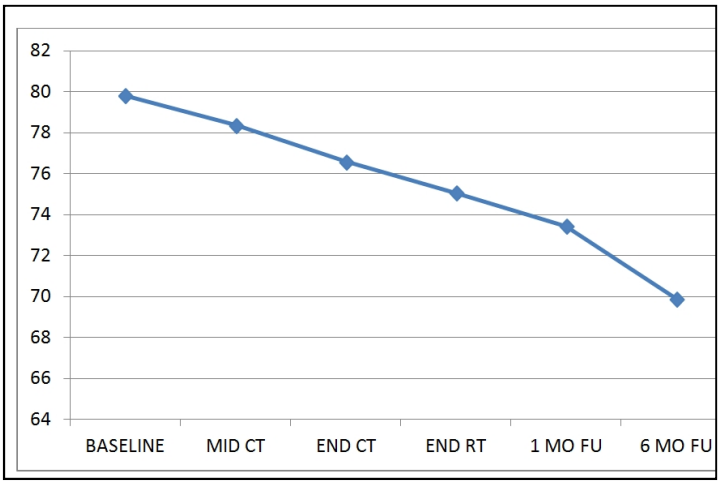

FIG. 2: Graphical representation of pattern of decline of FEV1/FVC ratio in the entire study group.
Y –axis represents FEV1/FVC ratios
Abbreviations: CT = Chemotherapy, RT= Radiotherapy, FU= Follow up, FAC=5 Fluorouracil, Adriamycin, Cyclophosthamide, AC= Adriamycin, Cyclophosphamide, T = Taxane

TABLE 7: Comparison of mean FEV1/FVC ratios (%) at different points of time and follow up period in the anthracycline based CT+RT group

Different points of study time	P values of mean FEV1/FVC ratio as compared with baseline	
	Anthracycline based CT+RT	A+T based CT+RT
Baseline and mid cycle chemotherapy	0.97	0.89
Baseline and end of chemotherapy	0.78	0.72
Baseline and end of radiotherapy	0.73	0.69
Baseline and 1 month follow up	0.087	0.08
Baseline and 6 months follow up	0.02	0.001

P < 0.05 "means statistically significant"

The FEV1/FVC ratio(in percentage) also revealed a definite decreasing pattern over different treatment time in the entire study group as evidenced from **Table 4** and **Figure 2**,which declines at statistically significant level as compared to baseline at 6th month follow up with p value 0.003 (**Table 4**). Separate analysis of mean FEV1/FVC ratios over time in anthracycline based chemotherapy and radiotherapy group (Table 5) as well as anthracycline and taxane based chemotherapy and radiotherapy group (Table 6) showed a similar declining pattern, which are statistically significant at 6 months follow up as compared to baseline in both the groups with p values 0.02 and 0.001 respectively (**Table 7**).

 ISSN 2330-4049

Discussion

Regarding pulmonary toxicities following treatment with chemotherapy and adjuvant radiotherapy in breast cancer patients several studies showed definitive influence of treatment on pulmonary function tests.

Tse-Kuan Yu et al.[16] in a phase 3 randomized study have shown that Patients with breast cancer treated with sequential paclitaxel, FAC, and radiation therapy appeared to have a very low rate of clinically relevant radiation pneumonitis that was no different from that of patients treated with FAC alone. But there was significant decrease in DLCO (diffusion capacity of lung for carbon monoxide) at long term (1 year) follow up.

Another study[12] have demonstrated that loco-regional radiotherapy in breast cancer results in reductions of DLCO, VC, FEV1 and RV. The slight reduction of FEV1 was completely explained by the decrease in VC, as the relation between FEV1 and VC was unchanged. Thus, no sign of obstructive disease was found. We suggest that the reduction of VC reflects decreased parenchymal elasticity in the irradiated part of the lung. The somewhat larger decrease in DLCO may also indicate an inflammatory reaction in the interstitial tissues.

In 1992, Marks et al.[17] reported severe pulmonary complications in 10% of the patients receiving loco-regional radiotherapy following high-dose chemotherapy (including carmustine) resulting in premature discontinuation of their radiotherapy. Dose-intensified chemotherapy (FEC-based) and loco-regional radiotherapy were not associated with increased pulmonary toxicity in our material and no course of radiotherapy treatment was prematurely discontinued. Gage et al.[18] have reported similar results to ours using the CTC high-dose chemotherapy. Thus, the results of Marks et al.[17] may have been influenced by delayed carmustine-induced pulmonary toxicity.

In our study, the breast cancer patients received either 6 cycles of FAC chemotherapy followed by adjuvant radiotherapy or 4 cycles of AC followed by taxane and adjuvant radiotherapy. Among total 58 study population only 2 patients developed overt radiological feature of radiation pneumonitis at 6 months follow up, definitive deterioration of pulmonary function tests were observed. Both the FVC (Forced vital capacity) and FEV1/FVC ratio have shown definitive declining trend with chemotherapy and radiotherapy and mean of those decreased to statistically significant level at 6th month of follow up. FEV1/FVC ratio decreased below 70% in about 67% patients at 6 months follow up. Separate analysis of PFTs in two different chemotherapy groups has shown similar changes.

Breast cancer treated with taxane and anthracycline-based chemotherapy regimens followed by radiation though did not develop overt radiation pneumonitis at significant levels, but declining trends of PFTs warn to continuously monitor those at different treatment times and follow ups. Before starting chemotherapy and radiation the baseline PFT must be within normal limit. Because both of these treatments have the potential to increase survival in properly selected patients, our data provide evidence that both treatments can be given sequentially without a concern for potential interactions that could result in a very serious pulmonary complication, but they result in definitive pulmonary damage.

Conclusion

The conclusion of our study was following anthracycline and/ taxane based chemotherapy and radiotherapy the breast cancer patients have shown definitive decrease in forced vital capacities and FEV1/FVC ratios. The declines were statistically significant at 6th month of follow up.FEV1/FVC ratio decreased below 70 % in about 67% of patients at 6 months of follow up.

Conflict of interest

The authors declare that they have no conflicts of interest. The authors alone are responsible for the content and writing of the paper.

References

1. Parkin DM, Whelan SL, Ferlay J, Raymond L, Young J.(eds) Cancer incidence in five continents VII. International agency for research on cancer, Lyon, France. *IARC Sci Pub* No. 143; 1997.
2. National Cancer Registry Programme Biennial Report (1988–89): An epidemiological study. Indian Council of Medical Research, New Delhi; 1992.
3. Berry DA, Cronin KA, Plevritis SK, et al. Effect of screening and adjuvant therapy on mortality from breast cancer. *N Engl J Med* 2005; **353**:1784.
4. Nabholtz JM, Gligorov J. The role of taxanes in the treatment of breast cancer. *Expert Opin Pharmacother* 2005; **6**:1073-94.
5. Shannon VR, Price KJ. Pulmonary complications of cancer therapy. *Anesth Clin N Amer* 1998; **16**:563– 86.
6. Ramanathan RK, Reddy VV, Holbert JM, et al. Pulmonary infiltrates following administration of paclitaxel. *Chest* 1996; **110**:289– 92.
7. Dimopoulou I, Galani G, Dafni U, et al. A prospective study of pulmonary function in patients treated with paclitaxel and carboplatin. *Cancer* 2002; **94**:452–8.

 ISSN 2330-4049

8. Henderson IC, Berry DA, Demetri GD, Cirrincione CT, Goldstein LJ,Martino S, et al. Improved outcomes from adding sequential paclitaxel but not from escalating doxorubicin dose in an adjuvant chemotherapy regimenfor patients with node-positive primary breast cancer. *J Clin Oncol* 2003; **21**:976–83.
9. Mamounas EP, Bryant J, Lembersky BC, Fisher B, Atkins JN, Fehrenbacher L, et al. Paclitaxel (T) following doxorubicin/cyclophosphamide (AC) as adjunct chemotherapy for node-positive breast cancer: results from NSABP B-28 [abstract 12]. *Proc ASCO* 2003; **22**:4.
10. Overgaard M, Hansen PS, Overgaard J, Rose C, Andersson M, Bach F, et al. Postoperative radiotherapy in high-risk premenopausal women with breast cancer who receive adjuvant chemotherapy. Danish Breast Cancer Cooperative Group 82b Trial. *N Engl J Med* 1997; **337**:949 –55.
11. Early Breast Cancer Trialists' Collaborative Group. Favourable and unfavourable effects on long-term survival of radiotherapy for early breast cancer: an overview of the randomised trials. *Lancet* 2000; **355**:1757–70.
12. Lind PA, Marks LB, Hardenbergh PH, Clough R, Fan M, Hollis D, et al. Technical factors associated with radiation pneumonitis after local /regional radiation therapy for breast cancer. *Int J Radiat Oncol Biol Phys* 2002; **52**:137– 43.
13. Botterman J, Tasson J, Schelstraete K, Pauw els R, VanDerStraeten M, DeSchryver A. Scintigraphic, spirometric and roentgenologic effects of radiotherapy on normal lung tissue. *Chest* 1990; **97**:97-102.
14. Kaufman J, Gunn W, Hartz AJ, et al. The pathophysiologic and roentgenologic effects of chest irradiation in breast carcinoma. *Int J Radiat Oncol Biol Phys* 1986; **12**:887–893.
15. Quanjer PH. Standardized lung function testing. Report from working party 'Standardization of lung function tests', European Community for Coal and Steel. *Bull Eur Physiopathol Resp* 1983; **19**:1–27.
16. Yu TK, Whitman GJ, Thames HD, Buzdar AU, Strom EA, Perkins GH, Schechter NR, McNeese MD, Kau SW, Thomas ES, Hortobagyi GN, Buchholz TA. Clinically relevant pneumonitis after sequential paclitaxel-based chemotherapy and radiotherapy in breast cancer patients. J Natl Cancer Inst. 2004 17; **96**:1676-81.
17. Marks LB, Halperin EC, Prosnitz LR, et al. Post-mastectomy radiotherapy following adjuvant chemotherapy and autologous bone marrow transplantation for breast cancer patients with⩾10 positive axillary lymph nodes. I*nt J Radiat Oncol Biol Phys* 1992; **23**:1021–1026.
18. Gage I, Bond S, Davidson NE, et al. Minimal acute toxicity with locoregional radiation therapy follow ing 2 high-dose chemotherapy regimens (HDC) supported with autologous marrow/stem-cell transplantation in high risk breast cancer patients (abstract). *Prog/Proc ASCO* 1998; **17**:120a.

ISSN 2330-4049

International Journal of Cancer Therapy and Oncology
www.ijcto.org

Human epidermal keratinocytes death and expression of protein markers of apoptosis after ionizing radiation exposure

Sharon Wong[1, 2], Han Hor Chor[1], Sathiya Moorthy[3], Chee Tian Ong[1,] Toan Thang Phan[1], Jaide Jay Lu[1, 4]

[1]*Department of Medicine, National University of Singapore, Yong Loo Lin School of Medicine, Singapore.*
[2]*Division of Radiation Oncology, National Cancer Centre, Singapore.*
[3]*Department of Pathology, Singapore General Hospital, Singapore.*
[4]*Department of Radiation Oncology, National University Cancer Institute, National University of Singapore, Singapore.*

Received October 31, 2013; Revised November 27, 2013; Accepted November 29, 2013; Published Online December 02, 2013

Original Article

Abstract

Purpose: Knowledge of the pathophysiology of the irradiated skin is important to understand the tolerance and cosmetic response of the human skin to radiation. There are limited studies on the effect of radiotherapy dosage and fraction size in inducing apoptotic cell death in human skin. The expression of apoptotic biomarkers within a controlled population in different fractionation schemes has also never been studied. This study aims to investigate radiation induced apoptotic cell death in human skin cells after fractionated radiation exposure and the expression of unique biomarkers that reflect cell death or biology using multiplexed immunoassays. **Methods**: Breast skin biopsies were obtained from a single individual and divided into small pieces. Each piece was irradiated under different radiotherapy treatment fractionation schedules to a total dose of 50Gy. The irradiated skin tissues were analysed using Tunnel, immunohistochemistry and Western blot assays for expression of apoptotic keratinocytes and biomarkers (p53, p21, and PCNA). Haematoxylin and eosin (H&E) immunostaining was performed to study the morphological changes in the skin cells. **Results:** Radiation is mostly absorbed by the epidermal layers and observed to damage the epidermal keratinocytes leading to the activation of apoptotic proteins. Apoptotic proteins (p53, p21 and PCNA) were confirmed to be up-regulated in radiation exposed skin cells as compared to normal skin cells with no radiation. There is strong correlation of apoptotic protein expressions with increased radiation dosage and dose fractionation. Statistical analysis with ANOVA revealed a significant increase of PCNA and p21 expression with increased radiation dosage and dose fractionation ($p < 0.05$). Immunohistochemically, 14 % (range 10.71% to 17.29%) of the keratinocytes were positive for PCNA and 22.5% (range 18.28% to 27.2%) for p21 after 2Gy of irradiation. The most widespread, intense and uniform staining for PCNA and p21 was observed in skin that had received 50Gy of irradiation. The maximum expression of p53 (range 37.09% to 50.91%) was reached at 10Gy. **Conclusion**: Findings from this study will assist clinicians in predicting radiation induced skin toxicity with the current changes in radiation fractionation protocols.

Keywords: Apoptosis; Fractionated radiation therapy; Immunohistochemistry; Skin

Introduction

Radiation therapy (RT) is a commonly utilized modality for the treatment of breast cancer. It is routinely employed in breast conservation therapy. Its role as adjuvant therapy in selected patients undergoing mastectomy for stages I and II disease is currently evolving, and has become an essential component of the combined modality approach for stage III disease. Postmastectomy Radiotherapy (PMRT) to the chest wall and to the regional lymphatics has shown to decrease locoregional recurrence and increase survival for women with large tumors and/or node-positive disease.[1-2] However, the risk of toxicity to skin and cosmesis must be weighed against local and regional recurrences.

A review of literature suggests that the risk of radiation induced skin damage is affected not only by individual variations in response to radiation, but also by the total dose received and fractionation.[3-7] There are also changes in post mastectomy radiotherapy schedules from conventional radi-

Corresponding author Dr. Sharon Wong; National Cancer Centre, Division of Radiation Oncology, 11 Hospital Drive, Singapore 169610; Email: ntrwmm@nccs.com.sg

Cite this article as:
Wong S, Chor HH, Moothy S, Ong CT, Phan TT, Lu JJ. Human epidermal keratinocytes death and expression of protein markers of apoptosis after ionizing radiation exposure. Int J Cancer Ther Oncol 2013; 1(2):01027. **DOI**: 10.14319/ijcto.0102.7

ISSN 2330-4049

otherapy at 50Gy at 1.8 to 2Gy per week to more aggressive schedules such as unconventional protocol.[8] Changes in radiotherapy practice over the years are due to the recognition of the importance of fraction size, fraction number, total dose and overall time for both tumour and normal tissue reactions. However, there is very limited knowledge on the extent of radiotherapy dose and fractionation schedules in inducing cellular radiation response in the human skin.

The practice of radiotherapy would also greatly benefit from the discovery of biomarkers that correlate with symptoms and side effects pertaining to tissues within the irradiated volume. Direct or surrogate biomarkers of radiation induced toxicity could potentially give clinicians the ability to use this information to individually plan patients treatments, develop Phase I trials with molecular targeted agents in combination with RT with more confidence regarding potential side effects and/or to intervene and reduce late effects with novel therapies directed against the signalling pathway(s) involved in the late injury.[9-10] However, the studies to date are limited and there is a rather weak correlation between the in-vitro and clinical data. The role of cytokines and apoptotic markers as biomarkers of radiation response to different radiation dose and fraction size has also never been studied.

In summary, this study aims to (1) look at radiation induced apoptotic cell death in human skin cells after exposure to post mastectomy treatment regimens and its relation to radiation fraction size. This study also (2) explores the proteomic expression of human skin cells as biomarkers for radiation response.

Methods and Materials

Biopsies and Irradiation

Breast skin biopsies were obtained from a single individual and divided into small pieces of 3 cm each, and were placed into 5 batches (Batch A, B, C, D and E). Each batch underwent a different radiotherapy treatment regimen, each receiving a total dose of 50Gy (**Table** 1). The human skin cell sections are irradiated daily and after each irradiation, one sample from each batch will be removed and stored in -80°C freezer for biochemical analysis. Each experiment was repeated three times and average readings obtained.

TABLE 1: Experimental design

Batch	Nos. of flasks	Dose per fraction	Duration
A-conventional	25	2.0 Gy	25 fractions
B	20	2.5 Gy	20 fractions
C	10	5.0 Gy	10 fractions
D	5	10.0 Gy	5 fractions
E	1	50.0 Gy	1 fraction
F-control	1	No radiation	-

*Each batch of skin tissues were irradiated under different radiotherapy treatment regimen, each receiving a total dose of 50Gy.

The human skin cell sections are irradiated using a Gammacell® 40 Exactor Low Dose-Rate Research Irradiator under different radiotherapy treatment schedules. Following irradiation, the skin sections were collected, fixed in 10% phosphate-buffered formalin for 10 hours at 4 C, dehydrated in ascending concentration of (50%, 70%, 80%, 95% and 100%) ethanol solution (Merck) for 45 minutes each. This was followed by two incubations in xylene (Merck) solution for 15 minutes each. Samples were then placed onto plastic cassettes and transferred into 60°C liquid paraffin tank (Leica) for 30 minutes. Samples were embedded and left to solidify on the -5°C cold plate. The sections were cut into 3 μm thickness using a microtome (Leica) and placed onto coated glass slides.

Measurement of Radiation Induced Apoptotic keratinocytes

Hematoxylin and Eosin (H&E) staining

Apoptotic cells are morphologically distinct due to cell shrinkage and nuclear condensation that stain darker by Haematoxylin and Eosin (H&E). Based on these criteria, irradiated sections were stained with H&E and apoptotic cells were counted.

TUNNEL assay

DeadEnd ™ Fluorometric TUNNEL System (Promega, Madison, WI) was used to detect apoptotic cells in tissue samples following manufacturer's protocol with some modifications. In brief, tissue sections after deparaffinization and rehydration were permeabilized with Proteinase K (30 μg/mL) solution, repeated fixation and wash steps. After equilibration, nucleotide mix and rTdT enzyme were added and DAPI nuclear staining dye was applied as counterstaining. The slides were mounted with cover slides and observed under x400 magnification for TUNNEL-positive cells.

Immunohistochemistry (IHC) Analysis of apoptotic biomarkers

Histological procedures

Serial paraffin sections of irradiated skin were dewaxed in xylene and then hydrated in descending concentrations of ethanol. Antigen retrieval was done by immersing the slides in 0.01 M Tris /0.001M EDTA buffer (pH9.0) and pressure cooked for 5 minutes. All sections were cooled under running tap water for 10 minutes. The Dako Envision+ kit was used for subsequent IHC steps. Briefly, endogenous peroxidase was blocked using 3% H_2O_2 for 30 minutes and washed in TBS-Tween 20 for 3 times. Non-specific binding was blocked using the Dako Protein Block, serum-free, for 5 minutes, followed by washes in TBS-Tween 20 for 3 times. Subsequently, sections were incubated with monoclonal anti-active p53 (Dako and BD Transduction Lab), PCNA (Santa Cruz) and P21 (Santa Cruz), in dilutions of 1:500 overnight (**Table 2).**

 ISSN 2330-4049

TABLE 2: List of antibodies used in immunohistochemistry procedures

	Antibodies	Product Code	Company	Clone
Primary	p53	P21020	BD Transduction Laboratories	Monoclonal
	p53	D0-7	Dako	Monoclonal
	PCNA	SC-56	Santa Cruz	Monoclonal
	p21	sc-817	Santa Cruz	Monoclonal
Secondary	Mouse IgG, HRP-conjugated,		Dako	Polyclonal
	Mouse IgM, HRP-conjugated,		Dako	Polyclonal
	Rabbit IgG, HRP-conjugated,		Dako	Polyclonal

After washing in TBS-Tween 20 for 3 times, the slides were incubated in secondary mouse antibody from Dako Envision+ kit for 1 hour. The slides were washed sequentially and incubated with DAB (3, 3-diaminobenzidine) for 5 minutes. Subsequently, slides were counterstained with Gill's III hematoxylin, dehydrated in ascending concentrations of ethanol, and cleared in xylene. Finally the sections were mounted using Depex (Merck). Non-immunised mouse antibody (IgG) was used for negative controls.

Briefly, tissue sectioned were screened under the microscope and evaluated under high power field (hpf, x 200). The stainings were visualized with an Olympus light microscope.

Histopathological evaluation

Sections of immunostained skin were evaluated under the microscope by an experienced pathologist (Singapore General Hospital, Singapore). The epidermal area in each biopsy sample was measured and both total and specifically stained keratinocyte nuclei were evaluated and counted. Since the number of positive cells was low in the irradiated tissue, we use the entire tissue section as reference determining the total number of keratinocyte nuclei. The difference between nonimmunoreactive (control) and immunoreactive (irradiated) keratinocyte nuclei was clear cut and cells were scored and the differences counted. The staining values are expressed as percentage of positive cells of the total number of keratinocytes evaluated with the control as a reference.

The staining intensity and reaction pattern was evaluated using the scale presented (**Table 3**).

Western Blot Analysis of Apoptotic biomarkers

Protein extraction from tissue culture cells

Skin tissues were minced and lysed directly in cell lysis buffer containing 20 mM Tris-HCI (ph 7.5), 1% Triton X-100, 100 mM NaCL, 0.5% Nonide P-40 and I mg/ml protease inhibitor cocktail. (Boehringer Mannheim, Mannheim, Germany). Cells were solubilized by passing solution through the pipette tip repeatedly followed by incubation on ice for 15 minutes.

Samples were then centrifuged at 4°C, 12,000*g* for 10 minutes and the supernatant containing the proteins were collected. Total cell lysates were then subjected to Western blot analysis.

Determination of protein concentrations

Protein concentration of cell lysates (CLs) was determined using Bradford protein quantification methods according to manufacturer's instructions. A standard curve was prepared using bovine serum albumin (BSA) with concentrations ranging from 0-2000 μg/ml the lysis buffer. Five and ten fold dilutions were carried out for each sample and 4 repeats were done for each standard or sample. 200μl of colorimetric assay reagent was added to each well. After the 96-well plate was incubated at 37°C for 30 minutes, protein concentrations were assayed by measuring absorbance at 570 nm with a reference wavelength of 690nm, using a photometric plate reader (BIO-RAD, Benchmark Plus™)

TABLE 3: The staining intensity and pattern was evaluated using the scale below

Staining Pattern	Score
No Staining at all, or membrane staining in less than 10% of the cells	**0**
A faint/barely perceptible membrane staining is detected in more than 10% of the cells. The cells are only stained in part of their membrane	**1+**
A weak to moderate staining of the entire membrane is observed in more than 10% of the cells	**2+**
A strong staining of the entire membrane is observed in more than 10% of the cells	**3+**

ISSN 2330-4049

TABLE 4: List of antibodies used in Western Blot Analysis

	Antibodies	Product Code	Company	Clone
Primary	p53	P21020	BD Transduction Laboratories	monoclonal
	PCNA	SC-56	Santa Cruz	monoclonal
	p21	sc-817	Santa Cruz	monoclonal

Table 5: Correlations between different radiation fractionation and TUNNEL staining

Total Dose	Dose fractionation[1]	Dose fractionation [2]	Dose fractionation [3]	Dose fractionation[4]	Dose fractionation[5]	Pearson's R	P
10Gy	2Gy Day 5	2.5Gy Day 4	5Gy Day 2	10Gy Day 1	---	0.49	<0.000
30Gy	2Gy Day 15	5Gy Day 6	10Gy Day 3	---	---	0.62	<0.000
50Gy	2GyDay 25	2.5Gy Day 20	5Gy Day 10	10Gy Day 5	50Gy Day 1	0.73	<0.000

*Nonparametric correlations of TUNNEL positive cells with different radiation fractionation are calculated. Both Pearson's coefficient of correlation (r_P) and the corresponding P value are shown. All statistical tests are two-sided. In all groups, there was a statistically significant correlation between TUNNEL positive cells and dose size fractionation. Radiation induced the formation of apoptotic cells and a noticeable increase was observed in skin tissues that received higher radiation dosage. These findings were confirmed by TUNNEL assay. There is also a significant (p<005) and strong correlation of apoptotic cells with increased fraction size.

Blocking, antibody incubation, washing and stripping

Equal amounts of protein samples were denatured, separated by 12% SDS-PAGE and transferred onto nitro-cellulose membrane by semi-dry blotting. The membrane was placed protein side up and incubated for 2hrs in blocking solution.

Primary antibodies were diluted in 5% milk and incubated with the membrane for 2hrs at room temperature. Secondary antibodies were diluted in 5% milk and incubated with the membrane for 1hr at room temperature. Following primary and secondary antibody incubations (**Table 4**) membranes were washed 5 times each time 10 minutes with 30ml washing buffer and incubated in sufficient volume of buffer diluted with horseradish peroxidase (HRP)-coupled secondary antibody at room temperature for 1 hour. The membrane was washed again with washing buffer for 5 times before incubation with Western lightning plus-ECL (Perkin Elmer) for a minute, exposed on X-ray films (Konica Minolta) and developed.

Computerized gel densitometry

A Bio-Rad gel scanner and densitometer program (Gel-Pro ® Analyzer version 4.5: MediaCybernetics, Maryland, USA) was used to assess concentrations of the bands obtained by Western blots. There were measured as total density units.

Statistical Analysis

Statistical Package for Social Sciences (SPSS), version 17.0 was the statistical tool used for data analysis. Nonparametric methods were used for the statistical analysis using one-way Anova (Analysis of Variance) - or Student's t-tests. A value of $P<0.05$ was considered to be statistically significant.

Results

Radiation induced apoptotic keratinocyte cell death is dose and fraction size dependent

Increased Apoptotic keratinocyte cell count:

Since it has been proposed that keratinocytes damaged by ionizing irradiation undergo apoptosis, we analysed the expression of apoptotic cells in the skin tissues of the volunteer using TUNNEL assay. The skin tissues were irradiated with different fractionation schedules. (**Table 5**)

Morphological changes of radiation induced apoptotic keratinocytes

Results showed that radiation is mostly absorbed by the epidermal layers and observed to damage the epidermal keratinocytes leading to apoptosis. These cells had characteristic dyskeratotic apoptotic cells with pyknotic nuclei in the irradiated sections. HE staining on control sections demonstrated normal epidermal morphology (**Figure 1A**) while irradiated sections demonstrated strong evidence of cellular damage caused by ionizing radiation (**Figure 1B-D**).

The keratinocytes were enlarged with cytological atypia **Figure 2**. The epidermis in the irradiated skin was thin, containing only one to three layers of keratinocytes and in some tissues; the epidermis layer was also detached from the dermis layer **Figure 3.**

 ISSN 2330-4049

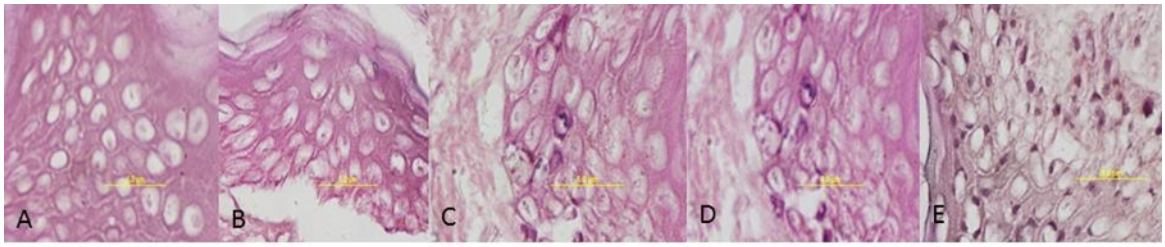

Dose series of Irradiated skin. Sections were stained with HE.
A- Control, B- 2Gy, C-5Gy, D-10Gy, E- 50Gy

FIG. 1: Morphological evaluation

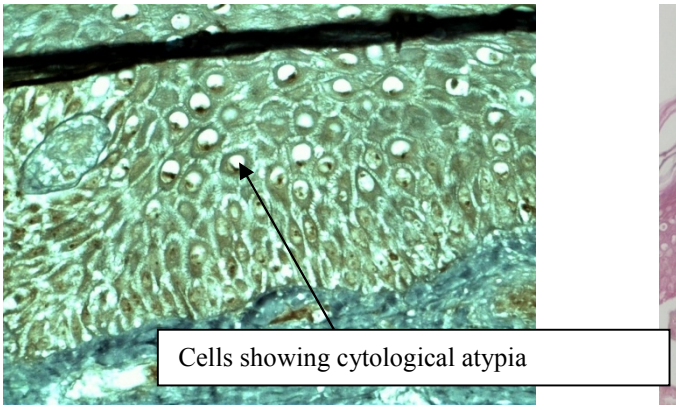

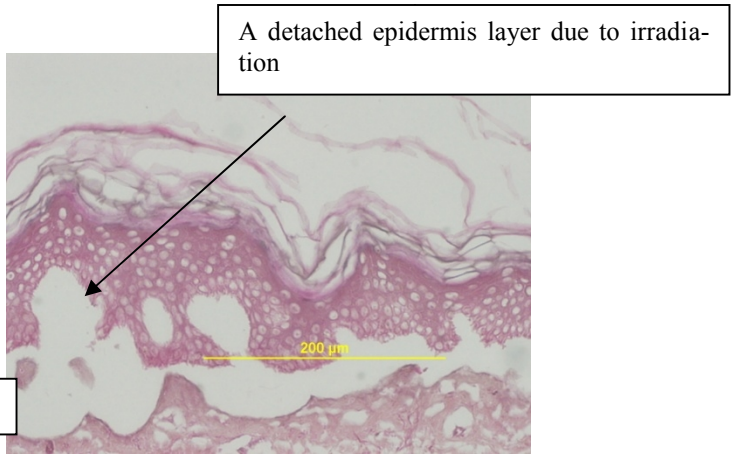

FIG. 2 (left): Shows morphological changes in cell after layer due to the irradiation.
FIG. 3 (right): HE slide showing a detached epidermis radiation exposure.

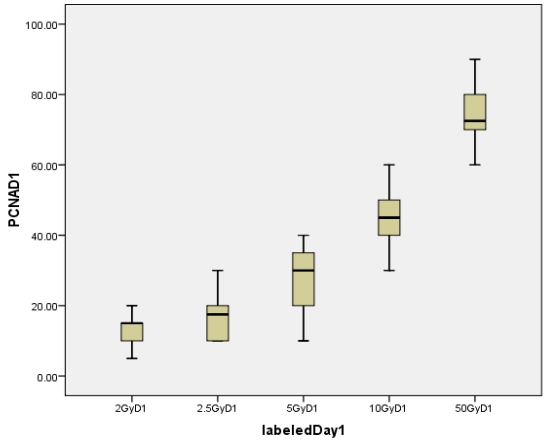

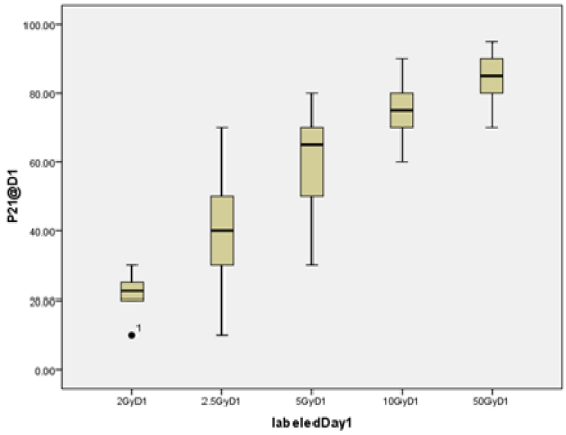

FIG. 4: The boxplot for PCNA immunoreactitivity in different radiation dosage starting from 2Gy to 50Gy. Bars represent the range within the different radiation dosage as indicated.

Expression of apoptosis related marker proteins with irradiation and this is dose and fraction size dependent

Accumulation of p53, PCNA and p21 proteins with increasing dose

We analyzed sections of paraffin-embedded skin biopsies of the volunteer for p53, PCNA and p21 apoptotic related

FIG. 5: The boxplot for p21 immunoreactitivity in different radiation dosage starting from 2Gy to 50Gy. Bars represent the range within the different radiation dosage as indicated.

marker proteins using western blot and immunohistochemistry analysis. Hardly any apoptotic positive cells were seen in the control epidermis before radiation. Skin tissues were irradiated with 2, 2.5, 5, 10 and 50 Gray. Apoptotic proteins (PCNA, P21) were confirmed to be up-regulated in radiation exposed skin cells as compared to normal skin cells with no radiation. There is strong correlation of apoptotic protein expressions with increased radiation dosage. (**Figures 4-5**)

ISSN 2330-4049

In contrast, P53 expression started to increase after 2Gy of radiation up to a maximum dose of 10Gy (**Figure 6**). At 2 Gy, a higher number of cells faintly positive for p53 extended from the suprabasal layer to the stratum granulosum. At more superficial locations, these cells became strongly stained by anti-p53. The maximum expression of p53 (median =44%, range 37.09% to 50.91%) was reached at 10Gy after irradiation exposure, and in most cases the p53 immunoreactivity appeared to be concentrated within the keratinocyte nuclei. At higher radiation dosage (> 10Gy), the epidermal sections showed a downward trend in the expression of P53. The irradiated keratinocyte nuclei appeared to be p53 negative or only faintly stained at 50Gy (median=7%, range 5.15% to 8.85%). Western blot analysis revealed similar results.

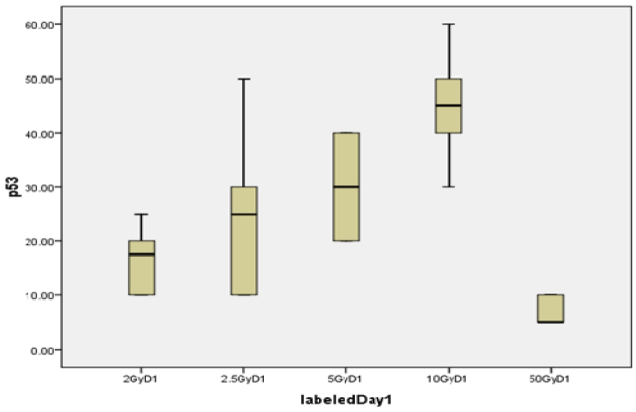

FIG. 6: The boxplot for p53 immunoreactitivity in different radiation dosage starting from 2Gy to 50Gy. Bars represent the range within the different radiation dosage as indicated.

Morphological changes of PCNA, P21 and P53 with increasing dose

Results unequivocally demonstrated that, in response to DNA damage, PCNA (**Figure 7**) and p21 (**Figure 8**) are up-regulated for cell cycle arrest to facilitate DNA repair.

As for p53, we hardly detected any cells stained with anti-p53 antibody in the control slide (**Figure 9**). P53 expression started to increase after 2Gy of irradiation and maximal expression of p53 was reached at 10Gy. Thereafter irradiated cells appeared to be p53 negative or only faintly stained at 50Gy.

Accumulation of p53, PCNA and p21 proteins with increasing fraction size

Subsequently, we tested by immunohistochemistry the expression of marker proteins of apoptosis, namely p53, P21 and PCNA with different radiation fractionations.

Repeated measures of ANOVA revealed that the effects of different radiation fractionation (2Gy, 2.5Gy, 5Gy, 10Gy and 50Gy) on human skin cells were significantly different from each other ($p<0.05$). There is a positive and significant correlation (Pearson's correlation r) between radiation fractionation and apoptotic protein expression (PCNA, p21 and P53), measured at different dosage. This correlation is strongest at higher dose (**Table 6 and 7**).

In summary, we have checked for associations between cytokine expression, radiation dose and type of fractionation regimen, given that both radiation and proteins expression are important variables in mediating radiation response. Results have shown that PCNA and p21 levels were significantly associated with dose and treatment regimen, while elevation of p53 was significant only up to 10Gy. These results were supported by western blot findings.

Western blot analysis revealed elevated levels of PCNA and P21 proteins in Irradiated keratinocytes and this is dose and fraction size dependent

Little or no immunoreactive band specific for p53, PCNA and p21 protein was observed in the lysates of non-irradiated control keratinocytes. Irradiated cell lysates revealed an accumulation of p53 protein which was detected at 2Gy and peaked at 5Gy. After 5Gy, the expression level slightly declined and was not detectable at 50Gy (**Figure 10).**

Regarding p21 and PCNA, a weak band was seen in control keratinocytes. Overexpression of p21 and PCNA protein was seen which increases with radiation dosage and fractionation (**Figures 11-14**).

This is one of the few studies that evaluated the difference in cellular response due to minor variations in the protocols of fractionation radiotherapy. For the evaluation of the effect of changes in dose/fraction, the human skin cells irradiated with the same total dose of 10Gy, 30 Gy and 50Gy were grouped according to the dose/fraction given. No significant difference in apoptotic cell death between groups of samples irradiated by dose fraction of 2Gy and 2.5Gy could be detected. However, irradiation with a higher dose/fraction of 5Gy and 10Gy resulted in a very significant elevation of mean % apoptotic cell death expression. Moreover, significant changes were also found at much lower total dose of 30Gy, where the treatment was given with a high dose/fraction of about 5Gy. Our results demonstrate that the increase in dose of radiation per fraction had much more impact on radiation induced apoptosis than elevation in the total dose, which may result in worst skin outcome. Our result is similar to previous study by Archambeau [11] who evaluated the effect of changes in dose/fraction using a swine skin model. Following irradiation there is a dose-dependent loss of basal cells. The fields treated with 2Gy daily dose fractions show no change in the basal cell density until total doses of 20-25Gy are delivered. This period is followed by

 ISSN 2330-4049

increasing cell loss up to 50Gy and necrosis is produced. A separate study by Raphael[12] looked at the effect of radiation fraction size on skin viscoelasticity. They also found that the increase in dose of radiation per fraction greatly increased skin stiffness. There is an intimate relationship between radiation-dose fractionation and clinical outcome of radiation therapy.

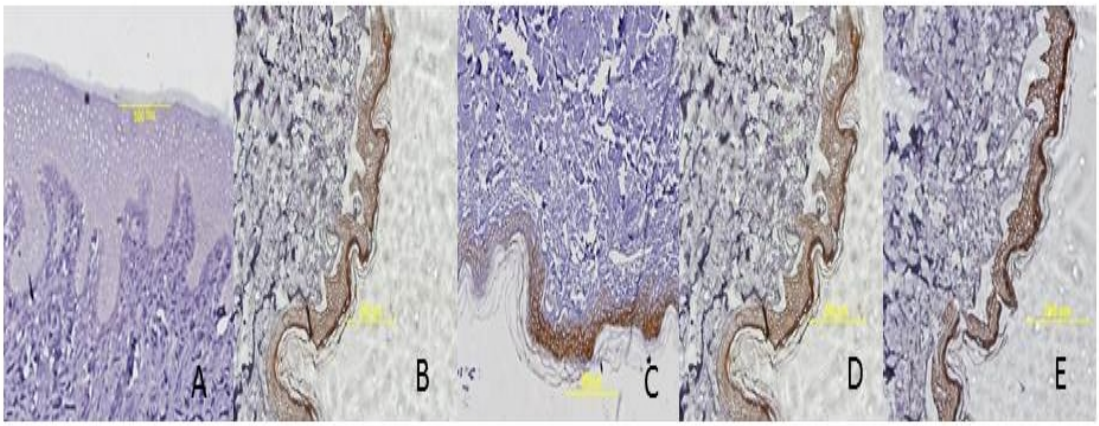

FIG. 7: Dose series of Irradiated skin. Sections were stained with monoclonal anti-PCNA; A-Control, B- 2Gy, C-5Gy, D-10Gy, E-50Gy

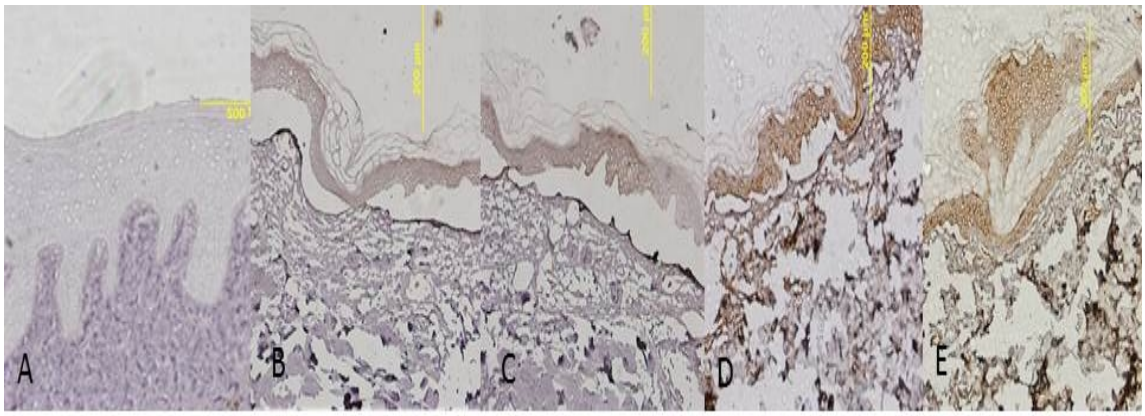

FIG. 8: Dose series of Irradiated skin. Sections were stained with monoclonal anti-p21; A-Control, B- 2Gy, C-5Gy, D-10Gy, E-50Gy

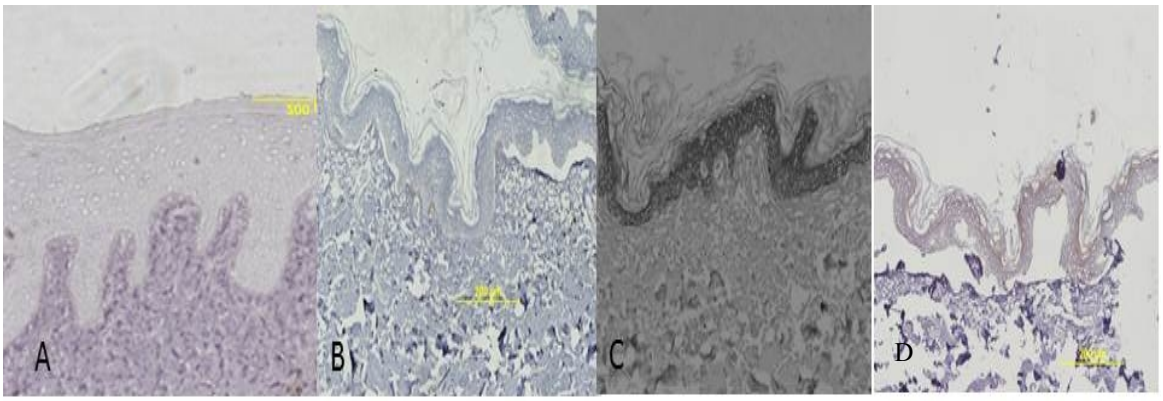

FIG. 9: Dose series of Irradiated skin. Sections were stained with monoclonal anti-p53; A-Control, B- 2Gy, C-10Gy, D-50Gy

ISSN 2330-4049

TABLE 6: Correlations between different radiation fractionation and PCNA expression

Total Dose	Dose fractionation[1]	Dose fractionation [2]	Dose fractionation [3]	Dose fractionation[4]	Dose fractionation[5]	Pearson's R	P
10Gy	2Gy Day 5	2.5Gy Day 4	5Gy Day 2	10Gy Day 1	---	0.59	<0.000
30Gy	2Gy Day 15	5Gy Day 6	10Gy Day 3	---	---	0.61	<0.002
50Gy	2GyDay 25	2.5Gy Day 20	5Gy Day 10	10Gy Day 5	50Gy Day 1	0.66	<0.000

TABLE 7: Correlations between different radiation fractionation and p21 expression

Total Dose	Dose fractionation[1]	Dose fractionation [2]	Dose fractionation [3]	Dose fractionation[4]	Dose fractionation[5]	Pearson's R	P
10Gy	2Gy Day 5	2.5Gy Day 4	5Gy Day 2	10Gy Day 1	---	0.657	<0.000
30Gy	2Gy Day 15	--	5Gy Day 6	10Gy Day 3	---	0.523	<0.002
50Gy	2GyDay 25	2.5Gy Day 20	5Gy Day 10	10Gy Day 5	50Gy Day 1	0.634	<0.000

*Tables 6 & 7: Nonparametric correlations of PCNA and P21 immunoreactive cells with different radiation fractionations are calculated. Both Pearson's coefficient of correlation (r_P) and the corresponding P value are shown. All statistical tests are two-sided.

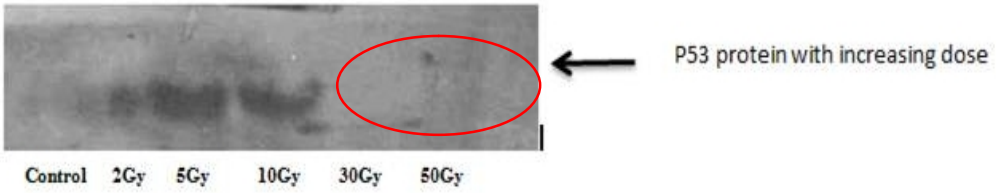

FIG.10: Little or no immunoreactive band specific for p53 was observed at dose above 10Gy

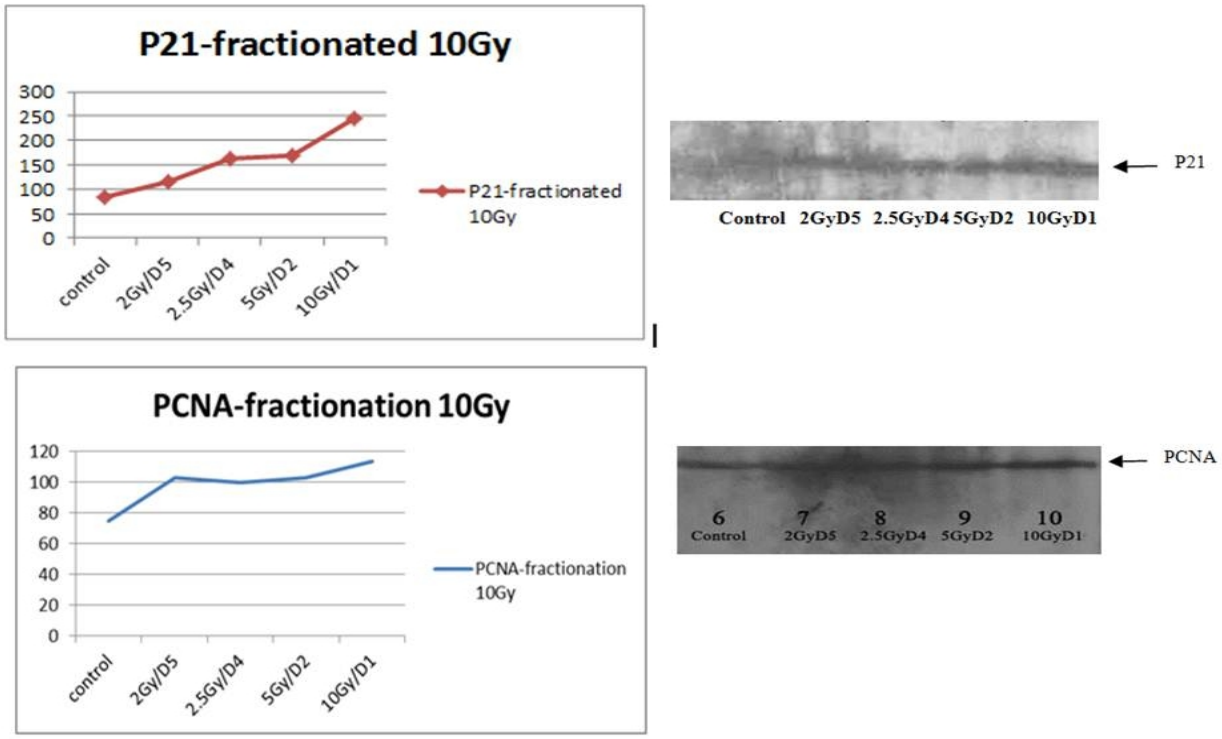

FIG.11 (top) **and FIG. 12** (bottom): Western blot analysis of P21 and PCNA reveals a higher level of protein with increasing fraction size at 10Gy

 ISSN 2330-4049

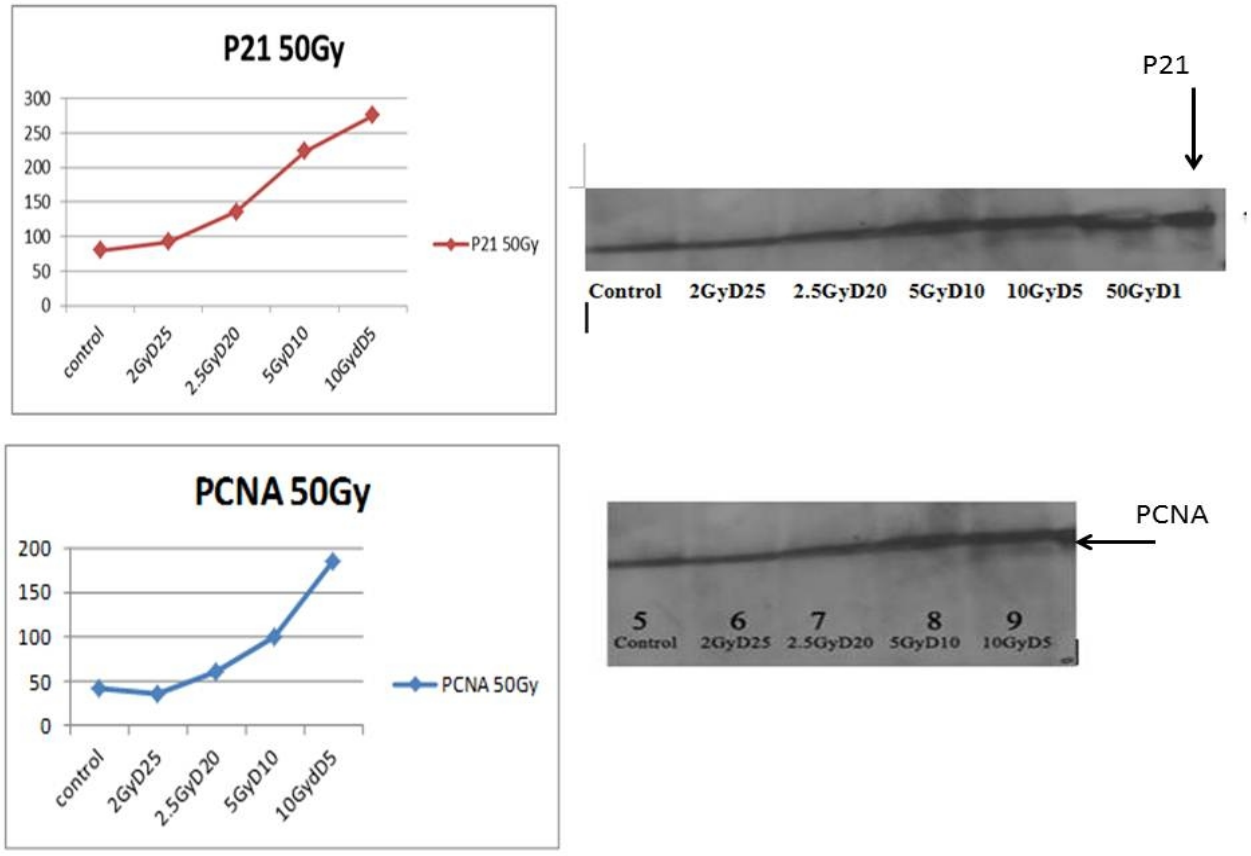

FIG.13 (top) **and FIG. 14** (bottom)**:** Western blot analysis of P21 and PCNA reveals a higher level of protein with increasing fraction size at 50Gy

Discussion

The practice of radiotherapy would greatly benefit from the understanding of apoptosis and its associated biomarkers that correlate with radiation dose and its side effects pertaining to tissues within the irradiated volume. This forms the basis of our study.

In this study we demonstrated dose-dependent keratinocyte apoptosis following irradiation that was associated with activation of apoptosis regulating biomarkers. We demonstrated that increasing radiation dosage led to increased keratinocyte death in human skin. Our results are in agreement with the findings of previously reported studies showing a dose related induced apoptosis using swine skin[11] and human cochlear cells.[13] Morphological evaluation was consistent with our findings. HE staining revealed an increased in the number of apoptotic cells with condensed nuclei surrounded by a bright halo. These morphological changes were similar to what has been described in Ponten F.[14] The keratinocytes were enlarged with cytologic atypia.

The relationship between the total dose of radiation and fractionation of the dose given is also crucial in radiotherapy with respect to the development of radiation induced effects in normal tissues. This elevates the therapeutic ratio and enables efficient tumour control while decreasing both early and late radiation effects in normal tissues.[12]

Cellular damage caused by ionizing radiation induces production and recruitment of specific proteins that have the potential to predict radiation induced toxicity in tissues within the irradiated volume.[15-16] Our interest in these proteins expression during Radiation Therapy is based in part on Rubin[17] and colleagues' description of a cytokine-linked continuum of early and late radiation responses. Rubin et al showed in murine and clinical lung models that radiation induced fibrosis is progressive after treatment and begins immediately following lung irradiation. Levels of IL-1, TGF beta and TNF alpha were observed to increase in lung tissue immediately after radiation exposure, however clinically appreciable lung fibrosis may occur months later. A number of clinical studies have also shown that cytokines are elevated during and after Radiotherapy for a variety of malignancies.[10, 18-19] Using this as a feasibility study, we measured the cytokines protein levels of p53, PCNA and p21 in human breast skin cells after receiving post-mastectomy radiotherapy treatment regimens as biomarkers for radiation

 ISSN 2330-4049

response. The radiation response of cytokines within a controlled population with the same dose but in different fraction size has never been studied before. Thus this is one of the first studies of its kind on cytokines expression in human breast skin after exposure to fractionated radiation.

Statistical analysis with ANOVA revealed a significant increase of PCNA and p21 expression with increased radiation dosage ($p<0.05$) and with different radiation fraction size ($p<0.05$). Our results showed that cytokines are up-regulated in response to radiation; and this is dependent on radiation dosage and fraction size. This is in agreement with previous studies that shown that these cytokines are radiation-inducible cytokine. Fredrik Ponten *et al* [14] investigated levels of p53 and p21 in skin exposed to different types of radiation. Results show an early onset of increased p53 levels and a correlation between p53 and p21 was evident. In other studies, p53, PCNA and p21 were induced in hairless mouse epidermis following UVB radiation[20], human skin response to x-ray treatment with release of p53 [21] and induced expression of p21 and PCNA proteins in UVB irradiated human epidermis.[22] However, drawbacks of these studies were the use of mice epidermis and UVB radiation and included a range of radiation dose. In our study, these factors were closely controlled. Human breast epidermis from a single donar and 50Gy of 6 MV ionizing radiation were used.

Results from our studies show predictable patterns of cytokine expression. PCNA and P21 levels elevated gradually from 2Gy to 10Gy, followed with a sharp increase at 50Gy. On the other hand, p53 was elevated at 2Gy and persisted until 10Gy, and then returned to baseline values. This pattern was also consistent with increasing fraction size. Not only did this study demonstrate the early and persistent elevation of cytokine production following irradiation, but it also determined consistent patterns of cytokines expression. A similar pattern of cytokine expression was observed in murine studies. Rubin[17] and colleagues studied cytokine induction in mice receiving thoracic irradiation. They found several cytokines were longitudinally elevated with consistent patterns between mice.

One question arising from our results is why p53 did not exhibit similar pattern with PCNA and p21 given that all are apoptotic inducing cytokines. P53 plays a crucial role in the protection against DNA damage allowing cell cycle arrest, DNA repair or apoptosis by transcriptional activation of p53 related genes such as p21 and Bax.[23] Ionizing radiation produces double and single strand DNA breaks. Cells respond to DNA photoproducts and DNA breaks by accumulation of functionally active p53 proteins.

Upon exposure to radiation, p53 is known to sense DNA damaged and to subsequently halt the cell cycle in the G1 phase, providing time for DNA repair. If the damage to the genome is too serious and repair likely to fail, p53 acts as an inducer of apoptosis.[14] Consistent with this report, we observed that these proteins are up-regulated in response to irradiation-caused DNA damage leading to cell cycle arrest to allow enough time for DNA repair. This observation is consistent with similar study in animal model showing stimulatory effect of UV radiation on the protein levels of p53 and downstream effector p21.[20] In a separate time-dose study by Peter Mab *et al* [21] human skin was exposed to UVB radiation and p53 expression was detection. P53 expression started to increase 3h after irradiation and reached a maximum at 12h after UVB exposure. However, epidermal sections at 36h appeared to be p53 negative or only faintly stained. This seem to suggest p53 has a short half life of less than 24h and is time -dose dependent. However, more studies are needed in the future to further support this anticipation, Further in this study, the radiation induced p21 protein was detected much sooner than PCNA, correlating well with the expression of p53. It seems likely that up regulation of p21 could have been mediated via p53 pathway by irradiation. The different time course of the expression also supports this hypothesis.

PCNA is implicated in DNA replication and repair by forming a sliding platform that could mediate the interaction of numerous proteins with DNA.[24] It is known that p21 binds to PCNA and inhibits PCNA function in DNA replication.[25] Therfore PCNA is regarded as an important target for p21 as well as reliable biomarker for cell proliferation. It has been observed that p53/p21 signal transduction pathway plays a significant role in the regulation of the PCNA response to ionizing radiation.[26] In view of the high affinity of PCNA to DNA strand breaks due to the ionizing radiation[27], it is logical to expect the rapid recruitment of PCNA to ionizing radiation induced strand breaks. In this study, we have demonstrated the induction of PCNA after radiation in human skin cells and this induction is dose and fraction size dependent.

The evidence from our study and clinical literature demonstrate a significant dose and fraction size response during RT. They also support the molecular rationale that increased cytokines expression may serve as indicators of increased normal tissue toxicity. The clinical research environment presents a number of unique challenges to prospective proteomics studies from sample collection to processing, storage and analysis. There are many sources of error (delays in sample collection or processing, misinterpretation of standard operating procedures (SOP) and so on) that can introduce a myriad of confounding variables, which in turn will render the resulting proteomic data inconclusive. We have considered these issues in details and study designs were carefully drawn out to minimize the influence of extraneous environmental factors that may affect our conclusions from these data. In addition our principal data were derived from a single

 ISSN 2330-4049

volunteer, thus avoided interindividual variations in the responses to DNA damage.

Another limitation of our work is the small sample size and limited apoptotic markers identified in skin relating to post-mastectomy radiotherapy. Future studies with bigger sample sizes are warranted to determine the cytokine changes after radiation exposure and how these relate to normal tissue radiation toxicity with greater certainty.

Conclusion

In summary, our results demonstrate the specific up-regulation of a number of apoptotic related marker proteins after irradiation and suggest that premature keratinocyte elimination occurs via apoptosis. Results also demonstrated that their increase expression or activation occurs in relation to radiation dose and fraction size. While total dose is critical in determining the severity of skin toxicity, skin effects are more severe following fractionations schedules that employ daily dose fractions of 5Gy or higher than follow dose schedules using 2-2.5Gy daily.

More importantly, based on our findings, there is a potential for the use of anti-apoptotic strategies which could be targeted at various regions of the apoptotic pathway to prevent radiation induced skin toxicity. Access of anti-apoptotic factors to the skin could possibly be delivered topically. The use of such a target-specific approach would minimize the systemic side effects of anti-apoptotic treatments. However, the mechanisms regulating the increase in cytokines in vivo in response to cellular damage and their role need additional study.

Taken together, all of the experiments discussed in this study lay the groundwork for future larger scale clinical trials within our institution and in collaboration with other clinical centers. Protein markers have potential as proxy indicators of radiation sensitivity and exposure. It is hoped that the preliminary work presented here will contribute to the identification of protein biomarkers that contributes not only to the advancement of radiation biology in the long-term, but allows us to make a difference in the lives of cancer patients. The very high incidence of breast cancer partially attributable to the ageing of their populations and the increasing use of surgery and postoperative radiotherapy for its treatment make the above type of study of special interest, with the side effects of radiotherapy an increasingly important issue.

Conflict of interest

The authors declare that they have no conflicts of interest. The authors alone are responsible for the content and writing of the paper.

References

1. Overgaard M, Jensen MB, Overgaard J, Hansen PS, Rose C, et al. Postoperative radiotherapy in high-risk postmenopausal breast-cancer patients given adjuvant tamoxifen: Danish Breast Cancer Cooperative Group DBCG 82c randomised trial. *Lancet* 1999; **353**:1641-1648.
2. Ragaz J, Jackson SM, Le N, Plenderleith IH, Spinelli JJ, et al. Adjuvant radiotherapy and chemotherapy in node-positive premenopausal women with breast cancer. *N Engl J Med* 1997; **337:** 956-962.
3. Turesson, I. Individual variation and dose dependency in the progression rate of skin telangiectasia. *Int J Radiat Oncol Biol Phys* 1990; **19**: 1569-1574.
4. Turesson I, Nyman J, Holmberg E, et al. Prognostic factors for acute and late skin reactions in radiotherapy patients. *Int J Radiat Oncol Biol Phys* 1996; **36**; 1065-1075.
5. Tucker SL, Turesson I, Thames HD. Evidence for individual differences in the radiosensitivity of human skin. *Eur J Cancer* 1992; **28A**: 1783-1791.
6. Bernier J, Thames HD, Smith CD, Horiot JC. Tumor response, mucosal reactions and late effects after conventional and hyperfractionated radiotherapy. *Radiother Oncol* 1998; **47**: 137-143.
7. Rojas A, Joiner MC. The influence of dose per fraction on repair kinetics. *Radiother Oncol* 1989; **14**: 329-336.
8. Vicini FA, Baglan KL, Kestin LL, Mitchell C, Chen PY, Frazier RC, Edmundson G, Goldstein NS, Benitez P, Huang RR, Martinez A. Accelerated treatment of breast cancer. *J Clin Oncol* 2001; **19**:1993-2001.
9. Jager JJ, Jansen RL, Arends JW. Clinical relevance of apoptotic markers in breast cancer not yet clear. *Apoptosis* 2002; **7**: 361-365.
10. Menard C, Johann D, Lowenthal M, Muanza T, Sproull M, Ross S, et al. Discovering clinical biomarkers of ionizing radiation exposure with serum proteomic analysis. *Cancer Res* 2006; **66**: 1844-1850.
11. Archambeau JO, Pezner R, Wasserman T. Pathophysiology of irradiated skin and breast. *Int J Radiat Oncol Biol Phys* 1995; **31**:1171-1185.
12. Gorodetsky R, Lotan C, Piggot K, Pierce LJ, Polyansky I, et al. Late effects of dose fractionation on the mechanical properties of breast skin following post-lumpectomy radiotherapy. *Int J Radiat Oncol Biol Phys* 1999; **45**:893-900.
13. Low WK, Tan MG, Sun L, Chua AW, Goh LK, Wang DY. Dose-dependant radiation-induced apoptosis in a cochlear cell-line. *Apoptosis* 2006; **11**:2127-2136.

 ISSN 2330-4049

14. Ponten F, Lindman H, Bostrom A, Berne B, Bergh J. Induction of p53 expression in skin by radiotherapy and UV radiation: a randomized study. *J Natl Cancer Inst* 2001 ;**93**:128-133.
15. Faulhaber O, Bristow RG. Basis of cell kill folowing clinical radiotherapy, In M. Sluyser(ed), Application of Apoptosis to Cancer Treatment. *Springer* 2005; 293-320.
16. Hagan M, Yacoub A, Dent P. Ionizing radiation causes a dose-dependent release of transforming growth factor alpha in vitro from irradiated xenografts and during palliative treatment of hormone-refractory prostate carcinoma. *Clin Cancer Res* 2004; **10**: 5724-5731.
17. Rubin P, Johnston CJ, Williams JP, McDonald S, Finkelstein JN. A perpetual cascade of cytokines postirradiation leads to pulmonary fibrosis. *Int J Radiat Oncol Biol Phys* 1995; **33**:99-109.
18. Okunieff P, Chen Y, Maguire DJ, Huser AK. Molecular markers of radiation-related normal tissue toxicity. *Cancer Metastasis Rev* 2008; **27**:363-374.
19. Kovacs CJ, Daly BM, Evans MJ, Johnke RM, Lee TK, et al. Cytokine profiles in patients receiving wide-field + prostate boost radiotherapy (xRT) for adenocarcinoma of the prostate. *Cytokine* 2003; **23**:151-63.
20. Gu M, Dhanalakshmi S, Singh RP, Agarwal R. Dietary feeding of silibinin prevents early biomarkers of UVB radiation-induced carcinogenesis in SKH-1 hairless mouse epidermis. *Cancer Epidemiol Biomarkers Prev* 2005; **14**:1344-9.
21. Mass P, Hoffmann K, Gambichler T, Altmeyer P, Mannherz HG. Premature keratinocyte death and expression of marker proteins of apoptosis in human skin after UVB exposure. *Arch Dermatol Res* 2003; **295**:71-79.
22. Ahmed NU, Ueda M, Ichihashi M. Induced expression of p16 and p21 proteins in UVB-irradiated human epidermis and cultured keratinocytes. *J Dermatol Sci* 1999; **19**:175-181.
23. Murphy M, Mabruk MJ, Lenane P, Liew A, McCann P, Buckley A, et al. The expression of p53, p21, Bax and induction of apoptosis in normal volunteers in response to different doses of ultraviolet radiation. *Br J Dermatol* 2002; **147**:110-107.
24. Warbrick E. The puzzle of PCNA's many partners. *Bioessays* 2000; **22**;997-1006.
25. Fotedar R, Bendjennat M, Fotedar A. Role of p21WAF1 in the cellular response to UV. *Cell Cycle* 2004; **3**:134-137.
26. Wenz F, Azzam EI, Little JB. The response of proliferating cell nuclear antigen to ionizing radiation in human lymphoblastoid cell lines is dependent on p53. *Radiat Res* 1998; **149**:32-40.
27. Moggs JG, Grandi P, Quivy JP, Jonsson ZO, Hubscher U, Becker PB, Almouzni G. A CAF-1-PCNA-mediated chromatin assembly pathway triggered by sensing DNA damage. *Mol Cell Biol* 2000; **20**:1206-18.

 ISSN 2330-4049

International Journal of Cancer Therapy and Oncology
www.ijcto.org

Getting the right balance in treatment of ductal carcinoma in situ (DCIS)

Ian S Fentiman

Department of Surgical Oncology, Guy's Hospital, London, UK.

Received October 28, 2013; Revised December 02, 2013; Accepted December 03, 2013; Published Online December 05, 2013

Review Article

Abstract

As a result of mammographic detection, ductal carcinoma in situ (DCIS) is an increasing problem in breast clinics. Both histopathology and molecular profiling can identify subtypes likely to progress to invasive disease, but there is no subgroup with a zero likelihood of subsequent invasion. In patients with low/intermediate grade DCIS, if breast irradiation is not being carried out after free margins have been achieved the patient should be aware of the risks of withholding and the benefits and morbidity of adjuvant radiotherapy. Either tamoxifen or an aromatase inhibitor may be of value in those with low/intermediate ER+ve disease if radiotherapy is being withheld. For those patients with extensive or multicentric DCIS, mastectomy is the appropriate treatment. This is best combined with sentinel node biopsy and all such cases should be offered immediate reconstruction.

Keywords: Ductal carcinoma in situ; High grade; Low/intermediate grade; Recurrence; Progression; Radiotherapy; Tamoxifen; Mastectomy

Introduction

In the not so distant past, no real distinction was made between invasive breast cancer and ductal carcinoma in situ (DCIS), both being treated by mastectomy, often including an axillary clearance. Such radical surgery for DCIS became questioned as results emerged from randomised trials indicating that breast conservation was a safe and effective alternative to mastectomy for invasive breast cancer.[1, 2, 3, 4, 5] At the same time, as a by-product of national mammographic screening programmes, the incidence of DCIS was increasing, representing up to a quarter of screen-detected malignancy. In the US in 1975 the incidence of DCIS was 2 per 100,000 and by 1985 was 10, rising to 22 in 1995 and 30 by 2005.[6]

Was it reasonable to offer a mastectomy for a non-life threatening condition? We know now that the answer is "yes and no". For some women, as a result of incomplete excision of DCIS, progression to invasive disease will reduce life expectancy. But are we yet in a position to individualise treatment for women diagnosed with DCIS? The aim of treatment is to eradicate the DCIS thereby reducing the risk of recurrence of DCIS or progression to invasive disease. DCIS is a miscellany of conditions with a spectrum of risk of malignancy and it is essential that it is not universally downgraded to being regarded as a benign precursor of with an attendant laissez faire attitude towards the management of high grade disease.

Corresponding author: Ian S Fentiman MD DSc FRCS; Professor of Surgical Oncology, Research Oncology, 3rd Floor Bermondsey Wing, Guy's Hospital, London SE1 9RT, UK.
Email: ian.fentiman@gstt.nhs.uk

Cite this article as:
Fentiman IS. Getting the right balance in treatment of ductal carcinoma in situ (DCIS). Int J Cancer Ther Oncol 2013; 1(2):01029. **DOI**: 10.14319/ijcto.0102.9

Histopathology

Randomised trials of treatment for DCIS have not only yielded evidence of relative efficacy of treatments tested but have also led to central pathological review by pathologists with a special interest in breast cancer. This has enabled the delineation of groups with differing risks of subsequent relapse or progression to invasive disease.

Pinder *et al* conducted a full pathological review of 1222/1694 (72 %) of specimens from women participating in the UKCCCR/ANZ DCIS trial.[7] Those pathological features associated with ipsilateral recurrence in univariate analysis included high cytonuclear grade, larger lesions, growth pattern, presence of necrosis or chronic inflammation, margin involvement or uncertainty of margin status and narrower margin width. The large group of high-grade lesions was subdivided to identify a very poor prognosis subgroup; DCIS of high cytonuclear grade, with >50 % solid architecture,

ISSN 2330-4049

comedo-type necrosis in >50% of ducts. After a median follow-up of 53 months, hazard ratios for ipsilateral in situ or invasive recurrence in low, intermediate, high and very high, grade were 0.42, 0.33, 0.62 and 1.00, respectively.

Because they found little difference in ipsilateral recurrence rates between low- and intermediate-grade groups they joined these two to form a 3 tier system: low/intermediate, high and very high. Results are shown in **TABLE 1**. Although the new categorisation does identify groups with different risks of DCIS relapse and progression to invasive disease, there is no group with a zero probability of invasive progression.

TABLE 1: Recurrence rates within 3 tier categorisation of DCIS from UKCCCR/ANZ DCIS trial.

Category	N	DCIS recurrence	Invasive progression
Low/intermediate	311	11 (3.5%)	8 (2.5%)
High	430	32 (7.4%)	14 (3.3%)
Very high	483	56 (11.6%)	32 (6.6%)

In the histopathological review of EORTC trial 10853, specimens from 863/1010 (85%) were examined and a multivariate analysis was conducted of clinicopathological features and relapse risk after a median follow-up of 5.4 years.[8] Significant variables to emerge from multivariate analysis included young age ≤ 40 years (hazard ratio 2.14), symptomatic DCIS (HR 1.8) solid and comedo growth pattern (HR 2.6 and 2.69), margin involvement (HR 2.07) and excision without radiotherapy (HR 1.7). It is noteworthy that margin status was a more major risk factor for recurrence than avoidance of breast irradiation.

It could be argued that what is important in treatment of DCIS is the avoidance of invasive relapse rather than recurrence of DCIS since this is not life threatening. The situation is however more complex. In EORTC 10853 there was no significant relationship between the type of DCIS and risk of progression to invasion. When however the risk of distant metastasis of invasive cancer was examined it was significantly elevated in those with high grade DCIS (HR 6.57).

Esserman *et al* have suggested the acronym IDLE (indolent lesions of epithelial origin) to encompass abnormalities which may not be precursors of invasive cancer, such as low grade DCIS.[9] This is good insofar as some patients will be saved from unnecessarily radical surgery but will be problematic if imperfectly characterised lesions are included, thereby placing them at increased risk of invasive disease.

Molecular profiling

Clark et al constructed tissue microarrays (TMA) for 188 cases of DCIS and examined expression patterns of estrogen receptor (ER), progesterone receptor (PR), HER2, EGFR, cytokeratin (CK) 5/6, CK14, CK17, CK18, b4-integrin, b6-integrin, p53, SMA, maspin, Bcl-2, topoisomerase IIa and P-cadherin. Hierarchical clustering analysis was undertaken to identify any natural groupings, and the findings were validated in an independent series of 75 cases. Although the intrinsic molecular subtypes could be identified in DCIS, subgroup frequency varied. In DCIS the triple negative and basal-like phenotype was very uncommon. Hierarchical cluster analysis identified three main subtypes of DCIS and the 4 main markers were ER, PR, Her2 and Bcl-2, related to conventional prognostic indicators. These subtypes ER-PR-BCL-HER2+, ER-PR-BCL-HER2-, R+PR+HER2-BCL- and ER+PR+HER2-BCL+ were confirmed in the validation series of DCIS cases.

Solin *et al* examined specimens from 327 women with pure DCIS who participated in Eastern Cooperative Oncology Group (ECOG) E5194 study.[10] Those with low or intermediate grade DCIS were observed without having breast irradiation and some took tamoxifen. Onco*type* DX breast cancer assay was performed to obtain a prospectively defined DCIS Score (based on 7 cancer-related genes (*Ki67, STK15, Survivin, CCNB1 (cyclin B1), MYBL2*, PR, *GSTM1* and 5 reference genes). The continuous DCIS Score was statistically significantly associated with the risk of developing an ipsilateral breast event (IBE). For the of low, intermediate, and high DCIS risk groups the 10-year risks of developing an invasive IBE, were 3.7%,12.3%, and 19.2%, respectively ($P \leq .006$). In multivariable analyses, factors significantly associated with IBE risk were DCIS Score, tumour size, and menopausal status.

Need for breast irradiation

The four major trials of treatment for DCIS had the main aim of determining whether radiotherapy was a necessary part of the treatment after excision of DCIS.[11, 12, 13, 14] All have shown the impact of breast irradiation on DCIS relapse and invasive progression. As an example, in EORTC 10853, the 10-year local relapse-free (LR) rate was 74 % in the group treated with local excision (LE) alone compared with 85% in those treated by LE plus RT (log-rank $P < .0001$; hazard ratio [HR] = 0.53). The risks of DCIS relapse and invasive progression were reduced by 48 % ($P < .0011$) and 42 % ($P < 0065$) respectively.

The effect of RT was homogeneous across all assessed risk factors, that is, there was no subgroup in which it could be shown that radiotherapy was redundant.[15] Despite this series with long term follow-up are published in which women with completely excised low and intermediate DCIS, <2cm are treated by wide excision and no radiotherapy. In a recent publication, Wehner *et al* reported 205 women treated with LE alone among whom the 6 years probability of relapse was 6.6%[16], similar to that in the low/intermediate category in the UKCCCR/ANZ DCIS trial.

 ISSN 2330-4049

Adjuvant tamoxifen

Tamoxifen has been tested in two prospective randomised trials, NSABP B 24[17] and UKCCCR/ANZ DCIS.[18] In B24, 1804 women with DCIS, including those with margin involvement, were treated by lumpectomy, radiotherapy, and tamoxifen 20 mg daily for 5 years or lumpectomy, radiation therapy, and placebo. To be eligible for UKCCCR/ANZ DCIS, the 1701 participants had complete local excision of DCIS and were randomised in a 2x2 factorial manner to observation, radiotherapy, tamoxifen or radiotherapy and tamoxifen. Long-term results are shown in **TABLE 2**.

In B24, after a median follow-up of 163 months, the overall ipsilateral breast recurrence rate was 19% in the placebo arm and 9% in the tamoxifen group.[19] There was a reduction in both DCIS relapse and invasive progression in the tamoxifen arm. Allred *et al* determined estrogen (ER) and progesterone receptors (PgR) in 732 (41%) of B24 participants.[20] ER was positive in 76% of patients. Those with ER-positive DCIS who received tamoxifen had significant reduction in subsequent breast cancer at 10 years (hazard ratio [HR], 0.49; $P < 0.001$). No significant effect was seen in ER-negative DCIS.

In UK/ANZ after 12.7 years median follow-up, tamoxifen reduced both ipsilateral DCIS relapse and contralateral events but had no impact on ipsilateral invasive progression.[21] The non-concordant results from the two trials may be a reflection of age differences. In the UK/ANZ trial where most cases were derived from the screening programme >90% were aged 50 years or older. In B24 however, most participants were younger with only 34% being aged >50.

Staley *et al* conducted a Cochrane review of post-operative tamoxifen for DCIS based on these 2 trials, totalling 3375 women.[22] They concluded that tamoxifen reduced incidence of both ipsilateral and contralateral DCIS (RR 0.50). There was a non-significant trend towards more endometrial cancer in the tamoxifen group but no impact on overall mortality.

Adjuvant aromatase inhibitors

No results are yet available from randomised trials such as IBIS-2 on the effect of aromatase inhibitors in post-menopausal women with ER positive DCIS.[23] Dixon *et al* reported that in a randomised neoadjuvant study of 206 postmenopausal women with invasive ER+ve breast 28 pre and post-treatment specimens contained ER+ve DCIS.[24] Both anastrozole and letrozole significantly inhibited proliferation. There was reasonable agreement between the fall in proliferation within both the invasive and in situ components.

Chen *et al* conducted a neoadjuvant trial in which 9 patients with ER-positive pure DCIS diagnosed by stereotactic core biopsy were treated with letrozole, followed by excision biopsy.[25] Proliferation and apoptotic markers were measured at baseline and at three months and compared with specimens from patients not given preoperative treatment. There was significant reduction of PR, and Ki67 as well as increase in CD68-positive cells. The authors questioned whether those responding might be able to avoid surgical intervention.

Magnetic resonance imaging (MRI)

MRI has been used particularly in women with dense breasts in an attempt to determine the extent of DCIS, in the hope that a one-stage operation can be performed. This may not always be helpful. Davis *et al* reviewed 218 patients with DCIS. Of whom 64 did not have a preoperative MRI, and154 who did.[26] Re-excision rates were similar (34% and 39 % respectively). Conversion rates to mastectomy were 9% and 8 %. Average specimen weights at definitive surgery were 50g and 49g respectively. The authors concluded that preoperative MRI did not add benefit to the care of women with DCIS.

A group from the Academic Medical Center Amsterdam evaluated preoperative MRI to try and identify those patients with DCIS who are at high risk of invasive breast cancer.[27] There were 125 with pure DCIS on core biopsy and 18 (14 %) had invasion on final histology. Suspicious enhancement on MRI was seen in 73 lesions, with a type 1 curve was seen in 12, type 2 in 19, and type 3 curve in 42. The most predictive features on multivariate analysis for excluding invasive disease were no enhancement or a type 1 curve and this had a negative predictive value 98.5 %.

Pilewskie *et al* reviewed 352 patients with DCIS of whom 217 received MRI and 135 did not.[28] There was no difference in terms of type of initial surgery and number of reoperations between the two groups. Successful breast conservation occurred more frequently in the no-MRI group. Additional biopsies were performed on 38 % of the MRI group compared with 7 % in the no-MRI group; ≥2 additional biopsies were performed in 18 % of the MRI group and 2 % of the no-MRI group ($p < 0.0001$). These yielded a cancer diagnosis in 26 % of MRI and 33 % of no-MRI patients. MRI was not as good as mammography in detecting size of DCIS lesions preoperatively 52 % of mammograms were accurate within 10mm in 52 % of cases compared with 41 % of MRIs.

These data suggest that MRI is likely to pick up suspicious looking lesions which are histologically non-malignant and also does not, in most cases, add precision to determination of extent of DCIS. Hence MRI should not be used in a screening role when DCIS has been diagnosed but be reserved for those cases where there is genuine difficulty in identifying multicentric or more extensive disease.

 ISSN 2330-4049

TABLE 2: Breast events in NSABP B24 and UK/ANZ DCIS trials.

Feature	NSABP 24		UK/ANZ DCIS			
Treatment	Placebo	Tam	Obs	Tam	RT	Tam+RT
Number	900	899	544	567	267	376
Ipsilateral DCIS	68(7.5%)	60 (6.7%)	96 (18%)	72 (13%)	16 (6%)	13 (4%)
Ipsilateral INV	81 (9%)	59 (6.5%)	52 (10%)	49 (9%)	10 (4%)	11 (3%)
Contralateral DCIS	25 (3%)	14 (1.5%)	9 (2%)	4 (1%)	2 (1%)	2 (1%)
Contralateral INV	48 (5%)	30 (3%)	20 (4%)	7 (1%)	5 (2%)	7 (2%)

Abbreviations: Tam = tamoxifen; Obs = Observation; RT = Radio therapy

Surgery

Although a small proportion of patients with DCIS present with symptomatic disease, a lump or nipple discharge, the majority of cases will be picked up following mammography. When micro calcification graded as M3, M4 or M5 is observed an ultrasound will be carried out to determine whether there is an associated mass and also to examine whether abnormal axillary nodes are present. In the absence of a mass, a stereotactic core is performed and a marker inserted at the site of the core biopsies. This obviates need for a subsequent stereotactic core since the marker acts as a target for an ultrasound guided wire localisation. In some cases the DCIS will be clearly identified and extent can be measured. If there is extensive micro calcification, by taking cores from close to the margins may be useful so that there is histological proof of extent. This may help to persuade the patient to undergo mastectomy rather than breast conserving surgery.

Localised wide excision

The standard method of dealing with an impalpable breast lesion was wire localisation under ultrasound or stereotactic guidance, followed by surgical excision under general anaesthesia.[29] Kohler *et al* evaluated ultrasound and mammography guided wire marking in 668 women with 741 impalpable breast lesions. Ultrasound was used in 418, mammography in 284 and for 39 lesions both techniques were combined. Specimen ultrasound suggested that 91 % of lesions were resected completely and specimen x-ray suggested complete resection in 89%. Histologically 20 % of the malignant lesions marked with sonography and 37 % of cancers marked mammographically had involved margins. Re-excision was necessary in 10 patients localised by ultrasound and in 25 patients who were x-ray localised.

Wire guided localisation (WGL) was usually successful but could be painful for the patient and occasionally the marker moved due to traction on the wire. To avoid this, in 1999, Luini *et al.* reported a new technique using a small quantity of 99mTc-labelled colloidal albumin is injected directly into the lesion under stereotactic-radiographic or ultrasonic guidance.[30] A gamma probe was then used to locate the lesion and guide the surgical excision. The results of radio-guided occult lesion localisation (ROLL) in 30 patients were compared with wire localisation in another 30 patients. In the WGL group, the mean distance from the lesion centre to the specimen margin was 25mm compared with 14mm in the radio-guided group so that ROLL removal reduced excision volume.

Several relatively small trials suggested that ROLL and WGL were equivalent.[31, 32, 33] Van der Ploeg *et al.* reviewed the available literature and concluded that ROLL was a promising technique, which achieved complete excision more frequently than WGL and was more accurate and faster.[34] Subsequently, contrary evidence came from a multicentre randomised controlled trial comparing ROLL and WGL for preoperative tumour localisation.[35] Complete tumour removal was achieved in 140/162 (86 %) patients in the ROLL group and 134/152 (88 %) patients in the WGL group. Re-excision was required in 12 % of the ROLL group versus 10 % in the WGL group. Mean specimen volumes were 71cm^3 versus 64cm^3 in the ROLL and WGL arms respectively. No significant differences were observed in the duration and difficulty of either the radiological or surgical procedures. It was suggested that ROLL cannot replace WGL as the standard of care.

Arentz *et al* hypothesized that the hematoma-directed ultrasound-guided (HUG) procedure to localise impalpable lesions would allow excision without the problems of WGL and decrease the high rate of margin positivity.[36] A multifrequency linear array transducer was employed intraoperatively for the HUG localisation, and a block of tissue surrounding the hematoma removed. Results were reported in 455 patients of whom 126 (28 %) had needle localization and 329 (72 %) underwent HUG. The previous core-biopsy site was successfully excised in all patients using HUG. Of those with cancer margins were positive in 24 % of HUG compared with 47 % of those needle localised. This suggests that HUG is more accurate in localising impalpable lesions than WGL but the technique is dependent upon the surgeon being trained in this aspect of ultrasound.

Margins

Although there is agreement that the aim is to achieve uninvolved margins, there has been disagreement concerning margin width. Dunne *et al* carried out a review of published trials examining outcomes after breast conserving surgery and

ISSN 2330-4049

radiotherapy for DCIS.[37] There were 4,660 patients and those with negative margins were at substantially reduced risk of relapse compared with those with positive margins (Odds ratio 0.36). Negative margins were better than close margins in terms of relapse (OR 0.59). A 2mm margin was better than <2 mm (OR 0.53). There was however no significant difference in relapse rate with margins 2-5 mm or >5mm.

Wang *et al* criticised the methodology used by Dunne, arguing that only randomised trials were included and here was duplication of data with multiple studies from the same institution drawing on overlapping patient sources.[38] Additionally, Dunne pooled study results and did not use them as a stratification factor. Wang *et al* identified 21 randomised and non-randomised studies with a total of 7564 women and performed a network meta-analysis. Of the patients, 3098 were treated by BCS alone and 4466 with additional radiotherapy. Ipsilateral relapse occurred in 565 (16 %) and 501 (11 %) respectively.

Comparing negative with positive margins, there was a reduced relapse risk both with radiotherapy (OR = 0.46), and without radiotherapy (OR = 0.34). For positive margins versus negative margin >0 mm, >2, >5 and ≥10 mm the ORs were 0.45, 0.38, 0.55, and 0.17 respectively. When comparing a negative margin >2 mm, with a negative margin of ≥10 mm the latter carried a lower risk of relapse (OR = 0.46). They concluded that within the constraints of satisfactory cosmesis, an attempt should be made to achieve wide negative margins but that further studies should determine whether margin thresholds >10 mm are of benefit.

Sentinel node biopsy

Ansari *et al* conducted a meta-analysis of results from 22 series of sentinel biopsy (SNB) in 3166 patients with a pre-operative diagnosis of DCIS.[39] The average rate of sentinel node involvement was approximately 7%. When however the post-operative diagnosis was DCIS alone the rate of nodal positivity fell to 4%. Studies predicting invasive disease after a core biopsy showing DCIS have shown that the significant variables were high grade DCIS, >2.5cm, <12 core biopsies, palpable mass, mass on imaging and inflammatory infiltrate in the core biopsy.

Osako *et al* investigated SNB in a large cohort of women with DCIS. The node was subjected to frozen section (FS) analysis in 338 patients treated between 2007 and 2009. For 285 who undergoing surgery between 2009 and 2011 the sentinel node (SN) was examined using the one-step nucleic acid amplification (OSNA) assay. More cases of SN metastases were detected by OSNA than FS (12/285 (4 % versus 1/338 (0.3 %). The majority were micrometastases. The characteristics of DCIS at high-risk of invasion (mass, size, grade, and comedo type, preoperative breast biopsy) did not apply to OSNA assay–positive DCIS.

For those patients having immediate reconstruction it is best that the SNB is carried out as a stand-alone procedure in order that the axillary nodal status in known before embarking on what may be a complex reconstruction. If this has not been carried out the need to carry out carry out a completion axillary clearance may compromise the achievement of a good cosmetic result.

Which patients with DCIS require a mastectomy?

There is probably less argument about indications for mastectomy in women with DCIS than there is concerning suitability for breast conserving surgery. An absolute indication is histologically proven presence of DCIS in more than one quadrant. In the event of multifocal rather than multicentric disease, the main consideration is whether the DCIS can be extirpated and still leaves the patient with a reasonable cosmetic result. Trials have varied in maximum allowable extent of DCIS but the clinical decision should be based on the extent of disease in relation to the size of the breast.

When the extent of DCIS mandates mastectomy a sentinel node biopsy should be performed. Upstaging from DCIS to invasive disease occurs in up to 20% of cases with pure DCIS on the original core.[40, 41] When invasive disease is present it is now accepted that; provided axillary ultrasound is normal, sentinel node biopsy is the best method of staging the axilla.[42] Ansari *et al* reported a meta-analysis of results from 22 series of sentinel biopsy in 3166 patients with a pre-operative diagnosis of DCIS.[43] The average rate of sentinel node involvement was approximately 7 %. When however the post-operative diagnosis was DCIS alone the rate of nodal positivity fell to 3.7 %.

The greater the extent of DCIS the higher the risk of associated invasion. In a series of 398 women with pure DCIS on core biopsy operated on at the MD Anderson Hospital 20 % were upgraded on final histology.[44] Multivariate analysis indicated that the significant prognostic variables included younger age, high grade DCIS and mammographic size ≥4cm. The same group reported later that invasive carcinoma was found at definitive surgery in 30 % of those with DCIS >15mm and only 11 % of those with DCIS ≤15mm.[45]

It is often assumed that a total mastectomy provides a cure for DCIS, with a zero risk of local recurrence. Unfortunately this is not true. Residual breast tissue may be left behind, particularly in the axillary tail and in the most inferior part of the breast. The larger series that have reported recurrence rates after mastectomy for ductal carcinoma. In situ are summarised in **Table 3**.[46, 47, 48, 49] This indicates that 1-2 % of patients will develop a relapse. Kelley *et al* used the USC Van Nuys Prognostic Index, which is an algorithm based on DCIS size, nuclear grade, necrosis, margin width, and patient age. Recurrence occurred in 11 patients, all of whom scored 10–12

 ISSN 2330-4049

using the USC/VNPI and all had multifocal disease and comedo-type necrosis.

TABLE 3: Recurrence after mastectomy for DCIS.

Author	N	Recurrence	Follow-up
Bedwani 1981[46]	112	1(1%)	60 months
Silverstein 1995[47]	228	2 (1%)	78 months
Van der Velden 2007[48]	408	4 (1%)	65 months
Kelley 2011[49]	496	11 (2%)	83 months

Management plan

An algorithm for management of DCIS is given in **Figure 1**. Treatment should not be planned until there is histological confirmation of the diagnosis of DCIS, accepting that up to 20 % of cases will eventually prove to have invasion/microinvasion. Outside of research protocols breast MRI should be confined to those cases where the extent of disease is indeterminate. All patients undergoing mastectomy for extensive DCIS should have a sentinel node biopsy as part of primary treatment. Sentinel node biopsy should also be considered for patients with DCIS ≥2.5cm having a wide excision because of the high risk of invasive disease being present.[39]

If a mastectomy is deemed necessary this will normally be a skin sparing procedure since this has been shown to be as effective as a standard mastectomy in terms of local control of disease and can help to achieve a better cosmetic outcome.[50] The Gustave Roussy Breast Cancer Study Group Data analysed 238 consecutive patients diagnosed with DCIS and who had undergone mastectomy and SNB between 2005 and 2011.[51] Of these, 57% had immediate breast reconstruction 43 % did not. The commonest reason for immediate reconstruction not being offered was that it had not been mentioned by the surgeon (33.4 %). The rate of immediate reconstruction was highest in those <50 and (52.2 %), and was lower among women with diabetes (0.7 %) or obesity (8.8 %). The choice of reconstruction was unaffected by tobacco use or positive lymph node status. This report from a centre of excellence highlights a potential lacuna in communication. Discussion of immediate reconstruction should be an intrinsic part of discussion between the surgeon and the patient with DCIS.

In a small series of 14 nipple-saving mastectomies (NSM), Nahabedian and Tsangaris reported that sensation was present in 43 %, delayed healing occurred in 29 % and symmetry was achieved in five of 50%.[52] Local relapse occurred 27%, and secondary procedures were required in 36%. Reviewing the evidence for efficacy and safety of nipple-preserving mastectomy in 2006, Garcia-Etienne and Borgen concluded that the published studies lacked the power to determine a role for NSM.[53]

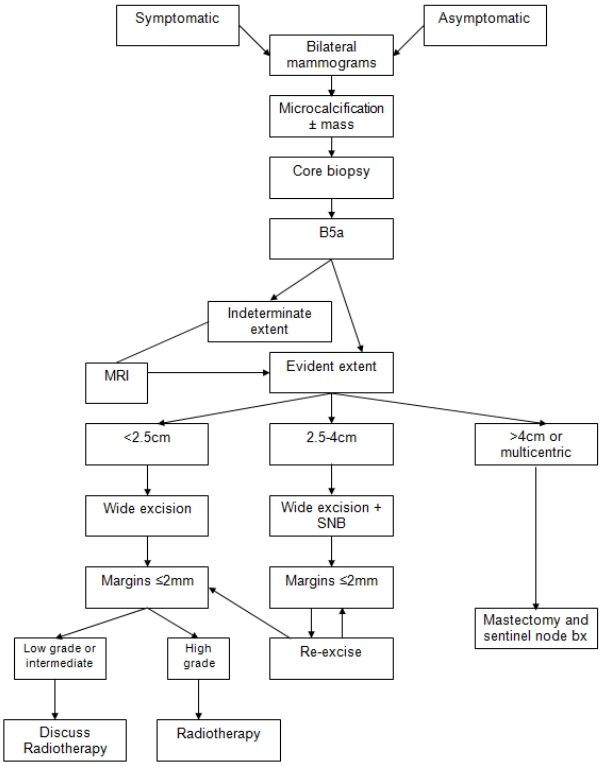

FIG. 1: Algorithms for DCIS management.

The situation changed when Petit *et al* reported a series of 570 patients with breast cancer treated by NSM were performed for carcinoma.[54] An immediate frozen section was taken from retroareolar tissue. If tumour was present the patient was not treated by NSM (63/570, 12%). Likelihood of areola positive histology increased with tumour size but was unrelated to the nodal status. The local recurrence rate was 0.9% per year. Provided that appropriate control is observed and in experienced hands, NPM is a safe surgical option in selected patients with DCIS.

Conflict of interest

The authors declare that they have no conflicts of interest. The authors alone are responsible for the content and writing of the paper.

References

1. Veronesi U, Saccozzi R, Del Vecchio M, *et al*. Comparing radical mastectomy with quadrantectomy, axillary dissection, and radiotherapy in patients with small cancers of the breast. *N Engl J Med* 1981; **305**: 6-11.
2. Fisher B, Redmond C, Poisson R, *et al*. Eight-year results of a randomized clinical trial comparing total mastectomy and lumpectomy with or without

ISSN 2330-4049

irradiation in the treatment of breast cancer. *N Engl J Med* 1989; **320**: 822-8.
3. Van Dongen JA, Bartelink H, Fentiman IS, et al. Factors influencing local relapse and survival and results of salvage treatment after breast-conserving therapy in operable breast cancer: EORTC Trial 10801, breast conservation compared with mastectomy in TNM stage I and II breast cancer. *Eur J Cancer* 1992; **28A**: 801-5.
4. Jacobson JA, Danforth DN, Cowan KH, et al. Ten-year results of a comparison of conservation with mastectomy in the treatment of stage I and II breast cancer. *N Engl J Med* 1995; **332**: 907-11.
5. van Dongen JA, Bartelink H, Fentiman IS, Peterse JL. Ductal carcinoma in situ (DCIS) of the breast –a therapeutic dilemma. *Eur J Surg Oncol* 1987; **13**: 123-126.
6. Virnig BA, Tuttle TM, Shamliyan T, Kane RL. Ductal carcinoma in situ of the breast: a systematic review of incidence, treatment, and outcomes. *J Natl Cancer Inst* 2010; **102**:170–178.
7. Pinder SE, Duggan C, Ellis IO, Cuzick J, Forbes JF, Bishop H, Fentiman IS & George WD. A new pathological system for grading DCIS with improved prediction of local recurrence: results from the UKCCCR/ANZ DCIS trial. *Br J Cancer* 2010; **103**: 94-100.
8. Bijker N, Petersee JL, Duchateau L, Julien J-P, Fentiman IS, et al. Risk factors for recurrence and metastasis after breast conserving therapy for ductal carcinoma in situ: analysis of European Organisation for Research and Treatment of cancer trial 10853. *J Clin Oncol* 2001; **19**: 2263-2271.
9. Esserman L, Shieh Y, Thompson I. Rethinking screening for breast cancer and prostate cancer. *JAMA* 2009; **302**:1685-1692.
10. Solin LJ, Gray R, Baehner FL, Butler SM, Hughes LL, et al. A multigene expression assay to predict local recurrence risk for ductal carcinoma in situ of the breast. *J Natl Cancer Inst* 2013; **105**:701–710.
11. Wapnir IL, Dignam JJ, Fisher B, Mamounas EP, Stewart J. Anderson SJ, et al. Long-term outcomes of invasive ipsilateral breast tumor recurrences after lumpectomy in NSABP B-17 and B-24 randomized clinical trials for DCIS. *J Natl Cancer Inst* 2011; **103**: 478–488.
12. Cuzick J, Sestak I, Pinder SE, Ellis IO, Forsyth S, Bundred NJ, Forbes JF, Bishop H, Fentiman IS, George WD. Effect of tamoxifen and radiotherapy in women with locally excised ductal carcinoma in situ: long-term results from the UK/ANZ DCIS trial. *Lancet Oncol* 2011; **12**: 21-29.
13. Donker M, Litiere S, Werutsky G, Julien JP, Fentiman IS, et al. Breast-conserving treatment with or without radiotherapy in Ductal Carcinoma In Situ: 15-year Recurrence Rates and Outcome After a Recurrence, from the EORTC 10853 Randomized Phase III Trial. *Journal of Clinical Oncology* 2013; **31**:4054-4059.
14. Holmberg L, Garmo H, Granstrand B, et al. Absolute risk reductions for local recurrence after postoperative radiotherapy after sector resection for ductal carcinoma in situ of the breast. *J Clin Oncol* 2008; **26**:1247–1252.
15. Correa C, McGale P, Taylor C, et al. Early Breast Cancer Trialists' Collaborative Group. J Natl *Cancer Inst Monogr* 2010; **2010**:162–177.
16. Wehner P, Lagios MD, Silverstein MJ. DCIS treated with excision alone using the national Comprehensive Cancer Network (NCCN) Guidelines. *Ann Surg Oncol* 2013; **20**: 3175-9.
17. Fisher B, Dignam J, Wolmark N, et al. Tamoxifen in treatment of intraductal breast cancer: National Surgical Adjuvant Breast and Bowel Project B-24 randomised controlled trial. *Lancet* 1999; **353**: 1993–2000.
18. Houghton J, George WD, Cuzick J, Duggan C, Fentiman IS, Spittle M; UK Coordinating Committee on Cancer Research; Ductal Carcinoma in situ Working Party; DCIS trialists in the UK, Australia, and New Zealand. Radiotherapy and tamoxifen in women with completely excised ductal carcinoma in situ of the breast in the UK, Australia, and New Zealand: randomised controlled trial. *Lancet* 2003; **362**:95-102.
19. Wapnir IL, Dignam JJ, Fisher B, et al. Long-term outcomes of invasive ipsilateral breast tumor recurrences after lumpectomy in NSABP B-17 and B-24 randomized clinical trials for DCIS. *J Natl Cancer Inst* 2011; **103**:478–488.
20. Allred DC, Anderson SJ, Paik S, et al. Adjuvant tamoxifen reduces subsequent breast cancer in women with estrogen receptor–positive ductal carcinoma in situ: a study based on NSABP Protocol B-24. *J Clin Oncol* 2012; **30**:1268-1273.
21. Cuzick J, Sestak I, Pinder SE, et al. Effect of tamoxifen and radiotherapy in women with locally excised ductal carcinoma in situ: long-term results from the UK/ANZ DCIS trial. *Lancet Oncol* 2011**;** **12**: 21-9.
22. StaleyH, McCallum I, Bruce J. Postoperative tamoxifen for ductal carcinoma in situ. *Cochrane Database Syst Rev* 2012; **10:**CD007847.
23. Cuzick J. Aromatase inhibitors in prevention – data from the ATAC (Arimidex, tamoxifen alone or in combination) trial and the design of IBIS-II (the second International Breast Cancer Intervention Study). *Recent Results Cancer Res* 2003; **163**:96–103.
24. Dixon JM, Faratian D, White S et al. DCIS and aromatase inhibitors. *J Steroid Biochem Mol Biol* 2007; **106**:173-9.

 ISSN 2330-4049

25. Chen YY, DeVries S, Anderson J, Lessing J, et al. Pathologic and biologic response to preoperative endocrine therapy in patients with ER-positive ductal carcinoma in situ. *BMC Cancer* 2009; **9**:285.
26. Davis KL, Barth RJ Jr, Gui J, et al. Use of MRI in preoperative planning for women with newly diagnosed DCIS: risk or benefit? *Ann Surg Oncol* 2012; **19**:3270-4.
27. Deurloo EE, Sriram JD, Teertstra HJ, et al. MRI of the breast in patients with DCIS to exclude the presence of invasive disease. *Eur Radiol* 2012; **22**:1504-11.
28. Pilewskie M, Kennedy C, Shappell C, et al. Effect of MRI on the management of ductal carcinoma in situ of the breast. *Ann Surg Oncol* 2013; **20**:1522-9.
29. Chaudary MA, Reidy JF, Chaudhuri R, Millis RR, Hayward JL, Fentiman IS. A new and improved device for the pre-operative localisation of impalpable breast lesions. *Br J Surgery* 1990; **77**: 1191-1192.
30. Luini A, Zurrida S, Paganelli G, et al. Comparison of radioguided excision with wire localization of occult breast lesions. *Br J Surg* 1999; **86**:522-5.
31. Medina-Franco H, Abarca-Perez L, García-Alvarez MN. Radioguided occult lesion localization (ROLL) versus wire-guided lumpectomy for non-palpable breast lesions: a randomized prospective evaluation. *J Surg Oncol* 2008; **97:**108-11.
32. Mariscal Martínez AM, Sola M, Perez de Tudela A. Nonpalpable breast cancer lesions: randomized comparison with wire localization in patients undergoing conservative surgery and sentinel node biopsy. *AJR* 2009; **193**:1001–1009.
33. Sarlos D, Frey LD, Haueisen H, Landmann G, Kots LA, Schaer G. Radioguided occult lesion localization (ROLL) for treatment and diagnosis of malignant and premalignant breast lesions combined with sentinel node biopsy: a prospective clinical trial with 100 patients. *Eur J Surg Oncol* 2009; **35**:403-8.
34. van der Ploeg IM, Hobbelink M, van den Bosch MA. Radioguided occult lesion localisation' (ROLL) for non-palpable breast lesions: a review of the relevant literature. *Eur J Surg Oncol* 2008; **34**:1-5.
35. Postma EL, Verkooijen HM, van Esser S, Hobbelink MG et al, Efficacy of 'radioguided occult lesion localisation' (ROLL) versus 'wire-guided localisation' (WGL) in breast conserving surgery for non-palpable breast cancer: a randomised controlled multicentre trial. *Breast Cancer Res Treat* 2012; **136:**469-78.
36. Arentz C, Baxter K, Boneti C, et al. Ten-year experience with hematoma-directed ultrasound-guided (HUG) breast lumpectomy. *Ann Surg Oncol* 2010; **17 Suppl 3**:378-83.
37. Dunne C, Burke JP, Morrow M, Kell MR. Effect of margin status on local recurrence after breast conservation and radiation therapy for ductal carcinoma in situ. *J Clin Oncol* 2009; **27**:1615-1620.
38. Wang S-Y, Chu H, Shamliyan T, et al. Network meta-analysis of margin threshold for women with ductal carcinoma in situ. *J Natl Cancer Inst* 2012; **104**:507–516.
39. Ansari B, Ogston SA, Purdie CA, et al. Meta-analysis of sentinel node biopsy in ductal carcinoma in situ of the breast. *Br J Surg* 2008; **95**: 547-554.
40. Sakr R, Antoine M, Barranger E, et al. Value of sentinel lymph node biopsy in breast ductal carcinoma in situ upstaged to invasive carcinoma. *Breast J* 2008; **14**: 55-60.
41. Van la Parra RF, Ernst MF, Barneveld PC, et al. The value of sentinel lymph node biopsy in breast ductal carcinoma in situ (DCIS) and DCIS with microinvasion of the breast. *Eur J Surg Oncol* 2008; **34**: 631-5.
42. Veronesi U, Paganelli G, Viale G, Luini A, Zurrida S, Galimberti V et al. A randomized comparison of sentinel-node biopsy with routine axillary dissection in breastcancer. *N Engl JMed* 2003; **349**: 546–553.
43. Ansari B, Ogston SA, Purdie CA, et al. Meta-analysis of sentinel node biopsy in ductal carcinoma in situ of the breast. *Br J Surg* 2008; **95**: 547-554.
44. Yen TWE, Hunt KK, Ross MI, et al. Predictors of invasive breast cancer in patients with an initial diagnosis of ductal carcinoma in situ: a guide to selective use of sentinel lymph node biopsy in management of ductal carcinoma in situ. *J Am Coll Surg* 2005; **200**: 516-526.
45. Huo L, Sneige N, Hunt KK, et al. Predictors of invasion in patients with core-needle biopsy-diagnosed ductal carcinoma in situ and recommendations for a selective approach to sentinel node biopsy in ductal carcinoma in situ. *Cancer* 2006; **107**: 1760-8.
46. Bedwani R, Vana J, Rosner D, et al. Management and survival of female patients with “minimal” breast cancer. *Cancer* 1981; **47**: 2769–2778.
47. Silverstein MJ, Barth A, Poller DN, et al. Ten-year results comparing mastectomy to excision and radiation therapy for ductal carcinoma in situ of the breast. *Eur J Cancer* 1995; **31**:1425–1427.
48. Schouten van der Velden AP, van Vugt R, Van Dijck JA, et al. Local recurrences after different treatment strategies for ductal carcinoma in situ of the breast: a population-based study in the East Netherlands. *Int J Radiation Oncology Biol Phys* 2007; **69**:703-10.

 ISSN 2330-4049

49. Kelley L, Silverstein M, Guerra L. Analyzing the risk of recurrence after mastectomy for DCIS: a new use for the USC/Van Nuys Prognostic Index. *Ann Surg Oncol* 2011; **18**:459–462.
50. Kroll SS, Schusterman MA, Tadjalli HE, Singletary SE, Ames FC. Risk of recurrence after treatment of early breast cancer with skin-sparing mastectomy. *Ann Surg Oncol* 1997; **4:**193-7.
51. Naoura I, Mazouni C, Ghanimeh J, Leymarie N, et al. Factors influencing the decision to offer immediate breast reconstruction after mastectomy for ductal carcinoma in situ (DCIS): the Institut Gustave Roussy Breast Cancer Study Group experience. *Breast* 2013; **22**:673-5.
52. Nahabedian MY, Tsangaris TN Breast reconstruction following subcutaneous mastectomy for cancer: a critical appraisal of the nipple-areola complex. *Plast Reconstr Surg* 2006; **117**:1083-90.
53. Garcia-Etienne CA, Borgen PI. Update on the indications for nipple-sparing mastectomy. *J Support Oncol* 2006; **4**:225-30.
54. Petit JY, Veronesi U, Rey P, et al. Nipple-sparing mastectomy: risk of nipple-areolar recurrences in a series of 579 cases. *Breast Cancer Res Treat* 2009; **114**:97-101.

 ISSN 2330-4049

International Journal of Cancer Therapy and Oncology
www.ijcto.org

Impact of heterogeneities on lateral penumbra in uniform scanning proton therapy

Suresh Rana, Hardev Singh

Department of Medical Physics, ProCure Proton Therapy Center, Oklahoma City, Oklahoma, USA.

Received October 5, 2013; Revised November 10, 2013; Accepted November 15, 2013; Published Online November 22, 2013

Original Article

Abstract

Purpose: In the treatment planning of uniform scanning proton therapy, an aperture block is designed for each beam with a margin, which typically includes the lateral penumbra measured in water (homogenous) medium. However, during real proton therapy treatment, protons may pass through tissues of different densities within the patient's body before they are stopped. The main aim of this study was to investigate the dependency of lateral penumbra on low- and high-density heterogeneities placed in the plateau and spread-out Bragg peak (SOBP) regions. **Method:** The measurements were performed by placing radiographic films at the isocenter (center of SOBP), and each proton beam was delivered with 150 monitor units using standard beam conditions of the institution. **Results and Conclusion:** The preliminary results from this study showed that the lateral penumbra of uniform scanning proton beams was less sensitive to the inhomogeneities introduced in the protons beam path. The low-density heterogeneity in the plateau region had more impact on the lateral penumbra when compared to the low-density in the SOBP region. In contrast, the placement of high-density heterogeneity (whether in the plateau or SOBP region) produced a very minimal difference. The overall difference in lateral penumbra among different phantoms was within ±1 mm.

Keywords: Lateral penumbra; Uniform scanning proton therapy; Inhomogeneity; SOBP

Introduction

In uniform scanning proton therapy planning, an aperture block is designed for each beam with a margin, which typically includes the width of the lateral penumbra. A sharp lateral penumbra is particularly important for the treatment sites that have organs at risk (OARs) abutting the target volume. Several groups[1-5] have performed the measurements and Monte Carlo simulation investigating the dependency of lateral penumbra of proton beams on different beam conditions and geometrical configurations, and it was found that lateral penumbra increases with an increase in range (or energy), depth, and air gap between the aperture/range compensator and phantom.

Corresponding author: Suresh Rana; Department Medical Physics, ProCure Proton Therapy Center, 5901 West Memorial Road, Oklahoma City, Oklahoma, USA.
Email: suresh.rana@gmail.com

Cite this article as:
Rana S, Singh H. Impact of heterogeneities on lateral penumbra in uniform scanning proton therapy. Int J Cancer Ther Oncol 2013; **1**(2):01026. **DOI**: 10.14319/ijcto.0102.6

The commissioning of treatment planning system (TPS) typically includes the measured data that are obtained in a homogenous medium. However, during real proton therapy treatment, protons may pass through tissues of different densities within the patient's body before they are stopped. The presence of heterogeneity along the protons beam path can change the energy spectrum of proton fluence, and this may change the width of lateral penumbra at a given depth as well as cause the degradation of the Bragg peak region. While previous studies have investigated the lateral penumbra of protons in a homogenous medium, the impact of high- and low-density heterogeneities on lateral penumbra for uniform scanning proton beams is yet to be investigated. The principal aim of this study was to perform the experimental measurements to investigate the dependency of lateral penumbra on inhomogeneities placed at different locations upstream from the measurement depth.

Methods and Materials

The measurements in this study were performed for uniform scanning proton beams on an IBA Cyclotron (IBA, Louvain-la-Neuve, Belgium). A detailed description on the uniform scanning proton therapy system has been provided elsewhere.[6, 7] In order to study the impact of heterogeneities

ISSN 2330-4049

on lateral penumbra, we manufactured one homogenous phantom and four inhomogeneous phantoms (**Figure 1**) utilizing solid-water plates (CIRS, Norfolk, VA), air, and poly-vinyl chloride (PVC) tile.

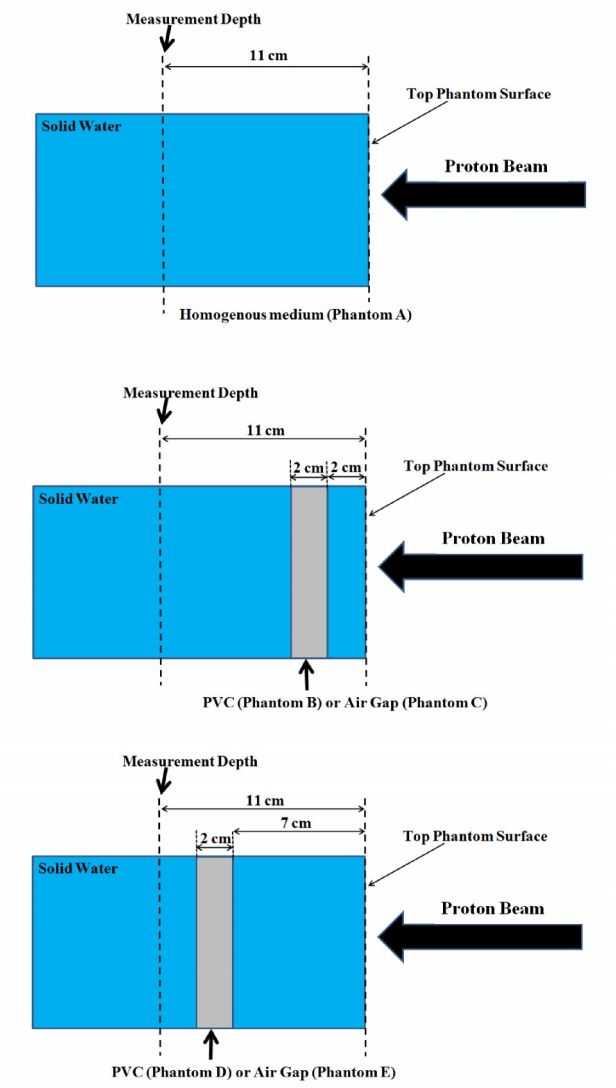

FIG. 1: Schematic diagram of homogenous *Phantom A* and inhomogeneous *Phantoms B, C, D,* and *E.* In each phantom, the measurement was always taken at 11 cm depth from the top surface of the phantom. Each phantom had a rectangular area of 30 × 30 cm^2.

Heterogeneities in the plateau region

An inhomogeneous *Phantom B* was manufactured by introducing a 2 cm thick PVC tile at the depth 2 cm downstream from the top phantom surface as shown in the **Figure 1**. An inhomogeneous *Phantom C* was manufactured by replacing the PVC tile in *Phantom B* with an air gap thickness of 2 cm.

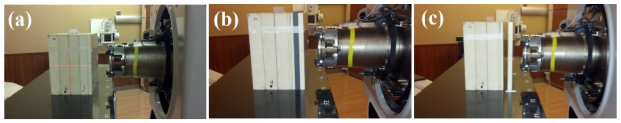

FIG. 2: An experimental setup showing (a) *Phantom A* (homogenous medium), (b) *Phantom B* (inhomogeneous medium with 2 cm thick PVC tile in the plateau region), and (c) *Phantom C* (inhomogeneous medium with 2 cm air gap thickness in the plateau region)

Heterogeneities in the spread-out Bragg peak (SOBP) region

As shown in the **Figure 1**, an inhomogeneous *Phantom D* consisted of a 2 cm thick PVC tile at the depth 7 cm downstream from the top surface of the phantom. An inhomogeneous *Phantom E* was created by replacing the PVC tile in *Phantom D* with an air gap thickness of 2 cm.

Lateral penumbra measurements and analysis

First, the measurements in each phantom were performed by placing radiographic films (Kodak, Rochester, NY; type EDR-2) at the isocenter, and each proton beam was delivered with 150 monitor units (MU). The measurements were taken for beam conditions listed in **Table 1**.

TABLE 1: Beam conditions and geometrical configurations for lateral penumbra.

Beam conditions	Values
Range	16 cm
Modulation	10 cm
Air gap	7 cm
Depth = center of SOBP = isocenter	11 cm
Range compensator thickness	0
Aperture diameter (circular)	10 cm
Snout	10

Abbreviations: SOBP = Spread-out Bragg Peak; Snout10 = maximum field size of 10 cm circular diameter at the isocenter plane.

(*Note: The measurement depth was always at the center of SOBP, which coincided with the isocenter. The proton beam was calibrated to deliver 1cGy absorbed proton dose to water per MU at the center of SOBP under reference conditions (range =16 cm, modulation = 10 cm, aperture = 10 cm, and air gap = 7 cm*).

Second, the Medical Film Processor (Konica Minolta Medical & Graphic, Inc., Tokyo, Japan; model SRX-101A) was used to develop the irradiated EDR-2 films. Third, the Vidar Scanner (Vidar Systems Corporation, Herndon, VA; model DosimetryPro Advantage) was used to scan the processed EDR-2 films. The OmniPro-I'mRT software, version 1.6.009 (IBA Dosimetry, Schwarzenbruck, Germany) was then used for film analysis in order to obtain the measured lateral penumbra (80%-20% distance).

 ISSN 2330-4049

Results and Discussion

Table 2 shows the measured lateral penumbra of uniform scanning proton beams in *Phantoms A, B, C, D,* and *E*. The results indicate that the lateral penumbra of X-magnet is always greater by 0.5 to 0.9 mm than that of Y-magnet. This was mainly due to the positioning of two scanning magnets in beam line with respect to the virtual source. Specifically, the X-magnet has a virtual source to isocenter distance (SAD) of 220 cm, whereas the Y-magnet has a SAD of 183 cm. Since the geometric penumbra becomes larger with an increase in SAD, the X-magnet with a larger SAD will have a wider geometric penumbra resulting increase in overall lateral penumbra when compared to the lateral penumbra of the Y-magnet with a smaller SAD.

Table 2: Measured lateral penumbra of uniform scanning proton beams in homogenous and inhomogeneous phantoms. (*Range =16 cm, Modulation = 10 cm, Aperture = 10 cm Circular Diameter, Measurement Depth = Center of SOBP = Isocenter*)

	Phantoms				
	A (mm)	B (mm)	C (mm)	D (mm)	E (mm)
X-magnet	4.2	4.5	3.8	4.5	4.1
Y-magnet	3.6	4.0	2.9	3.7	3.5
Average	3.9	4.2	3.3	4.1	3.8

Abbreviations: X-magnet = horizontal scanning magnet, Y-magnet = vertical scanning magnet.

(*Note: Phantom A has a homogenous (solid-water) medium, Phantom B has a PVC tile in the plateau region, Phantom C has an air gap in the plateau region, Phantom D has a PVC tile in the SOBP region, and Phantoms E has an air gap in the SOBP region*)

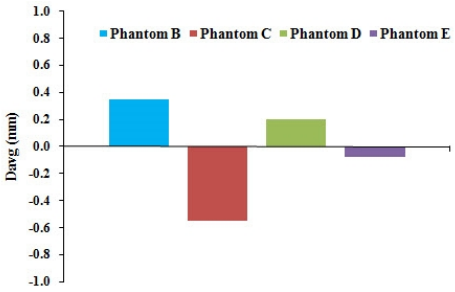

FIG. 3: Comparison of average lateral penumbra results in inhomogeneous phantoms with respect to average lateral penumbra in reference (homogenous) phantom A.

$$D_{avg} = \frac{(D_x + D_y)}{2}$$

where, D_x = difference in lateral penumbra of X-magnet between inhomogeneous phantoms (B, C, D, and E) and reference phantom A, and D_y = difference in lateral penumbra of Y-magnet between inhomogeneous phantoms (B, C, D, and E) and reference Phantom A.

Heterogeneities in the plateau region

The lateral penumbra in *Phantom B* was greater than that of *Phantom A* by an average difference of 0.3 mm. In contrast, the results in *Phantom C* are smaller by an average difference of 0.6 mm when compared to the ones in *Phantom A*. (**Figure 3**)

Heterogeneities in the SOBP region

In comparison to the *Phantom A*, the lateral penumbra in *Phantom D* was greater (average difference 0.2 mm), whereas the lateral penumbra in *Phantom E* was slightly smaller (average difference 0.1 mm). (**Figure 3**)

The results from this study demonstrated that, at a fixed depth, the high-density heterogeneity can increase the lateral penumbra, whereas the low-density heterogeneity will typically decrease the lateral penumbra. This is mainly due to change in range (or energy) of proton beam as range is dependent on the inhomogeneities introduced in the protons beam path. Additionally, the low-density heterogeneity in the plateau region (*Phantom C*) had more impact on the lateral penumbra when compared to the low-density in the SOBP region (*Phantom E*). (**Figure 3**) In contrast, the placement of high-density heterogeneity (whether in the plateau or SOBP region) produced a very minimal difference.

In this study, we investigated the impact of heterogeneities that have rectangular shape, and each inhomogeneous phantom contained either an air gap or a PVC tile. However, in the real clinical situations, proton beams may pass through multiple non-rectangular heterogeneities with various thicknesses before reaching the target. Although the average difference in lateral penumbra due to inhomogeneities is within ±1 mm, the difference may increase for inhomogeneities with thickness more than 2 cm.

Additionally, if the treatment setup has a proton beam passing through the immobilization devices, one should make an effort in reducing the air gap between such devices and the patient body surface. Since the beam aperture margins are typically selected based on the lateral penumbra of a proton beam for a specific range, it is imperative to investigate the accuracy of treatment planning system in predicting the range of proton beam in the presence of inhomogeneities. An inaccurate prediction of proton range by the treatment planning system will lead to wrong selection of the lateral penumbra, and the aperture margins based on the inaccurate lateral penumbra may lead to over-dose to the normal tissues or under-dose to the target volume during the real clinical treatment.

 ISSN 2330-4049

Conclusion

The preliminary results from this study showed that the lateral penumbra of uniform scanning proton beams was less sensitive to the inhomogeneities introduced in the protons beam path. In general, the high-density heterogeneity tend to increase the lateral penumbra, whereas the low-density heterogeneity slightly decreased the lateral penumbra when compared to the results in the homogenous medium. The overall difference in lateral penumbra among different phantoms in this study was within ±1 mm.

Conflict of interest

The authors declare that they have no conflicts of interest. The authors alone are responsible for the content and writing of the paper.

References

1. Urie MM, Sisterson JM, Koehler AM, Goitein M, Zoesman J. Proton beam penumbra: effects of separation between patient and beam modifying devices. *Med Phys* 1986; **13**:734-41.
2. Gottschalk B. Multileaf collimators, air gap, lateral penumbra, and range compensation in proton radiotherapy. *Med Phys* 2011; **38**: i-ii.
3. Oozeer R, Mazal A, Rosenwald JC, Belshi R, Nauraye C, Ferrand R, Biensan S. A model for the lateral penumbra in water of a 200-MeV proton beam devoted toclinical applications. *Med Phys* 1997; **24**:1599-604.
4. Safai S, Bortfeld T, Engelsman M. Comparison between the lateral penumbra of a collimated double-scattered beam and uncollimated scanning beam in proton radiotherapy. *Phys Med Biol* 2008; **53**:1729-50.
5. Rana S, Zeidan O, Ramirez E, Rains M, Gao J, Zheng Y. Measurements of lateral penumbra for uniform scanning proton beams under various beam delivery conditions and comparison to the XiO treatment planning system. *Med Phys* 2013; **40**:091708.
6. Zheng Y, Ramirez E, Mascia A, Ding X, Okoth B, Zeidan O, Hsi W, Harris B, Schreuder AN, Keole S. Commissioning of output factors for uniform scanning proton beams. *Med Phys* 2011; **38**:2299-306.
7. Zheng Y, Liu Y, Zeidan O, Schreuder AN, Keole S. Measurements of neutron dose equivalent for a proton therapy center using uniform scanning proton beams. Med Phys 2012; **39**:3484-92.

 ISSN 2330-4049

International Journal of Cancer Therapy and Oncology
www.ijcto.org

Evaluation of planned dosimetry when beam energies are substituted for a fraction of the treatment course

Samantha E Hawke, Angela Torrance, Lindsay Tremethick

Genesiscare, Radiation Oncology Victoria, Murray Valley Private Hospital, Wodonga, Victoria, Australia.

Received September 11, 2013; Revised October 31, 2013; Accepted November 10, 2013; Published Online November 22, 2013

Technical Report

Abstract

Purpose: The purpose of this technical study was to evaluate how the effect of changing beam energies for one to multiple fractions of a patient's plan affected the overall dose delivered to the planning target volume (PTV) and surrounding organs at risk (OAR's). **Method:** In this study, twenty-eight patient plans from treatment sites including the oesophagus, prostate, lung, spine, rectum, bladder, chest, scapula, and breast were evaluated in the Philips Pinnacle treatment planning system (TPS), of these 14 were originally planned with 15MV and 14 with 10MV. Each of these plans were substituted with a single to multiple fractions with 10MV and 15MV respectively while keeping the original monitor units the same. **Results:** It was determined that when the number of fractions of the substituted beam energy remained at one fifth or less of the overall fractions a change of dose of less than 2% to the PTV could be maintained. The OAR's dose, when the plan had 20% of its fractions substituted with a different energy, were found to change by on average up to 3.5% and 2.3% for original plan energies of 15MV and 10MV respectively. The dose change calculated in the TPS was then verified using ion chamber measurements for bladder and oesophagus treatment plans. **Conclusion:** Results appear to indicate that the site of treatment was not an important factor when changing energy but the overall number of fractions versus the number of fractions substituted with an alternative energy was fundamental. These results may be clinically useful when a radiotherapy department have machines with different photon energies. In the event of a break down, when a patient needs to be urgently treated, it may be possible to treat them on another machine with a different energy, without an immediate recalculation in the TPS. This decision would depend upon the percentage of fractions of their overall treatment needing to be treated before the machine was repaired.

Keywords: Radiotherapy; Fraction; Treatment planning system; Beam energy; Substitution

Introduction

Murray Valley Radiation Oncology Centre has two linear accelerators with different photon energies; a Varian 21iX with 6MV and 10MV photon beams and a Varian 21eX with 6MV and 15MV photon energies.[1] Problems arise when patients planned with 10MV or 15MV cannot be treated due to the machine with that energy capability breaking down. As this department is in a rural setting the patients cannot be treated in another department due to the distance of travel involved.

Corresponding author: Samantha E Hawke; Genesiscare, Radiation Oncology Victoria, Murray Valley Private Hospital, Nordsvan Dr., Wodonga, Victoria 3690, Australia.
Email: smayers@radoncvic.com.au

Cite this article as:
Hawke S, Torrance A, Tremethick L. Evaluation of planned dosimetry when beam energies are substituted for a fraction of the treatment course. Int J Cancer Ther Oncol 2013; 1(2):01014.
DOI: 10.14319/ijcto.0102.4

Previous studies have compared the same treatment plan being carried out on two separate energies for the entire duration of the treatment. In one study the difference between 6MV and 18MV for treatment of lung cancer was evaluated and it was observed that there was no clinically significant difference.[2] However these plans had been recalculated and optimised in the treatment planning system. It was found in another study that low energy beams provided better conformity to the target than high energy beams due to reduced lateral scatter.[3]

In a more recent study by Molazeda et al.[4] oesophageal and pelvis plans were compared using both 6MV and 15MV where all parameters entered in the treatment planning system (TPS) such as beam angle and weighting were kept the same. It was established that there was no significant difference in uniform dose coverage to the PTV in both the oesophageal and rectum plans when the energy was changed in the TPS. However it should be noted that in the study by Molazeda et al. the plan was recomputed to find the optimal

ISSN 2330-4049

monitor unit (MU) from each angle. This differs from what is being conducted in this technical note where all parameters, including the MU's are kept the same, and the plan recomputed to find the difference to the PTV and OAR's.

The purpose of this technical study was to investigate whether a patient could have treatment between one and several fractions of their whole treatment with substituted beam energy and to quantify the difference in dose to the planning target volume (PTV) and organs at risk (OAR).

Methods and Materials

Computation using TPS

The TPS used in this study was Pinnacle (Philips Healthcare, Andover, MA) version 9.2.[5] A variety of treatment plans generated using three dimensional conformal radiation therapy (3DCRT) were selected from the TPS with treatment sites including the oesophagus, prostate, lung, spine, rectum, bladder, chest, scapula and breast. Of the 28 plans selected half were planned with 15MV and half with 10MV. The number of fractions ranged from palliative treatments with 5 fractions to radical treatments with 34 fractions. In each case the energy of a single fraction was changed to 15MV if the plan was originally 10MV and 10MV if the original plan was 15MV. This was then repeated with 2, 3, 4, 5, 10 and all fractions being changed either to 15MV or 10MV. The modified treatment plan retained the same number of monitor units as the original plan. The calculation algorithm used in the TPS was collapsed cone convolution with a 0.28cm grid size. The percentage changes to the mean dose of the PTV and OAR's were evaluated. The average PTV volume for the plans investigated is shown in **Table 1.**

TABLE 1: Average PTV volume for plans investigated.

PTV	Average Volume (cm^3)
Oesophagus	310.88
Prostate	185.67
Lung	928.06
Spine	1183.85
Rectum	798.36
Bladder	741.83
Chest	606.42
Scapula	218.62
Breast	1866.32

Ion chamber measurements

Two bladder treatment plans were transferred onto a cylindrical phantom. The isocenter of the plans was moved to allow the ion chamber to be located within the PTV. The plan was modified so that trial 1 contained 5 fractions with 15MV and trial 2 with 4 fractions of 15MV and 1 fraction of 10MV. This second trial allowed for 20% of the treatment plan to be delivered with 10MV. The dose to the isocentres was recorded from the TPS for both trials. Both trials of the oesophagus plans were delivered to the cylindrical phantom with a Wellhofer cc13 chamber (Wellhofer Dosimetrie, Schwrazenbruck Germany) [6] (with a collecting volume of $0.13cm^3$ and previously known as an IC15) inserted at the centre. The ion chamber measurements were then compared with the TPS results.

Similarly two oesophagus treatment plans were transferred to a cylindrical phantom dataset where two plan trials were created. Trial 1 contained 5 fractions of 10MV and trial 2 contained 4 fractions of 10MV and 1 fraction of 15MV. Ion chamber measurements from the oesophagus trials were compared to the results from the TPS.

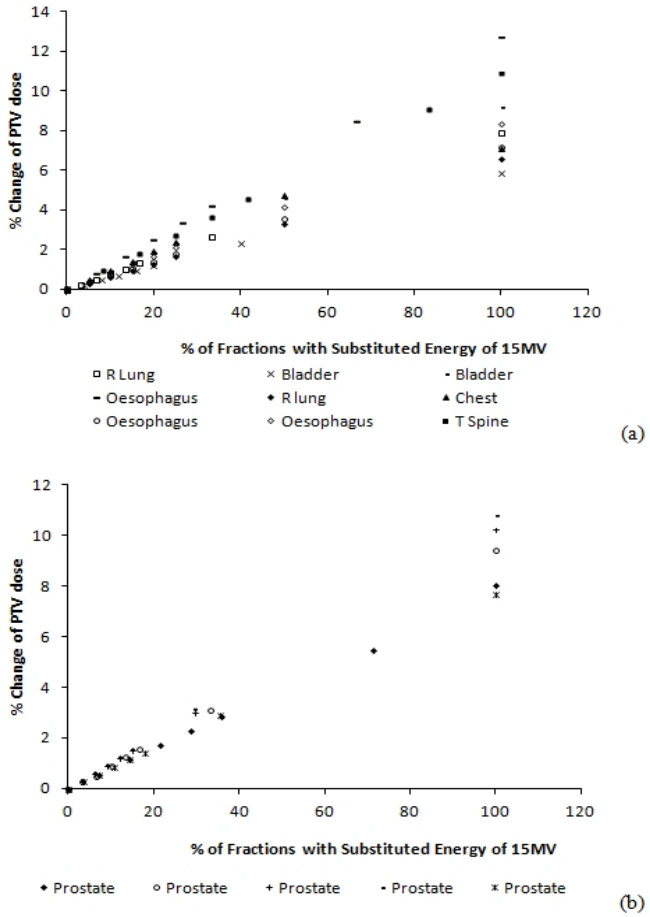

FIG. 1: A plot showing the change in the PTV dose when a percentage of the treatment was substituted with 15MV instead of the original planned 10MV for (a) three oesophagus plans, a spine plan, two bladder plans, a chest plan and two lung plans and (b) five prostate plans.

 ISSN 2330-4049

Results

Computation using TPS

Each of the patient plans investigated were plotted using the percentage change in dose to the PTV as a function of the percentage of fractions with the substituted energy. These findings are shown in **Figure 1** for a 10MV plan with 15MV substituted in for various numbers of fractions and **Figure 2** where a 15MV treatment plan had various numbers of fractions substituted with 10MV. Each of the different symbols represents an individual patient plan. The percentage change in the PTV dose was calculated using equation 1 where plan A is the dose to the PTV in the original plan and plan B is the dose to the PTV in the plan with the substituted fraction/s.

$$\%\ change\ of\ PTV\ dose = \frac{D_{plan\ B} - D_{plan\ A}}{D_{plan\ A}} \times 100 \qquad (1)$$

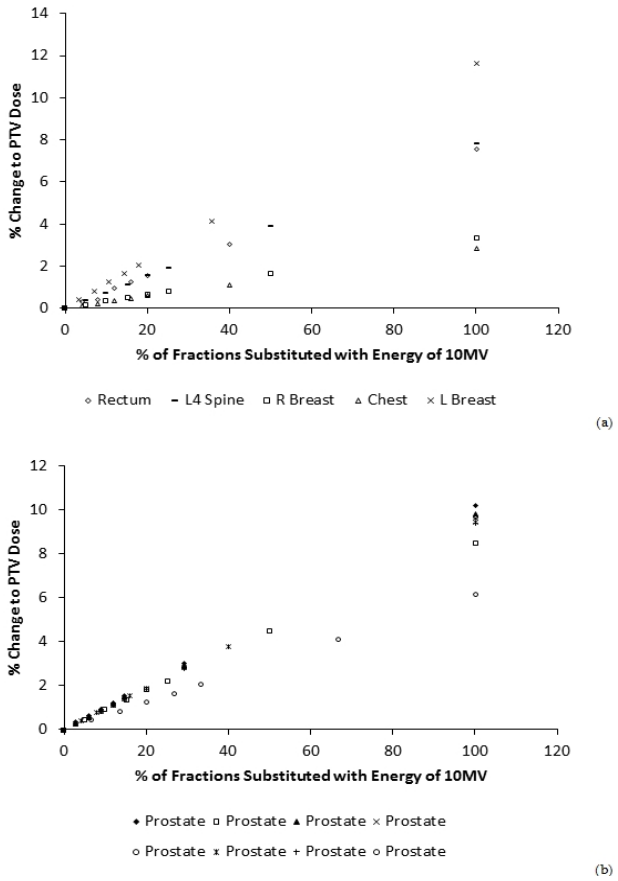

FIG. 2: A plot showing the change in the PTV dose when a percentage of the treatment was substituted with 10MV instead of the original planned 15MV for (a) a rectum plan, a spine plan, a chest plan and breast plan and (b) eight prostate plans.

The percentage change in the dose to the OARs were tabulated for each treatment plan when a fifth of the fractions had been substituted with 15MV for a 10MV plan, **Table 1**, and 10MV for a 15MV plan, **Table 2**.

TABLE 2: Percentage change for a fifth of the fractions of a 10MV plan substituted with 15MV for the organs at risk (OARs)

Treatment Site	OAR	Average of changes to Mean dose %
R Lung	Spinal Cord	0.3
	Heart	1.4
Bladder	Left femur	3.9
	Right Femur	1.9
Oesophagus	Spinal Cord	1.5
	Heart	2.9
	Left Lung	0.5
Chest	Right Lung	2.5
	Spinal Cord	1.4
	Spinal Cord	2.9
T- Spine	Left Lung	0.7
	Right Lung	3.1
	Bladder	3.2
	Rectum	1.8
Prostate	Left Femur	3.1
	Right Femur	1.7

TABLE 3: Percentage change for a fifth of the fractions of a 15MV plan substituted with 10MV for the organs at risk (OARs).

Treatment Site	OAR	Average of changes to Mean dose %
	Bladder	1.5
	Left Femur	2.3
Rectum	Right Femur	2.1
	Small bowel	2.1
	Spinal Cord	0.6
L4 Spine	Left Kidney	2.3
	Right Kidney	1.3
	Spinal Cord	0.4
Breast	Right Lung	2.4
	Left Lung	1.4
	Right Lung	1.2
Chest	Left Lung	1.5
	Spinal cord	0.7
	Bladder	2.2
Prostate	Rectum	1.9
	Left Femur	1.4

Ion chamber measurements

The TPS results for the bladder and oesophagus treatment plans are compared with ion chamber measurements, shown in **Table 4**. Trial 1 for the bladder treatment plans refers to 5 fractions of 15MV and trial 2 refers to 4 fractions of 15MV and 1 fraction of 10MV. Similarly for the Oesophagus trial 1 refers to 5 fractions of 10MV and trial 2 refers to 4 fractions of 10MV and 1 fraction of 15MV.

ISSN 2330-4049

TABLE 4: TPS calculation compared to ion chamber measurements for bladder and oesophagus treatment sites

Treatment Site	Δ^a	Δ^b
Bladder	1.2	0.6
Oesophagus	1.1	0.9

Abbreviations: Δ^a = Average % difference between ion chamber measurement of Trial 1 and 2; Δ^b = Average % difference between TPS and ion chamber measurement

Discussion and Conclusion

It can be seen from **Figure 1** that when the 15MV beam is substituted in for a 10MV plan the change to the PTV appears to follow a linear relationship with the number of fractions substituted. A similar phenomenon was also seen in **Figure 2**. More importantly the majority of the plans when substituted with 15MV for 20% of the fractions have a corresponding change in dose to the PTV of <2%. This is consistent with a study by Pokharel S[7] where 6MV prostate plans where substituted with mixed energy plans of 6MV and 16MV and the total dose to the PTV was found to vary by less than 1% from the original plan.

The International Commission on Radiation Units and Measurements (ICRU) recommend that the PTV dose remains within +7% and -5% of the prescription dose; therefore when considering if a plan could have one or multiple fractions with a substituted energy the dose to the PTV and the prescription dose needs to be considered.[8]

From **Table 2**, it is apparent that the average change to the OAR's for a substitution of a 15MV beam for 20% of a 10MV plan varies between 0.3% to 3.9%. For a 15MV plan substituted with 10MV for 20% of the fractions shows that on average the OAR's have a change of <2.3%. These findings are detailed in **Table 3**.

It was determined that up to 20% of the fractions for a 10MV or 15MV plan could be substituted with 15MV or 10MV respectively while maintaining the change to the PTV dose of less than 2%. These findings could be used as a general rule of thumb only for treatment plans generated using the 3DCRT technique in conjunction with the collapsed cone convolution algorithm and not for other techniques such as IMRT or VMAT.

These results were then verified using ion chamber measurements and comparing to the TPS results. It was seen from **Table 4** that the difference between ion chamber measurements and the treatment planning calculations were 1% or less, this can be attributed to the relative output for 10MV and 15MV being 1% above the ideal.

Neutron dose from the 15MV beam was not considered in this study as it has previously been shown that the absolute lifetime risk of malignancies caused by secondary neutrons in a 15MV beam during intensity modulated radiation therapy (IMRT) only increased slightly compared to the risk for a 6MV IMRT treatment.[9] 3DCRT has only a portion of the MU's delivered during IMRT and thus considered to have even less risk than IMRT treatment plans. The results here indicate the factors which need to be considered when substituting energy in for the planned energy are the number of fractions which will have a substituted energy as a percentage of the overall treatment.

Whilst beam substitution is not the recommended approach to treat patients when they are unable to be treated with the planned energy, this technical study suggests that patient dosimetry is not greatly affected if a treatment plan of 15MV or 10MV were to be substituted with 10MV or 15MV respectively for up to a fifth of the number of fractions.

Conflict of interest

The authors declare that they have no conflicts of interest. The authors alone are responsible for the content and writing of the paper.

References

1. Varian Medical Systems 2013 Available from: http://www.varian.com/us/oncology/radiation_oncology/clinac/.
2. Weiss E, Siebers JV, Keall P J. An analysis of 6MV versus 18MV photon energy plans for intensity-modulated radiation therapy (IMRT) of lung cancer. *Radiother Oncol* 2007; **82**: 55-62.
3. St-Hilaire J, Sevigny C, Beaulieu F, Gingras L, Tremblay D, Beaulieu L. Optimisation of Photon beam energy in aperture based inverse planning. *J Appl Clin Med Phys* 2009; **10**: 3012.
4. Molazeda M, Saberi H, Rahmatnezhad L, Molani A, Jabbari A. Evaluation the effect of photon beam energies on organ at risk doses in three-dimensional conformal radiation therapy. *Research Journal of Applied Science, Engineering and Technology* 2013; **6**:2110-2117.
5. Philips Radiation Oncology Systems. Pinnacle v9.2. Fitchburg, WI: 2013
6. Wellhofer Dosimetrie, inventor; IC-15. Schwrazenbruck Germany.

 ISSN 2330-4049

7. Pokharel S. Dosimetric impact of mixed- energy volumetric modulated arc therapy plans for high risk prostate cancer. *International Journal of Cancer Therapy and Oncology* 2013; **1**(1):01011.
8. Bestheda MD. Prescribing, recording and reporting photon beams. International Commission of Radiation Units and Measurements (ICRU) Report No. 50, 1993.
9. Kry SF, Salehpour M, Followill DS, et. al. The calculated risk of fatal secondary malignancies from intensity modulated radiation therapy. *Int J Radiat Oncol Biol Phys* 2005; **62**: 1195-203.

 ISSN 2330-4049

International Journal of Cancer Therapy and Oncology
www.ijcto.org

Sebaceous carcinoma of right upper eyelid: case report and literature review

Shurti Singh[1], Swarn Kaur[2], Alok Mohan[1], Sunder Goyal[3]

[1]*Pathology Department, MM Institute of Medical Sciences & Research, Mulana, India.*
[2]*Pathology Department, BPS Govt Medical College for Women, Khanpur, sonepat, India.*
[3]*Department of Surgery, Kalpana Chawla Govt Medical College, Karnal, Haryana, India.*

Received October 17, 2013; Revised October 27, 2013; Accepted October 27, 2013; Published Online November 15, 2013

Case Report

Abstract

Sebaceous gland carcinoma is a rare fast growing cutaneous cancer. It is derived from the adenxal epithelium of sebaceous glands. Sebaceous carcinomas are generally divided into those occurring in periocular or extraocular locations. Ocular sebaceous carcinomas occur most commonly in upper eye lid, in the elderly with a predilection for females and Asian populations. Due to its clinical resemblance with chalazion or other chronic inflammatory conditions, there is a delay in diagnosis. Due to its rarity, we present a case of sebaceous carcinoma of right upper eyelid in a 65-year-old female.

Keywords: Upper eyelid; ocular sebaceous carcinoma; chalazion

Introduction

Sebaceous carcinoma was first reported by Allaire in 1891. Its incidence is less than 1% of all skin malignancies. Sebaceous carcinoma is the fourth most common neoplasms of the eyelid and arises mainly from the meibomian or less commonly from Zeis glands. It is a rare but fast growing malignant neoplasm with a tendency for both local recurrence and distant metastases. Sebaceous carcinoma can either be ocular or extraocular, and extraocular type is rare.[1] Advanced age, Asian or South Asian race, women, previous irradiation to the head and neck, a genetic predisposition for Muir-Torre syndrome or possibly familial retinoblastoma are various predisposing factors for sebaceous carcinoma. It mostly spread to regional lymph nodes. It may invade orbit, and 22% of patients die due to visceral metastases.[2]

Case History

A 65-year-old female patient presented with a mass over right upper eyelid (Figure 1). Patient complained of decreased vision & foreign body sensation in the right eye for 6 months prior to reporting the case. Fine needle aspiration cytology (FNAC) was performed using standard technique. Staining was done with papanicolaou stain & May Grunwald Giemsa (MGG) stain. Smears demonstrated tumor cells arranged in irregular clusters and as single cells. The cells contain moderate amount of finely reticular cytoplasm with various degrees of vacuolization. Pleomorphic centrally located nuclei containing coarse chromatin & prominent nucleoli were seen (Figure 2).

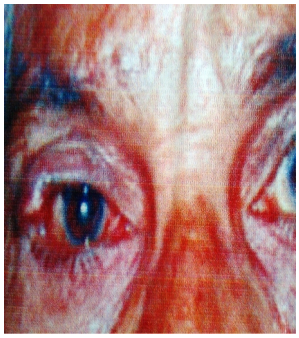

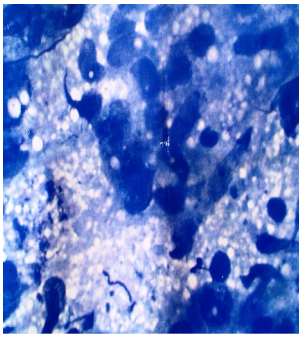

FIG. 1 (left): Patient Photo showing swelling right upper eyelid.
FIG. 2 (right): Cytological smear showing sebaceous carcinoma MGG (high power).

Tumor was excised and Oil red O staining of fresh frozen tissue was done for confirmation of sebaceous carcinoma. Histopathology revealed irregular epithelial lobules with atypical dark pleomorphic cells with abundant foamy, finely vacuolated cytoplasm & well defined borders. The tumor

Corresponding author: Sunder Goyal, MS, MNAMS, FAIS; Department of Surgery, Kalpana Chawla Govt Medical College, Karnal, Haryana, India. Email: goyal.sunder@yahoo.in

Cite this article as:
Singh S, Kaur S, Mohan A, Goyal S. Sebaceous carcinoma of right upper eyelid: case report and literature review. Int J Cancer Ther Oncol 2013; 1(2):01022. **DOI**: 10.14319/ijcto.0102.2

ISSN 2330-4049

cells manifested marked pleomorphism, prominent nucleoli & numerous mitotic figures (Figures 3 and 4). CAM 5.2 staining was done to differentiate between the normal & malignant sebaceous lesions. CAM 5.2 staining was strongly positive for sebaceous carcinoma.

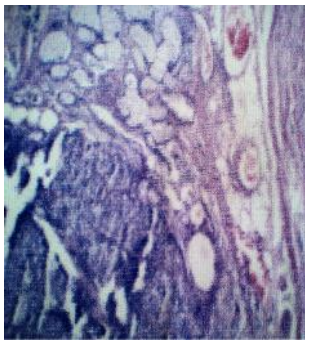

FIG. 3: Histopathology salide showing sebaceous carcinoma H&E under low power.

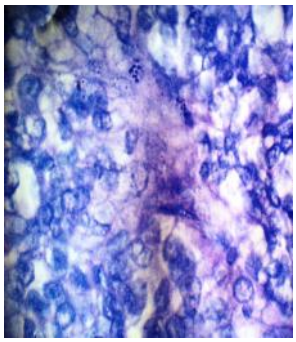

FIG. 4: Histopathology salide showing sebaceous carcinoma H&E under high power.

Discussion

Sebaceous carcinoma is a rare and destructive malignant neoplasm. It frequently occurs in adults with a female predominance.[3] This malignancy can occur as periocular and extraocular regions and the former type is about 75% of sebaceous neoplasms. Upper eyelid is affected two to three times more often than the lower eyelid due to high number of meibomian glands.[4] According to literature, ocular sebaceous carcinoma arose from the meibomian glands in 51 to 70% of cases; multicentric in origin in 12 to 24 %; and 4 to 10% arose from the glands of Zeiss; the few originated from the caruncle or orbit. Incidence of extraocular sebaceous carcinoma is about 25% of the sebaceous neoplasms and mostly effects the head and neck areas followed by trunk, salivary glands, genitalia, breast, ear canal, and the intra-oral cavity.[3]

The clinical presentation of ocular sebaceous carcinoma is varied and an accurate diagnosis is delayed for months to years. The mean delay from onset of disease to diagnosis is about 1 to 2.9 years. The most common clinical presentation is a small, erythematous or possibly yellowish, slowly enlarging, firm, deep seated papule or nodule on the upper eyelid. It may resemble with a chalazion, keratoconjunctivits or blepharoconjunctivitis. Numerous other inflammatory conditions, autoimmune diseases, infectious processes, and basal cell carcinoma may clinically imitate sebaceous carcinoma of the eyelid. Due to variable clinical presentations of ocular sebaceous carcinoma, a high degree of suspicion and ultimate biopsy of non-healing lesions is critical in making the final diagnosis. Sometime diagnosis is made only after metastases to the regional lymph node or parotid gland.[5]

TABLE 1: Classification of sebaceous carcinoma based on degree of differentiation by Font[6] (top) and Wolfe et al.[7] (bottom)

Classification by Font.[6]

Well Differentiated	Contains many neoplastic cells exhibiting sebaceous differentiation with abundant finely vacuolated cytoplasm. Areas of sebaceous differentiation are often toward the center of tumor lobules
Moderately Differentiated	Only a few areas of highly differentiated sebaceous cell are seen. The majority of the tumor is composed of neoplastic cells with hyperchromatic nuclei and prominent nucleoli and abundant basophilic cytoplasm
Poorly Differentiated	The majority of cells exhibit pleomorphic nuclei with prominent nucleoli and scant cytoplasm. A moderate increase in mitotic activity is present.

Classification by Wolfe et al.[7]

Grade I	Well differentiated; foamy cytoplasm present in all cells.
Grade II	Large vacuolated nuclei and foamy cytoplasm seen in most cells
Grade III	Small hyperchromatic nuclei and little cytoplasm present in most cells
Grade IV	Undifferentiated; small hyperchromatic nuclei and little cytoplasm; diagnosis requires positive fat stain, ultrastuctural study or areas of better differentiation.

Histologically, sebaceous carcinoma has to be differentiated from basal cell carcinoma, squamous cell carcinoma, trichilemmal keratinisation, sebaceous adenoma and sebaceous epithelioma. Special stains such as oil red O may be helpful in confirming the presence of fat, but requires frozen section. Immunohistochemical studies may also be employed to confirm the diagnosis. Sebaceous carcinoma cells express immunohistochemical markers such as cytokeratin, epithelial membrane antigen (EMA), Cam5.2 and anti-breast carcinoma associated antigen-225 antibody. The cause of sporadic sebaceous carcinomas is still unclear. Previous radiation to the area is a well-documented risk factor, especially in children.[8] Sebaceous carcinoma may be associated with use of oral diuretic like thiazide. The diuretic causes production of carcinogenic nitrosamines which may play a role in the carcinogenesis of the sebaceous carcinomas in these patients.[9] However, there is no firm etiologic link between diuretic use and the development of sebaceous carcinoma.

 ISSN 2330-4049

The molecular mechanisms for tumor development and progression are recently being studied. It has been assumed that the loss of p53 and the consequent disruption of genomic integrity might play a critical role in the progression of sebaceous carcinoma.[10] Ocular sebaceous carcinoma may metastasize via the lymphatics, the blood vessels, by the lacrimal secretory system, and the lacrimal excretory system. Metastases occur in approximately 8 to 25% of patients, and metastasize to regional lymph nodes, followed by involvement of the liver, lungs, brain, and bones. Lymphatic metastases involve preauricular, submandibular, or cervical lymph nodes, with or without secondary parotid masses. Distant metastases and recurrence rates are more common in the ocular type of sebaceous carcinoma.[11] Recurrence rates of ocular sebaceous carcinoma ranges from 11% to 30% with distant metastases occurring in 3% to 25% .[11] In sebaceous carcinoma of eye lid, there is local loss of the eyelashes due to tumour infiltration of the follicle. If tumor is one sided and every therapy is ineffective then there are more chances of sebaceous carcinoma. A full thickness eyelid biopsy combined with conjunctival map biopsies is necessary for the diagnosis.[12] Once a diagnosis of sebaceous carcinoma is considered, a detailed history and physical examination should be done. Colonoscopy and barium enema are essential to rule out internal malignancies associated with the Muir-Torre syndrome.

The primary treatment of sebaceous carcinoma is complete surgical excision. Mohs micrographic surgery is most commonly done.[13] Excision of tumor with frozen section is mandatory for proper management. Conjunctival map biopsies should be done at the time of surgery to assess for potential pagetoid spread. Microscopically it tends to extend far beyond its assessed clinical margins as it may spread by direct extension, be multifocal in advanced cases, and may develop "skip areas" after injury. Despite its ability to develop “skip areas”, Mohs micrographic surgery (MMS) is a ideal mode of treatment.[14] Subtotal or complete exenteration is required if the tumour is very large or recurrent with spread to bulbar conjunctiva, to the other eyelid, or to orbital tissue. Radical neck dissection along with partial parotidectomy is performed If it spread to regional lymph nodes.[12]

The missing tarsoconjunctival structures and skin should be reconstructed properly to protect the eye globe and should give a natural appearance with only minor deficiency. Ideally it should be one stage procedure. The vascularised temporal island flap can be used as one stage procedure. As it is fast growing cancer, postoperative patient should be followed up at 3 monthly interval during the first year, 6 monthly during the second year, and then on a yearly basis for life.[12] Cryotherapy can be utilized as adjunctive therapy to treat patients with residual conjunctival intraepithelial disease or in those patients in whom definitive surgical excision is not possible. Topical mitomycin C has also been used as an adjunctive therapy in patients with intraepithelial involvement.[15] Sebaceous carcinoma is relatively radio resistant, so, radiotherapy may be used as palliative therapy for inoperable patients.[13] Total dose of radiation is about >50 Gy. If radiation alone is used then tumor may reoccur within 3 years.

Finally, metastatic disease may be treated with a combination of excision, radiation, and chemotherapy. A schedule of intralesional 5-flurouracil in combination with intravenous 5-fluorouracil, doxorubicin, cisplatin, and vinblastine has been used.[16] Mortality rates irrespective of ocular or extraocular type ranges from 9% to 50%.[17]

Conclusion

Sebaceous carcinoma is a fast growing tumor and it is mostly seen on the eyelid. Since it clinically resembles other diseases, it presents challenge in diagnosis. Early, precise and prompt diagnosis is vital as it spreads out regionally as well to other distant organs. It may be associated with Muirre- Torre syndrome. The inconsistent appearance mostly causes delay in diagnosis, improper treatment, increased morbidity, and mortality.

Conflict of interest

The authors declare that they have no conflicts of interest. The authors alone are responsible for the content and writing of the paper.

References

1. Natarajan K, Rai R, Pillai SB1. Extra ocular sebaceous carcinoma: A rare case report. *Indian Dermatol Online J* 2011; **2**: 91–93.
2. Dasgupta T, Wilson LD, Yu JB. A Retrospective Review of 1349 Cases of Sebaceous Carcinoma. *Cancer* 2009; **115**: 158-165.
3. Lazar AJ, Lyle S, Calonje E. Sebaceous neoplasia and Torre-Muir syndrome. *Curr Diagn Pathol* 2007; **13**: 301–319.
4. Shields JA, Demirci H, Marr BP, et al. Sebaceous carcinoma of the eyelids. Personal experience with 60 cases. *Ophthalmology* 2004; **111**:2151–2157.
5. Shet T, Kelkar G, Juvekar S, et al. Masquerade syndrome: sebaceous carcinoma presenting as an unknown primary with pagetoid spread to the nasal cavity. *J Laryngol Otol* 2004; **118**:307–309.
6. Font RL. Eyelids and lacrimal drainage system. In: Spencer HW, ed. Ophthalmic Pathology: An Atlas and Textbook. 3rd ed. Philadelphia: WB Saunders; 1986; 2169–2214.

 ISSN 2330-4049

7. Wolfe JT, Yeatts RP, Wick MR, et al: Sebaceous carcinoma of the eyelid: errors in clinical and pathologic diagnosis. *Am J Surg Pathol* 1984; **8**:597–606.
8. Kivela T, Asko-Seljavaara S, Pihkala U, et al. Sebaceous carcinoma of the eyelid associated with retinoblastoma. *Ophthalmology* 2001; **108**:1124–1128.
9. Khan JA, Grove AS Jr, Joseph MP, et al. Sebaceous carcinoma. Diuretic use, lacrimal spread, and surgical margins. *Ophthal Plast Reconstr Surg* 1989; **5**:227–234.
10. Gonzalez-Fernandez F, Kaltreider SA, Patnaik BD, et al. Sebaceous carcinoma. Tumor progression through mutational inactivation of p53. *Ophthalmology* 1998; **105**:497–506.
11. Muqit MM, Roberts F, Lee WR, Kemp E. Improved survival rates in Sebaceous Carcinoma of the eyelid. *Eye* 2004; **18**:49–53.
12. Gardetto A, Rainer C, Ensinger C, Baldissera I, Piza-Katzer H. Sebaceous carcinoma of the eyelid: a rarity worth considering. *Br J Ophthalmol* 2002; **86**: 243–244.
13. Cook Jr. BE, Bartley GB. Treatment options and future prospects for the management of eyelid malignancies. An evidence-based approach. *Ophthalmology* 2001; **108**:2088–2100.
14. Snow SN, Larson PO, Lucarelli MJ, Lemke BN, Madjar DD. Sebaceous carcinoma of the eyelids treated by mohs micrographic surgery: report of nine cases with review of the literature. *Dermatol Surg* 2002; **28**:623-631.
15. Tumuluri K, Kourt G, Martin P. Mitomycin C in sebaceous gland carcinoma with pagetoid spread. *Br J Ophthalmol* 2004; **88**:718–719.
16. Tenzel RR, Stewart WB, Boynton JR, et al. Sebaceous adenocarcinoma of the eyelid. *Arch Ophthalmol* 1977; **95**: 2203–2204.
17. Doxanas MT, Green WR. Sebaceous gland carcinoma. Review of 40 cases. *Arch Ophthalmol* 1984; **102**: 245–249.

ISSN 2330-4049